



National Library
of Canada

Bibliothèque nationale
du Canada

Acquisitions and
Bibliographic Services Branch

Direction des acquisitions et
des services bibliographiques

395 Wellington Street
Ottawa, Ontario
K1A 0N4

395, rue Wellington
Ottawa (Ontario)
K1A 0N4

Your file Votre référence

Our file Notre référence

NOTICE

The quality of this microform is heavily dependent upon the quality of the original thesis submitted for microfilming. Every effort has been made to ensure the highest quality of reproduction possible.

If pages are missing, contact the university which granted the degree.

Some pages may have indistinct print especially if the original pages were typed with a poor typewriter ribbon or if the university sent us an inferior photocopy.

Reproduction in full or in part of this microform is governed by the Canadian Copyright Act, R.S.C. 1970, c. C-30, and subsequent amendments.

AVIS

La qualité de cette microforme dépend grandement de la qualité de la thèse soumise au microfilmage. Nous avons tout fait pour assurer une qualité supérieure de reproduction.

S'il manque des pages, veuillez communiquer avec l'université qui a conféré le grade.

La qualité d'impression de certaines pages peut laisser à désirer, surtout si les pages originales ont été dactylographiées à l'aide d'un ruban usé ou si l'université nous a fait parvenir une photocopie de qualité inférieure.

La reproduction, même partielle, de cette microforme est soumise à la Loi canadienne sur le droit d'auteur, SRC 1970, c. C-30, et ses amendements subséquents.

UNIVERSITY OF ALBERTA

**DEVELOPMENT OF PLASMA-SPRAYED HYDROXYLAPATITE
COATING SYSTEMS FOR SURGICAL IMPLANT DEVICES**

BY

DENISE LAMY



A THESIS

SUBMITTED TO THE FACULTY OF GRADUATE STUDIES AND RESEARCH IN
PARTIAL FULFILLMENT OF THE REQUIREMENTS FOR THE DEGREE OF
MASTER OF SCIENCE

IN

METALLURGICAL ENGINEERING

DEPARTMENT OF MINING, METALLURGICAL AND PETROLEUM
ENGINEERING

EDMONTON, ALBERTA

FALL 1993



National Library
of Canada

Acquisitions and
Bibliographic Services Branch

395 Wellington Street
Ottawa, Ontario
K1A 0N4

Bibliothèque nationale
du Canada

Direction des acquisitions et
des services bibliographiques

395, rue Wellington
Ottawa (Ontario)
K1A 0N4

Your file *Votre référence*

Our file *Notre référence*

The author has granted an irrevocable non-exclusive licence allowing the National Library of Canada to reproduce, loan, distribute or sell copies of his/her thesis by any means and in any form or format, making this thesis available to interested persons.

L'auteur a accordé une licence irrévocable et non exclusive permettant à la Bibliothèque nationale du Canada de reproduire, prêter, distribuer ou vendre des copies de sa thèse de quelque manière et sous quelque forme que ce soit pour mettre des exemplaires de cette thèse à la disposition des personnes intéressées.

The author retains ownership of the copyright in his/her thesis. Neither the thesis nor substantial extracts from it may be printed or otherwise reproduced without his/her permission.

L'auteur conserve la propriété du droit d'auteur qui protège sa thèse. Ni la thèse ni des extraits substantiels de celle-ci ne doivent être imprimés ou autrement reproduits sans son autorisation.

ISBN 0-315-88413-4

Canada

UNIVERSITY OF ALBERTA

RELEASE FORM

NAME OF AUTHOR: DENISE LAMY

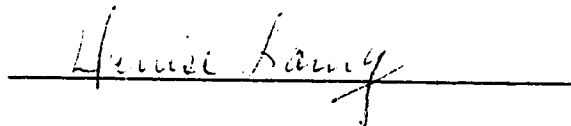
TITLE OF THESIS: DEVELOPMENT OF PLASMA-SPRAYED
HYDROXYLAPATITE COATING SYSTEMS
FOR SURGICAL IMPLANT DEVICES

DEGREE: MASTER OF SCIENCE

YEAR THIS DEGREE GRANTED: FALL, 1993

Permission is hereby granted to the University of Alberta Library to reproduce single copies of this thesis and to lend or sell such copies for private, scholarly or scientific research purposes only.

The author reserves all other publication and other rights in association with the copyright in the thesis, and except as hereinbefore provided neither the thesis nor any substantial portion thereof may be printed or otherwise reproduced in any material form whatever without the author's prior written permission.



10045-118 Street #803

Edmonton, Alberta

Canada

T5K 2K2

DATE: August 10, 1993

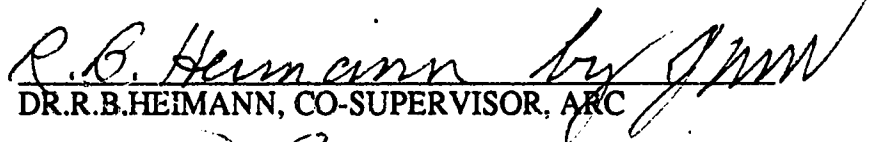
UNIVERSITY OF ALBERTA

FACULTY OF GRADUATE STUDIES AND RESEARCH

The undersigned certify that they have read, and recommend to the Faculty of Graduate Studies and Research for acceptance, a thesis entitled **DEVELOPMENT OF PLASMA-SPRAYED HYDROXYLAPATITE COATING SYSTEMS FOR SURGICAL IMPLANT DEVICES** submitted by **DENISE LAMY** in partial fulfillment of the requirements for the degree of **MASTER OF SCIENCE IN METALLURGICAL ENGINEERING**.


DR.J.M.WHITING, COMMITTEE CHAIRMAN


DR.A.C.PIERRE, CO-SUPERVISOR, U. OF A.


DR.R.B.HEIMANN, CO-SUPERVISOR, ARC


DR.F.ELLYIN, COMMITTEE MEMBER


DR.S.A.BRADFORD, COMMITTEE MEMBER

DATE: July 29, 1993

ABSTRACT

ABSTRACT

In orthopaedics, total hip joint replacement has been practiced for many years as a surgical procedure, and has contributed to the return to a normal life for many patients. Several designs and materials have led to the evolution of the artificial joint system. Application of a hydroxylapatite (HA) coating on metallic prostheses improves the stabilization of the implant within the bone. The hydroxylapatite coating becomes osseointegrated with bone, and the bond is stronger than bone itself. However, attachment of HA to metallic substrates needs improvement.

This study evaluates the effect, on the implant system, of adding an intermediary bond coat between titanium-based metal prostheses and the top hydroxylapatite coating. Investigations show that adhesion strength of the coating is higher with the presence of the bond coat than with HA alone. Thin coatings exhibit more consistent failure modes than thick coatings.

Long term studies are needed to confirm the beneficial effect of the established chemical bond from the titanium-based substrate up to the HA top coat, and to in-situ bone. More work is also needed to identify the exact nature of the intermediary substances.

PREFACE

PREFACE

The subject of this project is related to improving the attachment of a HA plasma-sprayed coating to its substrate through the development of a chemical bond obtained with the presence of an intermediary layer. Basically an advanced materials project linked to the plasma spraying technology, its *raison d'être* belongs to the medical domain: the search for suitable implantable materials for the human body. Therefore, this document is divided into two parts.

In the first part, a short review is made of what are the requirements for prostheses, followed by comments on metal and polymer materials, and by a more extensive section on ceramics as implantable materials. A review is included of the scientific (materials) and clinical (effects in the human body) literature on the calcium phosphate materials used in the human body.

The second part describes materials and methods, analyses performed, and results obtained with the multilayer implantable material.

In the context of this project, implants or prostheses are defined as artificial devices designed to replace a defectuous or missing part of the body.

ACKNOWLEDGEMENT

ACKNOWLEDGEMENT

The author expresses her appreciation and thanks to:

Dr. Robert B. Heimann, formerly of the Alberta Research Council, for his co-supervision of the project and for his numerous discussions and suggestions;

Dr. Alain C. Pierre, of the University of Alberta, for his co-supervision and guidance during this project;

Dr. Ted Heidrick and Mr. Chris Lumb, of the Alberta Research Council, for their contribution on administrative requirements related to this project;

Mr. Terry Sopkow, of the Alberta Research Council, for showing me how to use the plasma spray coating system;

Mr. Kelvin Kang, of the Alberta Research Council, for his indications in specimens preparation and photography;

Mrs. Tina Barker, of the University of Alberta, for her work on the scanning electron microscope and the x-ray diffraction spectra production;

Dr. Robert Pilliar (and his team) of the Centre for Biomaterials, in Toronto, for providing the tensile (adhesion) tests buttons and for performing the adhesion tests;

Onoda Cement, from Japan, for graciously providing the Ca_2SiO_4 powder;

Raymond, pour ses nombreux encouragements et pour sa compréhension.

TABLE OF CONTENTS

TABLE OF CONTENTS

CHAPTER	PAGE
1. STATEMENT OF WORK	...1
2. INTRODUCTION AND LITERATURE REVIEW	...4
2.1. Need for Implants	...4
2.2. Biomaterials Definition	...5
2.3. Performance Criteria for Biomaterials	...6
2.4. Ceramics as Implant Materials	...9
2.4.1 Nearly Inert Materials	...11
2.4.1.1. Alumina	...11
2.4.1.2. Zirconia	...15
2.4.1.3. Carbons	...15
2.4.1.4. Other Inert Materials	...16
2.4.2. Resorbable Materials	...16
2.4.2.1. Tricalcium Phosphate (TCP)	...17
2.4.2.2. Other Resorbable Ceramics	...18
2.4.3. Surface Reactive Materials	...18
2.4.3.1. Hydroxylapatite	...20
2.4.4. Calcium Phosphate-Based Materials (HA and TCP)	...21
3. MATERIALS AND METHODS	...42
3.1 Powder Characterization	...42
3.1.1. Particle Size and Size Distribution	...42
3.1.2. Chemical Composition	...45
3.1.3. Phase Identification	...47
3.1.4. Particle Morphology	...49
3.2 Plasma Spraying	...51
3.2.1. Spraying Parameters	...51
3.2.2. Specimen Preparation	...52
3.2.3. Wipe Tests	...52
3.2.4. Final Spray Parameters	...53

TABLE OF CONTENTS

3.3 Coatings Characterization	...54
3.3.1. Morphology	...54
3.3.2. Thickness	...54
3.3.3. Phase Identification	...54
3.3.4. Chemical Analysis of Interfaces	...55
3.3.5. Surface Roughness	...55
3.3.6. Mechanical Evaluation	...55
 4. RESULTS AND DISCUSSION	...58
4.1 Preliminary Work	...58
4.1.1. Steel Substrate	...58
4.1.2. Wipe Tests	...64
4.1.3. Pure Titanium Substrate	...71
4.2 Coating Systems Characterization	...78
4.2.1 Thick Coatings Morphology	...78
4.2.2 Thin Coatings Morphology	...83
4.2.3 Adhesion Test	...87
4.2.4 Thickness on Cross-Sections	...90
4.2.5 Phase Identification	...91
4.2.6 Chemical Analyses of Interfaces	...93
4.2.7 Surface Roughness	...101
 5. CONCLUSIONS	...103
 6. FUTURE WORK	...105
 7. REFERENCES	...106
 APPENDIX	
Plasma Spraying Equipment	...117

LIST OF TABLES

LIST OF TABLES	PAGE
Table 2.1 Estimate of market volume of biomaterials in the US.	...5
Table 2.2 Mechanical properties of biomaterials and bone.	...8
Table 2.3 Development of bioceramic implants.	...11
Table 2.4 Coefficients of friction for a variety of materials.	...13
Table 3.1 Particle size distribution table (by volume) for HA-Toronto.	...42
Table 3.2 Particle size distribution table (by volume) for HA-Bioland.	...43
Table 3.3 Particle size distribution table (by volume) for Ca ₂ SiO ₄ -Japan.	...44
Table 4.1 Parameters for Ca ₂ SiO ₄ on steel.	...58
Table 4.2 Surface roughness (Ra, in μm) according to surface preparation.	...59
Table 4.3 Parameters for HA on steel.	...60
Table 4.4 Wipe test for Ca ₂ SiO ₄ parameters.	...64
Table 4.5 Wipe test for HA parameters.	...65
Table 4.6 Parameters selected for spraying on titanium substrate.	...71
Table 4.7 Surface roughness and coating thickness for first series of titanium coupons.	...73
Table 4.8 Surface roughness of HA for the four coupons.	...73
Table 4.9 Spraying schedule and surface roughness for Ca ₂ SiO ₄ coatings.	...76
Table 4.10 Flat titanium coupons sprayed with "thick" coating layers.	...78
Table 4.11 Flat titanium coupons sprayed with "thin" coating layers.	...84
Table 4.12 Adhesion strength for thick coatings.	...87
Table 4.13 Adhesion strength for thin coatings.	...88
Table 4.14 Coating thickness with optical microscope.	...90
Table 4.15 Surface roughness measurements on flat coupons.	...101

LIST OF FIGURES

LIST OF FIGURES	PAGE
Figure 1.1 Schematic layering of the coating on the metallic substrate.	...3
Figure 2.1 Reactivity versus time after implantation.	...10
Figure 2.2 Two models of total hip replacement prostheses.	...12
Figure 2.3 Variety of available dental implants.	...14
Figure 2.4 Composition of inert, bioactive, and resorbable materials.	...19
Figure 2.5 Comparison of adhesive strength with bone of several biomaterials.	...27
Figure 2.6 Strength-time relationship for a) tibia with a bone plate and b) a femur possessing a hip prosthesis.	...32
Figure 3.1 Particle size distribution for HA-Toronto.	...43
Figure 3.2 Particle size distribution for HA-Bioland.	...43
Figure 3.3 Particle size distribution for Ca ₂ SiO ₄ -Japan.	...44
Figure 3.4 EDAX analysis for the Ca ₂ SiO ₄ powder.	...45
Figure 3.5 EDAX analysis for HA-Toronto.	...46
Figure 3.6 EDAX analysis for HA-Bioland.	...46
Figure 3.7 X-ray diffraction pattern for Ca ₂ SiO ₄47
Figure 3.8 X-ray diffraction patterns for HA-Toronto (top) and HA-Bioland (bottom).	...48
Figure 3.9 Raw HA-Toronto powder. 112 X.	...49
Figure 3.10 Raw HA-Bioland powder. 112 X.	...50
Figure 3.11 Ca ₂ SiO ₄ raw powder. 112 X.	...50
Figure 3.12 Specimens with thin HA coating used for bond strength evaluation.	...56
Figure 3.13 Schematic of the bonded structure used to evaluate the bond strength of plasma sprayed coatings.	...56
Figure 3.14 Tensile specimens with thick coatings (left) and thin coatings (right).	...57

LIST OF FIGURES

Figure 4.1	Ca ₂ SiO ₄ sprayed with conditions #3. 225 X.	...59
Figure 4.2	HA sprayed with conditions #2. 225 X.	...61
Figure 4.3	HA sprayed with conditions #3. 225 X.	...61
Figure 4.4	HA sprayed with conditions #4. 225 X.	...62
Figure 4.5	HA sprayed with conditions #5. 225 X.	...62
Figure 4.6	HA sprayed with conditions #6. 225 X.	...63
Figure 4.7	HA sprayed with conditions #7. 225 X.	...63
Figure 4.8	Glass slides for Ca ₂ SiO ₄ wipe tests.	...66
Figure 4.9	Glass slides for HA wipe tests.	...66
Figure 4.10	Example of a good splat for Ca ₂ SiO ₄ sprayed with conditions "2.3". 340 X.	...67
Figure 4.11	Example of a good splat for Ca ₂ SiO ₄ sprayed with conditions "3.3". 340 X.	...67
Figure 4.12	Example of splats for Ca ₂ SiO ₄ sprayed with conditions "1.1", which were considered inappropriate. 340 X.	...68
Figure 4.13	Example of splats for Ca ₂ SiO ₄ sprayed with conditions "3.6", which were considered inappropriate. 340 X.	...68
Figure 4.14	Example of a good splat for HA sprayed with conditions "5.3". 340 X.	...69
Figure 4.15	Example of a good splat for HA sprayed with conditions "1.2". 340 X.	...69
Figure 4.16	Example of splats for HA sprayed with conditions "3.6", which were considered inappropriate. 340 X.	...70
Figure 4.17	Example of splats for HA sprayed with conditions "4.6", which were considered inappropriate. 340 X.	...70
Figure 4.18	Top coat of HA sprayed with conditions set "1.2". Numbers on the side identify the coupons.	...72
Figure 4.19	Top coat of HA sprayed with conditions set "5.3". Numbers on the side identify the coupons.	...72
Figure 4.20	Coupon #5, coated with "Ca 2.3" and "HA 1.2". 225 X.	...74
Figure 4.21	Coupon #13, coated with "Ca 3.3" and "HA 1.2". 225 X.	...74

LIST OF FIGURES

Figure 4.22 Coupon #6, coated with "Ca 2.3" and "HA 5.3". 225 X.	...75
Figure 4.23 Coupon #20, coated with "Ca 3.3" and "HA 5.3". 225 X.	...75
Figure 4.24 Flat titanium coupons with thick HA coating and a thick bond coat.	...79
Figure 4.25 Flat titanium coupons with only a thick HA coating.	...79
Figure 4.26 Coupon #23, with thick Ca_2SiO_4 and thick HA layers. 112 X.	...81
Figure 4.27 Same cross-section from coupon #23. 225 X.	...81
Figure 4.28 Coupon #40, with only a thick HA coating. 112 X.	...82
Figure 4.29 Same cross-section from coupon #40. 225 X.	...82
Figure 4.30 Coupons sprayed with a thin coating system: coupons on the left had only the HA coating (3 passes) while coupons on the right had a Ca_2SiO_4 bond coat (2 passes) and the HA top coat (2 passes).	...83
Figure 4.31 Coupon #45, with thin Ca_2SiO_4 and thin HA layers. 112 X.	...85
Figure 4.32 Same coupon #45. 360 X.	...85
Figure 4.33 Coupon #47, with only a thin HA layer. 225 X.	...86
Figure 4.34 Same cross-section from coupon #45. 360 X.	...86
Figure 4.35 X-ray diffraction spectra. a) HA powder; b) HA as sprayed; c) HA after 24 hours at 330°C.	...92
Figure 4.36 Flat coupon #21, as sprayed. 112 X.	...94
Figure 4.37 Flat coupon #21, as sprayed. 225 X.	...94
Figure 4.38 Flat coupon #21, as sprayed: digital line scans through the cross-section.	...95
Figure 4.39 Flat coupon #21, as sprayed: digital line scan for Ti.	...96
Figure 4.40 Flat coupon #21, as sprayed: digital line scan for P.	...96
Figure 4.41 Flat coupon #21, after heat treatment. 112 X.	...98
Figure 4.42 Flat coupon #21, after heat treatment. 225 X.	...98
Figure 4.43 Flat coupon #21, after heat treatment: digital line scans through the cross-section.	...99
Figure 4.44 Flat coupon #21, after heat treatment: digital line scan for Ti.	...100
Figure 4.45 Flat coupon #21, after heat treatment: digital line scan for P.	...100

LIST OF FIGURES

Figure 4.46 Pure titanium bone screws with a bond coat, left, and with only HA, right.	...102
Figure 4.47 Sets of specimens sprayed with a variety of coating system.	...102
Figure A.1 Plasma spray coating system.	...117
Figure A.2 SG-100 plasma spray gun components.	...119
Figure A.3 Anode (#175), left, cathode (#129), centre, and gas injector (#130), right.	...119

1. STATEMENT OF WORK

Metallic implants, such as total hip replacement joints, have been developed for use inside the body. Materials selection and devices design have evolved with experience. Initially, materials selection was based on identifying the strongest and more inert materials. Requirements included high fatigue strength to resist the cyclic loading of the hip joint and good corrosion resistance. Alloys selected included some stainless steels and cobalt-based alloys. A study by Sutherby^[1] reviewed the corrosion of surgical implant materials such as stainless steel 316L and CoCrMo, or "Vitallium" alloy. He showed that self-passivation occurs in neutral saline solutions but that 316L stainless steel is more susceptible to spontaneous passive film breakdown. Current philosophy in the field of prostheses focuses on emulating the human body. In this regard, titanium possesses mechanical properties closer to the properties of bone than other alloys. However, there are still concerns about unknown effects of possible ion release. Therefore, some attention is now centered on providing coatings for prostheses fabricated with the above materials as well as others, such as titanium or its alloy, Ti-6Al-4V.

Another concern is proper immobilization of the prosthesis within the site of implantation. For biomedical reasons, the prosthesis cannot move, or problems will arise requiring the removal of the device. One solution for providing immobility has been the use of a bone cement called polymethylmethacrylate or PMMA. Attachment is immediate (upon surgery). This cement is relatively effective in older patients but a high failure rate is observed with younger, more active patients. PMMA is not an adhesive and does not provide chemical bonding. It does not bond to living bone^[2]; it merely acts as a filler to immobilize the device in place. Some problems identified with PMMA include heat released during in situ polymerization causing local morbidity of bone cells and release of toxic unreacted monomers^[3] with free monomer being transported within the circulatory system. In addition, PMMA deteriorates with time resulting in a loosening of the implant. For this reason the use of PMMA is only justified in older patients.

Lately, porous metal surfaces have been successfully used to allow early strong attachment with bone. However, for even earlier, stronger attachment, an apatite coating of the porous metal surface is sometimes used^[4]. Hydroxylapatite (HA) coating is now used as an alternative for obtaining a relatively early cementless attachment by chemical bonding as opposed to the mechanical bonding obtained with porous surfaces.

Hydroxylapatite has proven itself in several applications as an acceptable artificial material to be used inside the human body. When used as a coating for an implant such as an artificial hip joint, the HA coating becomes totally "integrated" with the surrounding bone. However, although the HA becomes well integrated within the body, with time it can delaminate from the metallic substrate implant. It is, therefore, the aim of this research to improve the bond strength between the HA and the metallic substrate. Titanium and its alloy are frequently used for total hip replacement due to their bone like mechanical properties (as compared to other alloys that are often too stiff). In this study titanium (and titanium alloy Ti-6Al-4V) coupons are used to develop an intermediate bond coat in order to demonstrate the possibility of establishing a chemical bond between the titanium substrate and the HA coating.

Heimann (1992)^[5] selected dicalcium silicate (Ca_2SiO_4 or " C_2S ") to develop a bond coat between the hydroxylapatite and the titanium substrate, for several reasons. First, it is possible to produce C_2S as a sprayable powder and to apply it to a substrate, as demonstrated by Uchikawa et al. (1988)^[6]. This group investigated the possibility of using various compounds of the CaO-SiO_2 system as coatings for industrial applications. They have produced thermally sprayable powders by the spray drying method. Among others, they evaluated the $2 \text{ CaO} \cdot \text{SiO}_2$ (Ca_2SiO_4 or C_2S) compound, which they produced with a $10 \mu\text{m} < \text{particle size} < 80 \mu\text{m}$. The $\gamma\text{-C}_2\text{S}$, observed by X-ray after spraying, was identified as $\alpha\text{-C}_2\text{S}$, $\alpha'\text{-C}_2\text{S}$, and $\beta\text{-C}_2\text{S}$. The resulting coating had a porosity of 10% and a bond strength of 9.6 MPa. Their work demonstrated that C_2S was usable as a plasma-sprayed coating for applications such as thermal barriers. Further investigation of C_2S by Ogawa et al. (1991)^[7] identified the composite $2 \text{ CaO} \cdot \text{SiO}_2\text{-CaO} \cdot \text{ZrO}_2$ ($\text{C}_2\text{S-CZ}$) in the range of 10 to 30 weight % CZ. (with NiCrAlY intermediate coating) as an alternate for a thermal barrier. They further demonstrated that this material (C_2S) can be applied by the plasma spraying process.

Second, when C_2S is sprayed onto a titanium substrate, it can react with the titanium oxide (TiO_2), which is on the titanium surface, to form a titanite (sphene) intermediate $\text{CaTi}[\text{O}(\text{SiO}_4)]$ thin layer. In addition, when the hydroxylapatite (HA) is sprayed on top of the Ca_2SiO_4 it can in turn react to form a silico-carnotite $\text{Ca}_5[(\text{PO}_4)_2(\text{SiO}_4)]$ at the interface, with some hydroxylapatite or $\text{Ca}_{10}(\text{PO}_4)_6(\text{OH})_2$ remaining to form the external top coat.

The schematic, shown in Figure 1.1, depicts the chemical bonding for attaching HA to the metallic implant while keeping the biocompatible HA in intimate contact with bone. Therefore, it is the aim of this research to produce and characterize the layered system obtained by spraying first a Ca_2SiO_4 bond coat on a titanium substrate, then a final $\text{Ca}_{10}(\text{PO}_4)_6(\text{OH})_2$ top coat. This work will include development of spraying parameters for the two types of powders.

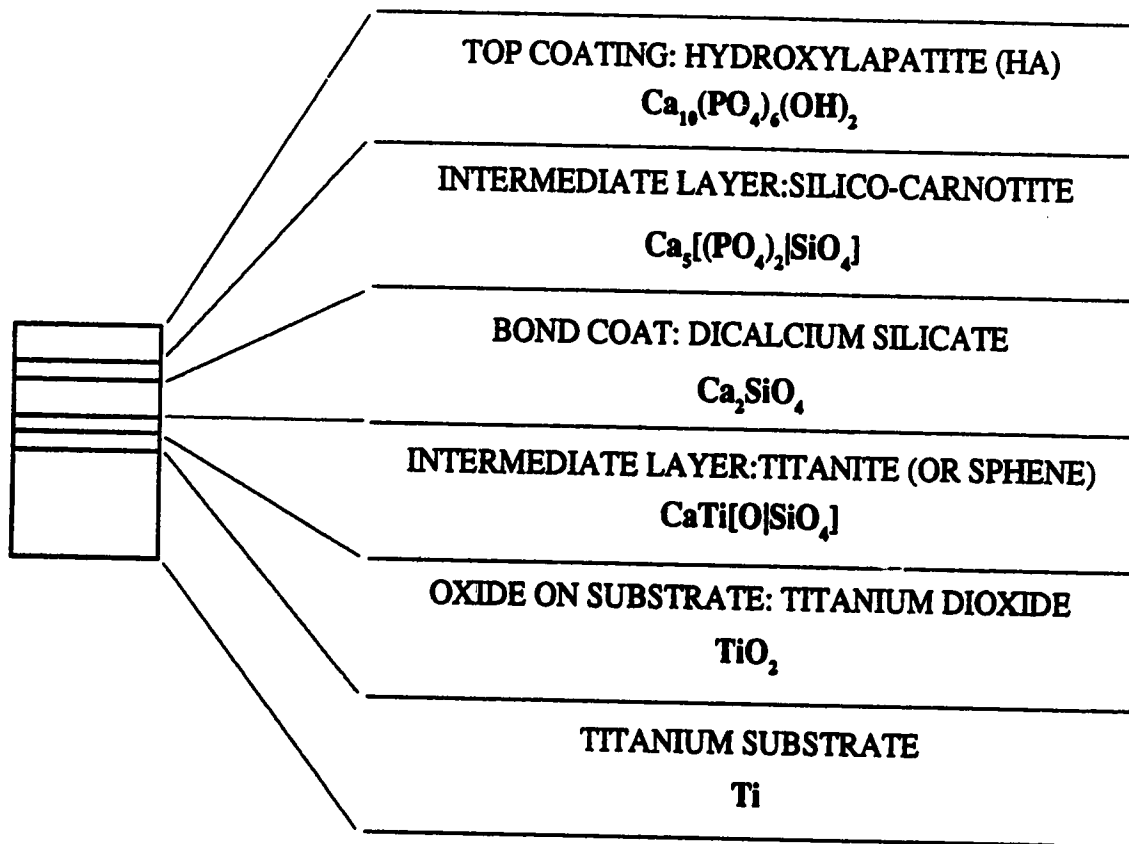


Figure 1.1 Schematic layering of the coating on the metallic substrate.

2. INTRODUCTION AND LITERATURE REVIEW

2.1 Need for Implants

The need for artificial or implantable materials in the human body is increasing every year as the general population expects to live retirement years in better physical condition, both in terms of general activities and in terms of ease of locomotion. Orthopaedics was the first clinical discipline to utilize implantable devices with the introduction of fracture plates at the beginning of the century. Now prostheses are currently used in orthopaedics, in the cardiovascular system [8, 9](valves, pace makers, vascular grafts), in intra-ocular devices, in hearing aids, in pumps which release periodically a dose of insulin^[10] etc. Conditions which require such artificial materials or devices vary widely from war wounds, accidents, illnesses, to congenital deformations or atrophies. In addition to these conditions, the average age of the population in the developed world has increased greatly during the last 30 years and, reflecting this phenomenon, an important proportion of the surgery work now occurring in hospitals is related to joint replacement.

Joint surgery underlines a frequent problem in the older population, namely, wear of the joints. With life span of patients reaching the mid 70's to mid 80's, there is growing acceptance by surgeons and the medical profession in general that a useful and comfortable lifestyle can be maintained when deteriorated body parts are replaced. As an example, about one third of the population in the USA above 35 years old (over 40 million people) has lost some or all of their teeth. Of these, 42% are older than 65 years of age and 4% of the 35 to 64 years of age are totally edentulous^[37]. Thus, many individuals could in the future benefit from dental implant therapy. Development of new materials and devices is motivated by the possibility of improving the quality of life while reducing the overall cost of health care^[12,13].

With a world-wide market of more than \$2.3 billion in 1983 (\$1.3 billion in cardiovascular prostheses and \$900 million in orthopaedics representing the two major areas) or close to 10% of all annual expenditures on medical equipment and material (excluding eyeglasses and hearing aids) prostheses have become a significant economic sector dominated by the United States, where the market has experienced a fairly strong growth^[14]. Rieger (1989)^[15] reported a study by Hench (1986) which gives an estimate of the market volume for biomaterials in terms of applications, Table 2.1. Numbers are given for 1986, as well as an estimate for 1996.

Table 2.1 Estimate of market volume of biomaterials in the U.S.^[15].

[15] W.Rieger, "Medical Applications of Ceramics", in "High-Tech Ceramics. Viewpoints and Perspectives", Zurich, Switzerland, 10-11 Nov. 1988. Publ. Academic Press Limited, London, p. 191-228, 1989.

REMOVED DUE TO COPYRIGHT RESTRICTIONS

2.2 Biomaterials Definition

The term "biomaterial" is a generic term referring to all materials designed for use under biological constraints. In the mid 70's^[16], a biomaterial was defined as a "systemically, pharmacologically inert substance designed for implantation within or incorporated with a living system". Now a biomaterial is expected to react with living tissue and to functionally incorporate with the living body. It may be constructed from any material including composites.

These biomaterials are of several types^[17, 92]: they may have the same structure as bone, a calcium phosphate implant similar to the calcium phosphate of bone, and thus prone to gradual colonization by bone cells^[18, 19]; they may be the biodegradable materials used as dressing which encourage cell growth before disappearing completely once new growth has been completed (such as lactic and glycolic acid copolymers which are used for deep biodegradable sutures)^[20, 21, 22]; or they may simply be inert materials with exceptional properties not likely to cause side-effects^[22]. The term "biomaterial" does not refer to a

living material, or at least, not at this time. The latest developments^[23] seem to indicate a need for more compatible interfaces: the key to successfully implanted devices resides in the organic / inorganic interface aspect of the materials.

A more extended definition of biomaterials includes the following (1987, as reported by Rieger, 1989^[15]):

- 1) Materials for long term implantation in human tissue, such as arterial and dental prostheses, prostheses of organs (heart, blood vessels), and artificial joints (hip, knee);
- 2) Products for prolonged contacts with vessels and tissue or bone;
- 3) Products for short-term contact with tissue or bone such as probes or instruments for tests and inspections;
- 4) Materials for obtaining and storing blood and blood plasmas;
- 5) Products used as instruments and tools during surgery.

2.3 Performance Criteria for Biomaterials

The choice of materials is governed by a variety of criteria^[11, 14, 24, 25, 93, 94]. One such criterion is aesthetic, closely related to social acceptability. The aesthetics of a prosthesis is secondary in comparison to performance but it plays an important role as a factor of social acceptance. For example, artificial skin for a missing member or for a third-degree burn victim must resemble natural skin to provide "social" comfort, both for the patient and for those around him. Other criteria are the availability of the materials, and the cost of the finished products.

Another set of criteria concerns biocompatibility of the material. Biocompatibility is concerned with the interaction between materials and the tissues of the bodies; it means the new material will not harm the host organism, i.e. it is non-toxic and it will not be rejected. In addition to this chemical compatibility, an implant must exhibit a strong bond with the

surrounding tissue, for fixation purpose, in applications where loading of the device is a factor^[24]. Comfort is also a part of biocompatibility. Nowadays, external prostheses are fabricated with much lighter materials (such as aluminum, celluloid fiber, Duralumin, lightweight wood and plastics) than were the first artificial limbs.

A third important criterion for choice is biofunctionality, or the mechanical adequacy for the purpose, i.e. the mechanical and physical properties that enable the implanted device to perform its function. In addition, biologic stability or the resistance of the materials to corrosion, wear, and mechanical constraints, is also important. For an internal prosthesis, the fatigue resistance of a material is a major consideration. For example, a heart beats 40 million times a year. Therefore, materials used in cardio-vascular devices must display good flexibility, hemocompatibility (blood compatibility), and biocompatibility in addition to wear resistance. Several materials are used, such as dacron, teflon, and urethane polymers, that offer good elasticity and elastomeric-like possibilities of durability as well as strong resistance to breakage. In general, implants alterations resulting from a reaction with the surrounding tissue or medium, such as corrosion, solubility or resorption should be kept as small as possible^[11].

Biological testing of implant materials is normally a long procedure, comparing the results to those obtained for known materials. The reference materials are stainless steel, cobalt-chromium-molybdenum alloys, UHMWPE, acrylate-based bone cements and alumina ceramics.

Traditionally, metals have been used inside and around the body. Examples include 316L stainless steel, various CoCrMo alloys such as Vitallium, pure titanium or titanium alloy such as Ti-6Al-4V^[26]. However, a limited number of metals or alloys qualify as implantable materials because the human body is highly corrosive for metals^[1]. In some cases, metal alloys can cause inflammation in the implanted area. In addition, metal ions leaving the implant and entering the bloodstream cause serious complications. Bone is a living tissue continuously changing, and responding to tensile or compressive stresses. Therefore, the strongest implant material is not necessarily the best: the use of stiff metals generally prevents bone remineralization and can cause bone resorption. However, the modulus of elasticity of titanium alloy (Ti-6Al-4V) is approximately one-half of the more traditional implant alloys (CoCrMo and stainless steels). The titanium alloy has a good fatigue strength, a good fabricability, and is readily available. Consequently, titanium is

often used for the stem component of the total hip replacement prostheses. Table 2.2 shows the properties of bone and of some biomaterials.

Table 2.2 Mechanical properties of biomaterials and bone^[15].

- [15] W.Rieger, "Medical Applications of Ceramics", in "High-Tech Ceramics. Viewpoints and Perspectives", Zurich, Switzerland, 10-11 Nov. 1988. Publ. Academic Press Limited, London, p. 191-228, 1989.

REMOVED DUE TO COPYRIGHT RESTRICTIONS

Polymer based devices have a wide range of applications within the body^[17, 20, 21]. One example is polymethylmethacrylate (PMMA) which serves as a sealant for hip prostheses but this product sometimes causes inflammation. Therefore, alternate methods of attachment have to be developed.

In the musculoskeletal system, osseous (i.e. bone) components have been traditionally repaired with the living autogenous bone, which is bone harvested from the skeletal structure of the same individual^[27]. The grafting of autogenous bone is normally successful, but it requires a second surgical procedure and the patient may not be strong enough to sustain this additional stress, which may cause local morbidity at the site of extraction^[28]. Another limitation arises if the patient himself does not have a proper supply of healthy bone. Allogeneous bone, which is bone originating from someone else, or banked bone, eliminates the need for the second surgical procedure. However, banked bone is not always available^[29] and its clinical performance is not satisfactory. New bone formation occurs at a slower rate and its cost can be high. In addition, this type of graft exhibits a higher resorption rate, a larger immunogenic response and there have been concerns regarding the transmission of live virus through its use^[28]. The solution appears to be the use of a suitable artificial graft material.

Ceramics appear to be a good choice as a material for joints. One likely candidate for the ball component of a hip joint is alumina, with its excellent biocompatibility and wear

resistance, good mechanical properties and low friction coefficient. Ceramic coatings for the metallic stem component of the hip joint will provide improved attachment. The tendency is now to combine the advantages of several materials by fabricating composite materials with more complex characteristics. Another area of exploration is centered on developing a bioactive interface by addition, for example, of heparin directly to the surface of prostheses made of polymer^[29].

2.4 Ceramics as Implant Materials

Numerous applications for advanced ceramic materials have emerged in the field of medicine during the past two decades. As biomaterials, ceramics can be utilized in load-bearing and non-load-bearing functions, in resorbable or non-resorbable situations, as structural parts or coatings on surgical implants made of other materials. Load-bearing applications, using non-resorbable materials include knee and hip implants, dental implants, bone plates, artificial heart valves, artificial tendons and the coatings on metal prostheses. Non-load-bearing applications are temporary space fillers which can be penetrated and resorbed by the reconstructed natural tissue, such as reconstruction of maxillo-facial defects^[15].

The requirements for the bioceramic materials vary with the application. The materials are grouped into three large categories, according to their chemical reactivity with the environment: The bio-inert or nearly inert materials, the bioactive or surface-reactive materials, and the resorbable materials. In addition, composite materials are formed from the materials above or with polymers and metals.

Figure 2.1 shows a comparison of the relative chemical reactivity of the material groups as a function of time after implantation. The rate of change of pH and ion solubility serve as indicators of the reactivity because of their good correlation with in vivo tissue reactions. This visualization of materials reactivity was developed by Hench^[30].

- [15] W.Rieger, "Medical Applications of Ceramics", in "High-Tech Ceramics. Viewpoints and Perspectives", Zurich, Switzerland, 10-11 Nov. 1988. Publ. Academic Press Limited, London, p. 191-223, 1989.

REMOVED DUE TO COPYRIGHT RESTRICTIONS

Figure 2.1 Reactivity versus time after implantation^[15].

In this figure, totally resorbable compositions, such as $\text{Ca}_3(\text{PO}_4)_2$ (calcium phosphate)(A), show rapid ion dissolution and pH change. Nearly inert compositions, e.g. alumina (D), show little chemical activity even after thousands of hours of exposure to extremes of physiological pH, resulting in no interfacial bonds with living tissues. Surface-reactive bioglasses (B) and bioglass-ceramics (C) exhibit an intermediary behavior.

Examples of bio-inert materials are oxide ceramics such as alumina and zirconia-TZP (tetragonal zirconia polycrystals), and biocarbons. Hydroxylapatite and bioglasses are examples of bioactive materials, and calcium phosphates are examples of resorbable materials. Table 2.3 gives examples of the development of some of those materials over the years.

Table 2.3 Development of bioceramic implants^[15].

- [15] W.Rieger, "Medical Applications of Ceramics", in "High-Tech Ceramics. Viewpoints and Perspectives", Zurich, Switzerland, 10-11 Nov. 1988. Publ. Academic Press Limited, London, p. 191-228, 1989.

REMOVED DUE TO COPYRIGHT RESTRICTIONS

2.4.1 Nearly Inert Materials

The term "bio-inert", as stated by Boretos, 1987^[31], refers to materials that are essentially stable with little or no tissue reactivity when implanted within the human body. Any minor degradation products that could occur are readily assimilated by the body and do not produce adverse tissue responses.

2.4.1.1 Alumina

Alumina (Al_2O_3) is the most widely used bio-inert ceramic. This material has two advantages over other biomaterials such as metals and polymers: low wear rates and low concentration of inert wear particles in the surrounding tissue. Alumina is used in load-bearing hip prostheses as ball and cup components, shown in Figure 2.2, and in dental implants, because of its combination of excellent corrosion resistance, good biocompatibility, high wear resistance, and reasonable strength.

[90]L.M. Sheppard, "Cure it With Ceramics". Advanced Materials and Process, No. 5, p.26-31, 1986.

REMOVED DUE TO COPYRIGHT RESTRICTIONS

Figure 2.2 Two models of total hip replacement prostheses^[90].

Although some dental implants are a single-crystal sapphire (α -Al₂O₃ or corundum), most alumina devices have a fine-grained polycrystalline structure. The properties of medical-grade alumina are summarized by Rieger, 1989^[15] as follows: very fine grain size, no glassy phase in the grain boundary, theoretical density, and a very low content of ir purities (<0.05%). The high purity and high density are required for the high reliability and life expectancy of prostheses. Strength, fatigue resistance, and fracture toughness of polycrystalline α -alumina depend on the grain size and on the amount of sintering aid.

The wear and friction behavior of artificial joint components, which are of importance in long-term implantation, have been determined. Coefficients of friction are provided in Table 2.4 for various combinations of hip articulations, including ceramic-UHMWPE (UHMWPE = ultra-high-molecular-weight-polyethylene). The favorable wear characteristics of alumina can be attributed to the formation of adsorbed water layers on the surface.

Table 2.4 Coefficients of friction for a variety of materials^[31].

[31]J.W.Boretos, "Bioceramics Come of Age". Chemtech, No. 4, p.224-231, 1987.

REMOVED DUE TO COPYRIGHT RESTRICTIONS

The existence of wear and wear debris in implants systems is of special concern for systems implanted in younger patients, who will use the prostheses for longer periods. Clinical observations show that ceramic-ceramic total hip replacements (THRs) provide the least wear and debris, giving a long life expectancy of the prostheses.

In addition to satisfying the technical requirements such as strength, wear and friction behavior, and corrosion resistance, the material must satisfy the biological requirements such as body tolerance (biocompatibility) and biological stability. The biocompatibility of surgical grade alumina has been ensured by means of animal tests followed by clinical experience over a long period of time (in Germany, since 1973, also in France and in Japan, as reported by Rieger (1989)^[15]). When fabricated with a high-density and small grain size, alumina produces less wear debris in comparison to other materials.

Single-crystal alumina and single-crystal alumina with a polycrystalline crown are both used successfully for blade and screw type dental implants. More than 60,000 successful dental implants have been performed from 1977 to 1987. Alumina is highly successful for all teeth, including molars and incisors. Tooth implants also serve as anchors for bridges and dentures. Shapes of ceramic tooth implants differ depending on location and function within the mouth. Figure 2.3 shows a variety of dental implants available.

[31]J.W.Boretos, "Bioceramics Come of Age". Chemtech, No. 4, p.224-231, 1987.

REMOVED DUE TO COPYRIGHT RESTRICTIONS

Figure 2.3 Variety of available dental implants^[31].

2.4.1.2 Zirconia

Zirconia possesses a higher bending strength, higher fracture toughness and lower Young's modulus than alumina and, therefore, can be considered a good candidate to replace alumina in load bearing implants.

The most advanced zirconia material today is TZP (polycrystalline tetragonal zirconia stabilized by MgO (magnesia) or Y₂O₃ (yttria)). TZP is characterized by an extremely small grain size of less than 0.5 μm after sintering. It is a candidate material for the production of femoral heads in total hip replacements. The use of TZP allows the reduction of the diameter of the femoral head, improving the degree of freedom for three-dimensional mobility of the implant. However, wear of TZP in ceramic-ceramic articulating surfaces seems unacceptably high, due to the lower hardness of zirconia (as compared to alumina). Nevertheless, the mechanical advantages of TZP could be used by matching a ceramic TZP ball with an UHMWPE socket.

Unlike the 20 years of alumina research, no long term clinical studies of zirconia products are available. A short 14 weeks study with animals, rats implanted with yttria stabilized TZP in cylindrical shapes in the lower back, indicates that no difference occurs in the tissue response while comparing surgical-grade alumina and TZP.

2.4.1.3 Carbons

The carbons are another dense inert ceramic implant materials. They are used in various forms as bio-inert implant materials. Three classes of carbon materials are used, corresponding to the method of production:

a) Pyrolytic carbon, or low-temperature isotropic carbon (LTI), is produced in a fluidized bed by the pyrolysis of methane at temperatures above 1000 °C. Prosthetic heart valves, percutaneous access devices for dialysis, and dental implants are partly made of LTI.

b) Vapor deposited carbon, or ultra-low-temperature isotropic carbon (ULTI), is produced by vacuum deposition from gaseous precursors containing carbon to form an impermeable isotropic deposit. It serves as coatings in heart pacemakers and on sealing rings for heart valves. The thickness of this coating is usually less than 1 μm .

c) Glassy carbon, or vitreous carbon, has been evaluated for dental implant applications. It is made by controlled heating of carbonaceous precursors and subsequent elimination of volatile constituents. Vitreous carbon gets its name from its glossy black appearance and its conchoidal fracture pattern. It is not a glass, however, but rather a polycrystalline solid with a very small grain size.

The excellent biocompatibility of carbon materials is attributed to the absence of molecules or ions having metallic character or producing adverse effects (no blood clotting, no break up of red blood cells). Carbons are stable and non-reactive with respect to tissue. In addition, wear resistance is very high, providing smooth and abrasion-resistant surfaces. As a result, heart valves made from LTI carbon can withstand the rigors of millions of openings and closings. Thousands of devices have been made since their introduction some 15 years ago.

2.4.1.4 Other Inert Materials

Spinel (MgAl_2O_4) together with corundum ($\alpha\text{-Al}_2\text{O}_3$) is used to produce ceramic dental crowns that are strong enough for utilization as posterior as well as anterior teeth. This 70% alumina crown provides a more precise fit than previously available crowns because it undergoes minimal shrinkage during firing.

Some electrical and electrode insulating materials are made of tantalum covered by tantalum pentoxide. These electrodes show promise for stimulation of nerves deep within tissues of the body.

2.4.2 Resorbable Materials

The second large bioceramic category is resorbable materials. These materials are designed to degrade gradually over a period of time and to be replaced by the natural host tissue. They are temporary space fillers or scaffolds for new tissue to develop. They have been used to treat defects of the face and jaws, to fill up periodontal pockets, and to serve as artificial tendons and composite bone plates. Natural tissue reconstruction occurs

simultaneously with resorption. During the remodeling process the load-bearing capacity of the prosthesis is weakened and therefore, temporary fixation or immobilization of the repair is required. In addition, large quantities of materials may be replaced and it is necessary that the biomaterials consist only of metabolically acceptable substances.

As the ceramic dissolves, it becomes more and more porous, allowing the ingrowth of more supporting tissue. The advantage of such a prosthesis is that it is replaced by normal functional bone, thus eliminating any long-term functional or biocompatibility problems.

Different properties are required according to applications. Fast-degrading materials are needed when tissue is to be replaced, such as for periodontal defects and open spaces in bone due to surgical procedures. Slow-degrading ceramics are important when tissue is to be augmented, for example, filling of open spaces between the spine, or reconstructing the bone ridge after extraction of numerous teeth.

2.4.2.1 Tricalcium Phosphate (TCP)

The most widely used resorbable ceramics are based on tricalcium phosphate or TCP ($\text{Ca}_3(\text{PO}_4)_2$) also called β -whitlockite. TCP has a close chemical resemblance to bone material, hydroxylapatite (HA): $\text{Ca}_{10}(\text{PO}_4)_6(\text{OH})_2$. TCP is slowly degradable in a reaction with aqueous media inside the human body, and forms a substance crystallographically identical to HA. This product, used to fill bone gaps, is resorbed during the healing and restoration process by the bone tissue: The bone tissue grows into the pore structure of the phosphate material which is gradually dissolved. At the same time, mineralized bone is formed. Thus the main application for TCP is bone regeneration, in non-load-bearing conditions. Owing to the low-strength characteristics of the material, non-load-bearing conditions have to be ensured over a relatively long period up to 3 months. The applicability is therefore restricted to the non-stressed regions of the skeleton.

The in vivo behavior of calcium phosphates depends not only on their chemical composition, but also on their porosity and surface properties such as roughness and charge, as well as their texture. Traces of impurities, especially Mg^{2+} and F^- ions, have a strong influence, affecting the composition and solubility of the HA formed.

2.4.2.2 Other Resorbable Ceramics

Examples of other resorbable bioceramics are CaSO_4 (plaster of Paris), which was the first bioceramic ever tested, and CaCO_3 , in the form of coral skeletal (replaniform) replicas, which display good resorption characteristics. Plaster of Paris is the most rapidly resorbed implant material in dogs. It is a completely safe implant material for filling osseous defects and does not generate foreign body giant-cell activity. However, variable resorption rates and poor mechanical properties have prevented plaster implants from being used widely.

Calcium aluminates ($\text{CaO} \cdot \text{Al}_2\text{O}_3$) have also been investigated as resorbable ceramics for orthopaedics applications. The advantage of this material as a resorbable implant is that the various phases hydrolyze at different rates, thus providing a means of controlling the resorption rate as well as the tissue response. These characteristics permit one to engineer an optimal resorption rate. A disadvantage is that Al ions will be released in large concentrations into the body with unknown results.

2.4.3 Surface Reactive Materials

The third large category of bioceramics is surface reactive materials. The concept of bioactive or surface-reactive materials is intermediate between bio-inert and resorbable materials. A bioactive material, after Hench and Wilson, 1986^[19],

"is one that elicits a specific biological response at the interface of the material which results in the formation of a bond between the tissues and the material".

Such materials include bioactive glasses such as Bioglass[®], bioactive glass-ceramics such as Ceravital[®], or dense A/W (apatite-wollastonite) glass-ceramic, dense hydroxylapatite such as Durapatite[®] or Calcitite[®] or bioactive composites such as Palavital[®] or stainless steel fiber reinforced Bioglass[®]^[32].

The successful approach is to use a composition that forms a chemical bond at the interface between the implant and the host tissue. The time dependence of bonding, the strength of bond, the mechanism of bonding, and the thickness of the bonding zone differ for the various materials. Therefore, relatively small changes in the composition of a biomaterial

will determine whether it is bio-inert, resorbable or bioactive. An example of this composition is given in Figure 2.4, for the bioglass group in which, for a constant amount of 6% phosphate (P_2O_5), the variation in silica (SiO_2), sodium oxide (Na_2O), and calcia (CaO) gives different products.

[15] W.Rieger, "Medical Applications of Ceramics", in "High-Tech Ceramics. Viewpoints and Perspectives", Zurich, Switzerland, 10-11 Nov. 1988. Publ. Academic Press Limited, London, p. 191-228, 1989.

REMOVED DUE TO COPYRIGHT RESTRICTIONS

Figure 2.4 Composition of inert, bioactive, and resorbable materials^[15].

The composition in the middle of the diagram (region A) forms a bond with bone and is therefore called the Bioglass® bone bonding boundary. In this region, apatite is formed more rapidly for compositions located in the cross-hatched area of the diagram. Silicate glasses within region B, such as window, bottle glass, or microscope slides, behave as nearly inert materials and lead to the formation of a fibrous capsule at the implant tissue interface. Glasses within region C, the CaO poor region, are resorbable and disappear within 10 to 30 days of implantation. Glasses within region D, the silica poor region, are biologically inactive.

The surface activity can be controlled by the composition of the implant, as described above. Substitution of fluoride ions for oxygen ions in the glass network will decrease the surface reactivity of the material while B_2O_5 (5-15%) results in a much more reactive glass. Consequently, it is possible to achieve a spectrum of physiological responses to the surface-reactive implants, and an order-of-magnitude difference in reactivity is possible with small adjustments in the formulation. It may be possible to design an implant surface

from these materials to produce specific in vivo tissue responses controlled by the local metabolic activity.

The mechanism of bone bonding to bioactive glasses appears to be initiated by the formation of a silicon-rich gel on the implant surface to a thickness of up to 200 μm followed by a nucleation of hydroxylapatite (HA) crystals. Li, 1992^[33] demonstrated that apatite formation can be induced by silica gel in a simulated body fluid. He compared the apatite formation at the surface of a pure silica gel, pure silica glass, and a pure quartz single-crystal, when immersed in a simulated body fluid. Only silica gel among these three silica materials induced apatite formation in the body environment. Chemically, the main difference between these three materials is the density of silanol (SiOH) which is more important on the surface of the silica gel. This showed the importance of a preliminary apatite layer formation for further bone bonding.

The strength of the bonding zone between bioactive implants and hard tissues is a function of the composition and the thickness of the bonding layer. Since the thickness of the bonding layer changes with time, the strength also changes with time. The bonding zone of the bioactive glasses is composed of the hydrated silica layer and the apatite layer. Consequently, the strength is also a function of the extent of hydration of the silica layer.

Hench and collaborators^[19, 34, 35, 36, 102] and others^[103] have done extensive work on Bioglass® and related compositions, as surface-reactive materials.

2.4.3.1 Hydroxylapatite (HA)

Another important calcium phosphate-based surface-reactive material is hydroxylapatite (HA) or $\text{Ca}_{10}(\text{PO}_4)_6(\text{OH})_2$. Due to its chemical formulation, hydroxylapatite, the main mineral constituent of bone, is biocompatible and does not induce foreign body reaction. On the contrary, it is integrated into normal bone. It is used as implants in various forms: as a solid dense body with little porosity, as granular particles, as a porous structure or as a coating on metallic implants. Coatings of HA on metal implants (such as titanium alloy Ti-6Al-4V) are utilized to facilitate body acceptance of implants and attachment to osseous tissue by growth of bone. Coatings are applied mostly by the plasma spraying technique, to a thickness of approximately 50 μm .

The size and volume of pores in HA determine its biodegradability after implantation: if the density of the material is low, a high degree of degradation occurs whereas with reduced microporosity, degradation slows down. Granular particles of size 20-60 μm have been used in alveolar ridge augmentation by injection into tooth sockets. A surface roughness (or macroporosity, as Klein et al.(1988) call it) of 150 to 250 μm allows bony ingrowth into the macropores and along the surface of the materials. Connective tissue eventually fills the pores.

A variety of shapes and sizes of HA blocks and granules have been used to prevent resorption of alveolar bone after premature loss of teeth. Anatomically shaped implants maintain the stability of the alveolar contour. After a few weeks, prosthetic appliances such as fixed bridge work are inserted. Sintered HA powder can be formed into various shapes with macroporous structure for use as bone replacement and for bony ingrowth. However, load-bearing applications seem to be less successful except for tooth implants or in middle-ear channel wall prostheses. Where there is no need for mechanical strength, as in the middle ear, bony ingrowth into porous nonresorbable HA can provide a good functioning structure with integration of implant and host bone.

HA has also been used in combination with alumina to coat a titanium dental implant (tooth root). The structure provided a base for the subsequent attachment of a crown. HA coatings seem to stimulate the direct chemical bonding of tissue to prostheses and of bone ingrowth. In the next section, further details will be provided on the calcium phosphate-based materials among which are HA and TCP.

2.4.4 Calcium Phosphate-Based Materials (HA and TCP)

Calcium phosphates exist under several forms with a varying Ca/P ratio, among which is HA with a Ca/P ratio of 1.67; human bone mineral (non-stoichiometric HA) is calcium deficient and can have a Ca/P ratio as low as 1.5. Other forms include brushite, $\text{CaHPO}_4 \cdot 2\text{H}_2\text{O}$, which is more acidic than HA, α -TCP, β -tricalcium phosphate (TCP), $\text{Ca}_3(\text{PO}_4)_2$ or $\text{Ca}_3\text{P}_2\text{O}_8$ which has a Ca/P ratio of 1.5, and tetracalcium phosphate, $\text{Ca}_4\text{P}_2\text{O}_9$ or $\text{Ca}_4(\text{PO}_4)_2\text{O}$, which is more basic than HA, with a Ca/P ratio of 2.0. HA is generally nonbioresorbable and therefore suitable for long term restorative and preservative

clinical procedures. Tricalcium phosphate (TCP) is chemically similar to HA but is not a natural component of bone mineral. It is partially bioresorbable which is desirable for repair of nonpathologic sites where resorption of the implant material with concurrent replacement by bone is expected.

Hydroxylapatite or $\text{Ca}_{10}(\text{PO}_4)_6(\text{OH})_2$, one form of the calcium phosphate-based materials, is the main mineral constituent of bone and teeth. The adult body has 2 kilograms of HA^[16] which makes up 60 to 70% of the bone material and 98% of the dental enamel^[38]. Bone in the human body, however, is a non-stoichiometric form modified by monovalent and divalent ions such as Na^+ , K^+ , Mg^{2+} , CO_3^{2-} , and other ions^[24]. The human skeleton is composed^[39] of two phases: one continuous phase of collagen and other proteins, usually called the bone matrix, and a discontinuous phase of very small crystals with an approximate structure of $\text{Ca}_{10}(\text{PO}_4)_6(\text{OH})_2$. These HA crystals are embedded in the matrix.

Apatite is a general term^[16] for crystalline minerals with a composition of $\text{M}_{10}(\text{ZO}_4)_6\text{X}_2$ where

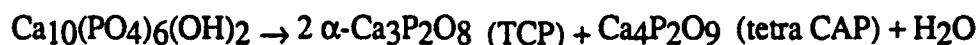
$\text{M} = \text{Ca, Sr, Ba, Cd, Pb, etc.}$

$\text{Z} = \text{P, V, As, S, Si, Ge, etc.}$

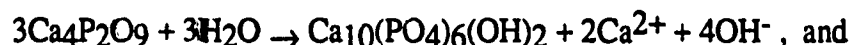
$\text{X} = \text{F, Cl, OH, O, Br, Vacancy, etc.}$

In the case of hydroxylapatite, "M" stands for "Ca", "Z" stands for "P", and "X" stands for "OH".

The normal thermal decomposition of HA is as follows, according to Newesly et al.(1980)^[124]:



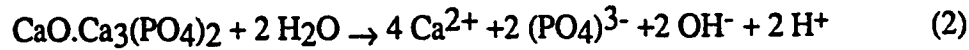
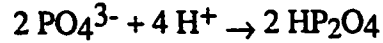
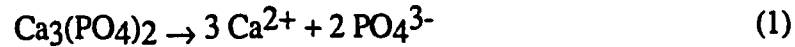
The authors state that in aqueous surroundings such as body fluids, HA is the only stable phase and results of hydrolysis of the two other forms (TCP and Tetra CAP) may be:



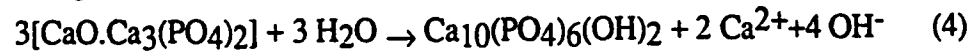
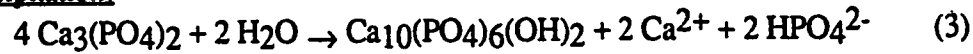
TCP in presence of water is unstable and transforms to HA^[40]. When TCP is sintered in water vapor containing atmosphere at temperatures up to 1200-1300 °C, it transforms to HA.

Klein et al.(1990)^[86] and Klein et al.(1991)^[25] summarize the chemical reactions occurring *in vivo* as being composed of a dissolution phase and a reprecipitation phase, as follows:

Dissolution:



Reprecipitation:



In the remaining part of this work, hydroxylapatite will be abbreviated as HA and tricalcium phosphate as TCP. Albee, in 1920, as reported by Denissen et al.(1980)^[40] was the first to use calcium phosphate-based material inside the body. He used a slurry of TCP as a stimulus to osteogenesis.

The Government Industrial Research Institute of Nagoya, Japan, studied extensively the calcium phosphate-based materials. Much of the preliminary work consisted in developing preparation methods for the various materials followed by their basic characterization. The objective of this group is to use sintered β -TCP within the body with the possibility of this material being replaced by intrinsic bone, after implantation. This is expected because of the high rates of dissolution and absorption of TCP in the living body. However, depending on the location of implantation, the material requires initial high strength, not seen in HA or TCP materials when they are used alone. Therefore, the basis of their work is to find materials, either as mixtures, compounds, or coatings, etc., to associate with TCP for later implantation.

Toriyama et al.(1987 a)^[46] sintered mixtures of various amounts of HA and TCP, and measured their bending strength. The flexural strength was the highest for the powder containing 17 mol% of β -TCP sintered at 1300 °C, at a value of 187.3 MPa. However, this material has a higher solubility than HA and β -TCP, limiting its usage within the body.

Sintering characteristics of β -TCP powders synthesized by 3 methods were studied. Mechanochemically synthesized β -TCP was obtained as a dense sintered body at the low

sintering temperature of 1050 °C. This temperature is 50 °C lower than that of the wet-synthesis method or 100 °C lower than that of the dry-synthesis method. However, formation of α -TCP during the sintering process decreased the bending strength and chemical corrosion resistance of the sintered body^[47]. Further work by the same group^[48] consisted in improving the strength by adding MgO. The role of MgO was to replace calcium ions and to inhibit the formation of α -phase during the sintering step. In addition to these effects, this contracted the crystal lattice and the bending strength increased to 197.1 MPa, which corresponds to the bending strength of dense human bone. Optimum amount of MgO was 0.18 wt%, at a sintering temperature of 1100 °C. Toriyama et al.(1988)^[49] investigated further additions to β -TCP, such as Al_2O_3 and SiO_2 , in order to develop higher strength materials. These additions, when present together, also prevented the phase transformation of β -TCP into α -TCP. The composite ceramic of β -TCP-2 wt% Al_2O_3 -6 wt% SiO_2 attained a bending strength of 270.7 MPa at a sintering temperature of 1280 °C. The objective was also to limit the total quantity of additives to an arbitrary 10 wt% TCP in order, hopefully, to retain the compatibility with living tissue, which is the main purpose of producing this category of materials.

Toriyama et al.(1989)^[50] further pursued their investigation of β -TCP to develop a method of preparation for β -TCP raw material powder suitable for further sintering. Calcination at 720 °C for about 12 hours was determined to be the optimum condition to obtain fine powder with little agglomeration.

The materials previously discussed, β -TCP, β -TCP with MgO additives, and β -TCP with Al_2O_3 and SiO_2 additives, were evaluated for biocompatibility. The MgO or Al_2O_3 - SiO_2 additives used to increase the strength of the sintered ceramics did not decrease the biocompatibility of β -TCP^[51] as indicated by in vitro cell growth studies.

The high strength β -TCP's materials discussed above, are sufficiently strong for use as a substitute for dental roots and for bones where they are exposed to relatively simple forces. However, they are not appropriate for articulations or other areas subjected to high fatigue and impact loading. For such applications, various composites were investigated.

A β -TCP- Al_2O_3 - SiO_2 composition was used as a coating on a higher strength substrate material. It was applied as a slurry over a sintered alumina ceramic substrate^[52]. Optimum adhesion of the coating was obtained by first firing at 1300 °C the alumina substrate coated

with a slurry containing 20% of β -TCP (25% Al_2O_3 and 75% SiO_2) to form anorthite ($\text{CaAl}_2\text{Si}_2\text{O}_8$). Second, this composite was coated with a slurry containing 80% β -TCP (5% Al_2O_3 and 15% SiO_2) and fired at 1200 °C to 1300 °C.

Kawamoto et al.(1991)^[53] of the same research group, used a similar process to coat a yttria-partially stabilized zirconia (PSZ) with a pure β -TCP. An intermediate bond coat of magnesium metaphosphate was required to achieve the bonding of the β -TCP to the substrate. However, destabilization of the Y-PSZ was observed in the reaction layer with the apparition of YPO_4 and with the transformation of tetragonal zirconia to monoclinic.

To preserve the PSZ structure^[54], a calcium metaphosphate was used as an intermediary bond coat. On top of the bond coat a mixed slurry of calcium metaphosphate and tetracalcium phosphate was reacted by heating at 1200 °C for 40 minutes. This top layer adhered well to the substrate and was identified as β -TCP. Further work^[57] consisted in heating the mixed slurry in the presence of water vapor. HA was obtained, in addition to β -TCP, when heated to 1100 °C, while calcium pyrophosphate ($\text{Ca}_2\text{P}_2\text{O}_7$) and α -TCP were formed above 1200 °C. The desirable phases for further implantation are HA and β -TCP.

In a similar manner, Yamashita et al.(1988)^[43] prepared a dense composite of HA and PSZ. The product was obtained by sintering in presence of a stream of water vapor to prevent the decomposition to TCP. The objective was to produce the HA-PSZ composite in order to obtain a material stronger and tougher than pure HA. Such a product could see applications as a structural implantable material, where HA per se does not have appropriate mechanical properties.

Similar work, without a substrate, was performed by Monma (1987)^[41]. He confined his studies to the preparation of various calcium phosphate-based compounds and the measurement of their properties. Examples include sintering α - and β -TCP at high temperatures followed by a water post-sintering treatment. He observed the change in porosity and tensile strength as some HA was obtained.

Toriyama et al.(1991)^[55] also produced a β -TCP coating onto a titanium substrate, by a sintering reaction. A low temperature of reaction was required to prevent the structural transition of the titanium that occurs at 882 °C and to prevent oxidation that occurs in air

above 900 °C. The choice of liquid phase sintering permitted to achieve good adhesion of the coating at a low temperature of reaction. They used mixtures of CaCO_3 , TiO_2 , H_3PO_4 , and Na_2CO_3 . Previous studies had shown that $\text{CaO-TiO}_2\text{-P}_2\text{O}_5$ glass crystallizes into β -TCP and $\text{CaTi}_4(\text{PO}_4)_6$ by addition of Na_2O with long heat treatment period. After applying the mixture as a slurry, β -TCP and $\text{CaTi}_4(\text{PO}_4)_6$ were obtained by heat treating for 24 hours at 800 °C. The strength of adhesion is provided by the presence of the titanium oxide (TiO_2) formed at the surface of the titanium substrate during the heat treatment process.

Clinical work was performed by Oonishi et al.(1987)^[4] on dogs to compare various HA coatings. HA was plasma sprayed on titanium cylindrical substrate either as a 100% HA coating or as a 80% HA / 20% alumina mixture. Such coated cylinders and other uncoated titanium substrates were implanted in dogs' tibiae. As time elapsed from 4 to 13 weeks, adhering strength of coated cylinders was comparatively higher, with the HA-20% alumina-coated cylinder having a strength 20 % lower than the 100%-HA coated cylinder, while shot blasted titanium controls had the lowest value.

Further work by Oonishi (1989)^[91] and Oonishi (1990)^[42], included a whole range of biomaterials: 1- Non-porous materials with and without a HA coating, as discussed above. 2- Porous titanium alloy beads with and without a HA coating. 3- α -TCP bioactive bone cement and PMMA bone cement. 4- Bioactive bone cement made by interposing HA granules between polymethylmethacrylate cement and the bone. The author calls this "the interface bioactive bone cementation technique".

Porous metal (case 2) with HA coating was better than that without coating, producing earlier and stronger fixation. Problems with fatigue and peeling of HA from the base metal were eliminated when the beads were coated with HA. Pain is observed by some patients on weight-bearing after implantation, because complete initial fixation is not obtained and micro-movement of the component occurs. As HA bonds chemically to the bone, pain on weight-bearing is eliminated due to the absence of micro-movement.

In case 3, α -TCP with polyacrylic acid, α -TCP with citric acid and PMMA, all shaped into cylindrical forms, were implanted. The α -TCP with citric acid showed better bonding strength, although the HA coated titanium cylinder had a larger adherence strength between HA and bone.

In case 4, fine HA granules were placed as a thin layer on top of PMMA cement, thus interfacing with bone. New bone tissue filled all the space after 6 weeks. Push-out tests showed that the bond strength of both bone cement to HA and that of the HA granule layer to bone were adequate, according to Oonishi. He has used the interface bioactive bone cementation technique in total hip replacement and total knee replacement since 1984, in about 250 cases. The patients were pain free after surgery. As the HA bonds chemically to the bone, the pain while weight-bearing due to micro-movement never occurs. This type of bone cementation technique combines the advantages of both conventional PMMA bone cement fixation and cementless fixation with HA coatings on the components. This bioactive bone cement hardens during surgery within 10 minutes. Figure 2.5 compares the adhesive strength of the materials discussed above, as a function of time of implantation.

REMOVED DUE TO COPYRIGHT RESTRICTIONS

[42]H. Oonishi, "Mechanical and Chemical Bonding of Artificial Joints",
Cli. Mater., Vol.5, No. 2-4, p. 217-233, 1990.

Figure 2.5 Comparison of adhesive strength with bone of several biomaterials^[42].

Problems with fatigue and peeling of the HA from the base metal when HA is coated on a flat surface have not been solved. These problems are eliminated when HA is coated on the surface of titanium alloy beads. Oki et al.(1991)^[45] reported an experiment where they sprayed HA over the top of an intermediate layer of porous pure titanium covering a solid titanium substrate. The application was dental implants. They used the intermediate titanium coating to impart a rough porous finish and the HA to enhance fixation between implant and bone.

Another type of bioactive bone cement^[2] was evaluated as a potential candidate either for fixing various kinds of implants to the surrounding bones or for use by itself as a bone filler. The product, a $\text{CaO-SiO}_2\text{-P}_2\text{O}_5\text{-CaF}_2$ glass powder, when mixed with an ammonium phosphate solution, sets within 4 minutes, forming $\text{CaNH}_4\text{PO}_4\cdot\text{H}_2\text{O}$ at its outer layer (without temperature increase, contrary to commercial PMMA bone cement). When placed in simulated body fluids, HA progressively replaces this layer. When implanted within bone, the absence of fibrous tissue indicates a tight chemical bond between the cement and bone. The chemical bond is attributed to the formation of HA within the body, as demonstrated by implantation in rat tibiae. This showed how HA material is produced within the body, through indirect routes.

The need for prosthesis stabilization has long been recognized. Early on clinicians noted that polished implant surfaces tended to be isolated by the body within a non-adherent membranous sheath, thus preventing full stabilization. These observations led to the preparation of implant surfaces with substantial porosity or macroroughness that were more likely to induce interdigitation of the bone, ensuring some mechanical integration of the implant with the host tissue.

Homsy et al.(1972)^[58] discussed the evolution of the means for prosthesis stabilization. Some implants used in dentistry had macroroughness to which were later added macro-perforations into the implant to encourage through tissue and bone growth. This philosophy in design was also applied to orthopaedic endoprostheses. However, apparently some movement of the implants still occurred with these designs, even though bone growth through perforations occurred. Next step in design was to provide microporosity to the surface. Several advantages were expected: to provide much greater area for mechanical interdigitation between the implant and the host tissue; to improve the vascularization of tissue next to the implant; to induce more rapid fixation. Work with a variety of systems, including metallic microporous structures, non-degradable ceramic (calcium aluminate and aluminum oxide) or slowly soluble ones, and various carbon-based materials was conducted, demonstrating the possibility of growing tissue within pores. However, all the studies were conducted under mechanically static conditions (cylinders inside long bones). Pilliar (1987)^[114] also reviewed the porous-surfaced orthopaedic implants.

The need for a low modulus implant material was identified as essential for appropriate transmission of load between the supporting tissue and the prosthesis. In this regard, some work on HA was initiated, in the US, by Jarcho et al.(1976)^[59]. They developed one form of the calcium phosphate material, durapatite[®], which is a 100% dense polycrystalline form of HA, characterized by a high flexural strength of 195.6 MPa. Trial implants in dogs in form of durapatite[®] plugs and particulates showed material stability. Both types were surrounded by normally calcified bone, as shown by histological observations, after 6 month implantation with no inflammation and no fibrous tissue. Although the implant material was of a dense nature with little surface relief, bone was strongly bonded to the ceramic, suggesting chemical bonding.

Hench et al.(1977)^[35] used Bioglass[®] as an alternate material for providing hip prosthesis stabilization. To achieve the high strength necessary for hip prostheses, they applied the bioglass material as a coating to metal and ceramic materials such as 316L surgical stainless steel and high-density alumina.

In a clinical study with humans, Golec (1985)^[60] used "subperiosteal" implants coated with HA through an activated sintering process, developed by the company Calcitek, Inc., and called Calcite[®]. The proprietary process enabled HA to be chemically bound to metal. The interface between bone and ceramic is stronger than either the ceramic or bone alone, as previously demonstrated by Kay et al.(1986)^[61]. This clinical experiment involved the successful implantation of various types of maxillary and mandibular implants with Calcite[®] coating (HA) showing the versatility of this type of HA-coated implants.

This HA coating process on surgical alloys was proposed^[61, 65] as an alternative to existing metallic porous orthopaedic implants which rely on bony ingrowth for their stabilization. HA was coated on smooth Ti-6Al-4V alloy, CoCrMo alloy and on porous pure titanium. Results of the materials characterization showed these composites could be used for applications in orthopaedics as demonstrated by the interfacial strength measured between the alloy and the HA coating. Those implant systems later evaluated in dogs^[62] and compared with the same non-coated alloys, indicated that HA coated porous systems had increased amount of bone ingrowth and a higher degree of mineralization at early time periods compared to the non-HA coated systems. The coating provided a chemical rather than a simple mechanical type of interlocking. In addition, the HA made the surface more suitable for bone formation, thus decreasing the time to reach maximum interface strength.

Following the above results, HA coated porous titanium implants were used^[63] to evaluate the biological response in dogs, in load-bearing applications such as hip joints. As well, non-coated porous titanium materials were used as controls. An increased amount of bone ingrowth was present earlier in the HA coated system as compared to the non-HA coated system. The bone was also better "organized" and had a higher degree of mineralization. Similar implantation was performed by Kent et al.(1986)^[64] with dental implants. The non-coated implant interface was completely lined with fibrous tissue while the HA coated implants resulted in a bone-implant interface. The apparent chemical bonding of bone to HA coated endosseous dental implant provides an increased stability and retention as compared to un-coated implants.

Kay et al.(1987)^[66] underlined the importance of obtaining a crystalline HA during processing because of its in-vivo biostability as opposed to amorphous materials which result in less stable coatings upon implantation, according to them. However, long term studies are required. They recommended as well that implants should not depend uniquely on coatings for primary attachment as significant shear forces are encountered. They suggested the addition of macroscopic steps or grooves at the surface of implants to prevent pure shear conditions at the metal-coating interface. HA coatings provide, through total bony encapsulation, a positive stress transfer from the implant to the bone.

Further quantitative work^[67] of coated and uncoated press-fit metallic implants subjected to shear load in service (in vivo) was performed. Cylindrical shape Ti 6Al-4V alloy implants were placed in the femur of dogs. Push-out strength of the implants was recorded after 5 weeks and 10 weeks and, in both cases, HA-coated implants displayed much higher strength values: 3.70 MPa and 4.44 MPa for HA coated system versus 0.18 MPa and 0.17 MPa for uncoated specimens.

A longer term study was performed^[68] by implanting both granular and solid HA ceramic forms in the femurs of dogs. Up to eight years after implantation in bone, both the HA granules and solid discs were well tolerated with no inflammation present. Dense lamellar bone interfaced directly on all surfaces, with very rare cases of resorption in some granules. Besides a few cracks observed in the dense material, there was no change in the implants after long term implantation. Host tissues responded to the implant as if it were normal bone. However, this study did not evaluate the implants in a load-bearing type of application.

Jarcho (1986)^[38] reviewed the properties and applications for calcium phosphate bioceramics. Examples of clinical practice described include alveolar ridge augmentation, preservation of alveolar bone after tooth extraction, and repair of periodontal osseous lesions. He also discussed the biologic response obtained with this class of materials. He stated that calcium phosphate biomaterials are not "osteogenic" per se, because they do not induce bone to form in unexpected sites such as muscle. They also do not stimulate a more rapid bone growth in bone implant sites. What they do is to provide a physical matrix such as a scaffold^[69] suitable for deposition of new bone. These materials are rather called "osteoconductive" or "osteophilic". He also showed that calcium phosphate ceramics are well tolerated by soft tissues although they are usually surrounded by a fibrous tissue capsule when implanted in those sites.

Animal and human studies reviewed by Jarcho showed that chemical composition and porosity of these materials influence their bioresorbability. It can result from simple chemical dissolution in biologic fluids or from cell-mediated processes such as phagocytosis. HA dissolves far less readily than TCP in a variety of fluids. TCP can gradually resorb at a rate similar to the rate of bone ingrowth. This assumes that TCP is a completely bioresorbable substance. However, available studies on this subject report conflicting results. Jarcho (1986)^[38] observes that predictable rates of bioresorption have not been achieved with TCP ceramics.

Subperiosteal dental implants made of CoCrMo (Vitallium) have been used in the past. However, there are concerns about the metallic ions released in the surroundings. Kay et al.(1987)^[66] suggested that those accepted implant models could be coated with dense HA. In vitro tests indicated a 10-fold decrease in metallic ion release when HA-coated CoCrMo alloy was compared with uncoated metal. In other words, HA coatings make the metallic implants more biocompatible.

A different substrate surface was coated by Rivero et al.(1988)^[70]. A titanium alloy Ti-6Al-4V solid core was covered by a fiber mesh of pure titanium used to produce a macroporous surface onto which HA was deposited. After spraying, the deposit was identified as TCP and some HA. These coated cylinders were implanted in dogs humeri as non weight-bearing implants. Measurements of shear strength indicated that the HA coated implants had higher values only at the 4 weeks period. However, the transformation of

HA to TCP was not discussed. This prevented from associating the shear strength values to the exact nature of the coating.

Berndt et al.(1990)[24] carried out an excellent review of the material and clinical considerations related to the thermal spraying of HA on metallic substrates for orthopaedic applications. They described the factors which can influence the bioresorption of materials, such as physical and chemical properties of the implants. They stated that resorbability of HA can be increased by porosity, reduction in grain size and the presence of crystal imperfections. In terms of chemical properties, ionic substitutions (CO_3^{2-} or Mg^{2+}), the presence of β -whitlockite (TCP) and impurities have the same effects. Biological factors as well contribute to bioresorbability. These factors include pH drop due to cell-mediated factors (living body reaction, by macrophages, osteoclasts and fibroclasts), osteolytic infection and disease, degree of bone contact, type of bone, etc. Brown et al.(1991)[133] reported that bone-prosthesis intergrowth does not occur when the gap between the two interfaces is greater than about 10 μm . The time required for bioresorption and the amount of resorption within the body change according to the above factors. Materials selection is a function of whether we want resorbability to occur or not to occur at the implantation site. For example, in the case of fracture healing of bones, the pin used to stabilize a fracture slowly dissolves and progressively loses its strength if properly manufactured. For the opposite case, selection of a ceramic coated implant is more appropriate where bone cannot regenerate enough to repair any previous damage. These two phenomena are well schematized in Figure 2.6, which shows the strength-time relationship for these two cases.

REMOVED DUE TO COPYRIGHT RESTRICTIONS

[24]C.C. Berndt, G.N. Haddad, A.J.D. Farmer, and K.A. Gross, "Review Article - Thermal Spraying for Bioceramic Applications", Materials Forum, vol. 14, p. 161-173, 1990.

Figure 2.6 Strength-time relationship for: (a) tibia with a bone plate and (b) a femur possessing a hip prosthesis[24].

Berndt et al.^[24] also reviewed the characteristics of various implant stabilization methods. Thermosetting cement (PMMA) stabilizes the implant by adhesion. Disadvantages include mortality of cells from the exothermic reaction in situ and cement failure with time. Thus reliability of this fixation technique is questioned if it is to be used over periods of more than 10 years. The main advantage is its immediate bond formation. An alternate fixation method consists in promoting bone ingrowth into a porous surface. A porous beaded surface or titanium fiber pads are used. The material is pressure sintered onto the surface to provide a surface with controlled pore size to allow bone ingrowth. These have seen long term failure which might occur by destruction of bone inside the macropores. Superior bonds are obtained with surface active ceramic coatings deposited on a metallic substrate. In this case, osseous tissue grows against the material where it forms an intimate bond. In this perspective, results from plasma spraying of HA show that bone bonding to HA coatings is the same as to HA bulk implants.

At this time Ti-6Al-4V is the main metallic substrate material in use. Advantages of this alloy are as follows: it is less susceptible to corrosion than other alloys such as 316L SS and CoCrMo alloys; it has a lower elastic modulus, relatively closer to values for bone (106 GPa vs. 7.30 GPa for cortical bone) as compared to the two other materials; it is less dense, and therefore, more compatible with the biological system. This is required because an applied stress in the femur would otherwise cause a difference in deformation between the bone and the implant. This mechanical incompatibility would be transferred to the interface in the form of deformation stresses and strains. A very stiff implant is subjected to all the mechanical loading and does not allow stress transfer to the surrounding bone. Such conditions produce stress shielding and bone degradation (resorption and loosening of the prosthesis). HA has a modulus similar to the alloy, (100 GPa) and therefore the strain at the coating/substrate interface will be minimized when the prosthesis is stressed. The stress anticipated for in vivo orthopaedic implants is estimated as three to four times the body weight (Semlitsch, as reported by Sahay et al.(1990)^[3].

Berndt et al.(1990)^[24], report that no bond coats are used for HA coatings on Ti-6Al-4V substrates. According to de Groot et al.^[80], HA can form CaTiO_3 and TCP through a chemical reaction with titanium dioxide (at the surface of the alloy), at 1000 °C. They expect that a chemical bond will form if HA is deposited at high temperatures onto a titanium substrate by the plasma spraying process. The CaTiO_3 , a compound formed from both the substrate and the HA coating, acts as a bond layer. This adhesion of HA to Ti

alloys could be stronger (up to 60 MPa) than bonding mechanisms by normal mechanical interlocking. However, chemical evaluations are required to demonstrate the existence of the bond coat described above.

Problems surrounding the plasma spraying of HA coatings were reviewed by a powder manufacturer^[73] and by a manufacturer of coated devices^[75]. Such problems include the obtaining of pure stoichiometric powders and deposits. Another problem is the requirement by the biomedical community for a highly crystalline product which is difficult to obtain by the plasma spraying process, characterized by rapid solidification. A problem of color also exists because HA, known to be white, is susceptible to the pick-up of color centers from minor element contamination. Yet, these elements are still within acceptable levels recognized and accepted for human use.

According to Harris (1990)^[73], the rapid solidification effects of plasma spraying exclude high crystallinity of this material without the use of post-spray thermal treatments or the use of substrates heated to high preheat temperatures. However, he remarked that long term histology (tissue) studies in the human species for plasma sprayed HA is not available. He further stated that if a proper Ca/P ratio is present in a form which can be acted upon, "bonding is inevitable" and the question of crystallinity vis-a-vis amorphous content is immaterial (although most users insist on >90% crystalline HA in the powder, with the remainder β -TCP).

Salsbury, 1991^[75], as a manufacturer of coated devices, also reviewed the characterization of HA coatings, in terms of purity and crystallinity, since it is recognized that plasma spraying can alter both the purity and crystallinity of HA. The usual impurities seen in HA coatings are α - and β -TCP and occasionally some calcium oxide or calcium pyrophosphate. The major concern with HA coating analysis has been quantifying the amount of amorphous HA present because it is known that amorphous HA resorbs. He observed that microcrystalline HA has a broad peak centered around 32° while synthetic amorphous HA has a broad peak centered around 30°. Plasma sprayed HA resembles synthetic amorphous HA. However, after mild heating (300 to 400 °C for several hours) "crystal maturing" occurs, and the amorphous component disappears from the spectrum, showing signal intensity similar to synthetic HA powder. Contrary to Harris, Salsbury claims that value of 65-70% crystallinity must be achieved in order to prevent complete deterioration of the coating.

In the mean time, Wolke et al.(1990)^[83] and Koch et al.(1990)^[85] performed a more systematic study of the effect of the plasma spraying process on calcium phosphate-based materials in term of structural changes. Wolke et al. evaluated the influence of the particle size of HA material, comparing powders with particle size 1-45 μm and 1-125 μm . Koch et al. compared the behavior of the three materials, HA, β -TCP, and tetracalcium phosphate (tetra-CaP), all 50 μm and smaller in particle size.

All specimens were produced with the same plasma spraying conditions, after sandblasting, ultrasonic cleaning and drying of the substrate (Ti-6Al-4V and/or stainless steel). XRD patterns showed that HA powders (1-125 μm) had transformed to an amorphous coating containing some calcium oxide, when sprayed with argon and 10% hydrogen, while spraying with nitrogen did not alter significantly the material, with only some peak broadening observed. The finer powder (1-45 μm) sprayed in nitrogen was almost completely transformed into an amorphous phase. After a heat-treatment for 1 hour at 600 °C in an inert furnace to prevent oxidation of the metal, the structure had completely reverted to a fully crystalline HA. In vitro incubation for 3 months in Michaelis Buffer pH 7.2 at 37 °C, also displayed an increase in crystallinity, with no amorphous phase left, with the HA-125. This phenomenon was also observed after implantation for 6 weeks in rabbit tissue. A very hot flame gives an amorphous coating with the formation of calcium oxide. The cooler nitrogen plasma results in a higher crystallinity (for coarser powder). The particle size of 1-45 μm gives an entirely amorphous phase, but a heat treatment increases the crystallinity. After incubation in vivo or in vitro the amorphous phase disappeared.

Under similar spraying conditions, β -TCP turns into less stable α -TCP, HA does not change although the crystallite size decreases 10- to 100-fold, and tetra-CaP only shows a limited line broadening of the x-ray diffraction pattern and a lesser decrease in crystallinity than HA. β -TCP transforms to α -TCP at ~ 1100 °C and HA is stable to temperatures up to 1300 °C. Tetra-CaP is thermodynamically stable at temperatures up to 1600 °C. The tensile strength of the three coatings was similar, suggesting either that chemical adhesion due to possible reactions at higher temperatures between HA and the surface does not play a significant role, or that similar reactions might happen with other calcium phosphates as well. However, the substrate was stainless steel, as opposed to the Ti alloys discussed by de Groot et al.(1987)^[39].

A comparison of various fabrication processes of HA coating^[69] included thick coating techniques ($>10\ \mu\text{m}$) such as thermal spraying, various dipping techniques, isostatic pressing/sintering, and electrophoresis, and thin coating techniques ($<10\ \mu\text{m}$) such as ion beam techniques. Plasma spraying was reported by far the most widely used process for thick coatings. Observations from many researchers are as follows: more rapid attachment of bony tissues to HA-coated surfaces, long term histocompatibility (cellular compatibility) of HA coatings, structural water is often depleted in sprayed HA, and degree of crystallinity varies as a function of processing. Plasma spraying is currently the method of choice for depositing HA coatings on devices now in clinical use. However, decomposition of HA at elevated temperatures through the loss of structural water is not well understood in the context of non-equilibrium processing conditions. Overall the basic processing-structure-properties-performance relationships are not well understood and warrant further studies, in particular optimization of coated devices for long term use in humans.

Important consideration in plasma spraying concerns the surface preparation of the implant substrate before applying the HA coating. Yankee et al.(1991)^[137] evaluated the effect of two grit types and other grit blasting processing variables followed by cleaning procedures in terms of adhesion measurements of HA coatings. Results of these tests indicate that adhesion strength is a function of the substrate surface preparation and the cleaning procedure. An ultrasonic cleaning procedure (ASTM F-86)^[76] was slightly better than air blast cleaning for samples having equivalent surface roughness. In addition, Al_2O_3 grit blasting particles tended to embed more in the Ti-6Al-4V substrate than SiC particles which break apart rather than remain embedded.

Yankee et al.(1991)^[74] also investigated the deposition of individual HA particles as spread on a substrate in order to determine optimal spraying parameters. In particular, they studied plasma gas flow rates and percent secondary gas as a function of the splat characteristics, while maintaining constant all other spraying parameters. Two variables, splat spreading and splat morphology, were determined, as a function of the processing conditions. They expressed droplet spreading in term of an equivalent mean diameter and droplet morphology in term of a dimensionless shape factor relating perimeter and area.

Rejda et al.(1977)^[77] conducted an animal study with implanted cylinders. These were made of a porous biodegradable ceramic based on tricalcium phosphate (TCP) with a

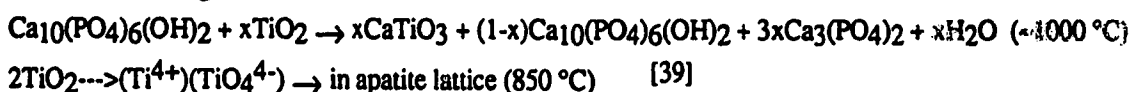
macroporosity of 20% (pores >100 μm) and a microporosity of 30% (pores $\approx 1\text{-}2\ \mu\text{m}$). Histological (tissue) inspection showed bone ingrowth in the large pores (>100 μm) and general bone tissue contacts at the interface. After two months, resorption of the TCP material had occurred, with new bone directly deposited on the implant material. Large pores in the ceramic are gradually penetrated by osteoblasts, while osteoclasts create new space within the ceramic.

Denissen et al.(1980)^[40] used commercial HA raw powder to prepare, by compression followed by sintering, a dense HA material. The obtained material had properties they considered essential for implantable tooth roots: 1) chemically close to the normal hard tissue material (HA); 2) mechanical properties sufficient for implant design and use in clinical dentistry; 3) close to 100% density (microporosity must be minimal to obtain maximum biostability and minimum degradation). They fabricated tooth root implants which were successfully implanted in humans.

Further work with dense HA by de With et al.(1981)^[78] indicated that this material remains stable while bone ingrowth without fibrous encapsulation still occurs. However, in vitro mechanical evaluation showed that subcritical crack growth occurs in wet environments, with a significant degradation of strength with time. This restricts the applicability of this material to non-stressed region of the skeleton.

Driessen et al.(1984)^[79] also demonstrated this failure mode by implanting in dogs sintered HA tooth material. To prevent mechanical failure, they used pre-stressed implants. The cylindrical implants were pre-stressed using a bolt and screw and then implanted in the lower jaw of dogs. After 1 1/2 years implantation, no fracture had occurred, as compared with 50% implant failure for non-stressed components.

As an alternate solution, de Groot et al.(1987)^[80] suggested using HA as thin coatings on metallic substrates when tensile loading is expected. Plasma spraying as a coating technique to applied HA was first reported by this group, as indicated by Berndt et al.^[24]. They chose titanium as a substrate based on literature data^[81] indicating that, in theory, HA reacts with titanium and its oxides at elevated temperatures, creating a chemical bond between coating and substrate, as follows:



Selection of the coating thickness is a compromise between best mechanical properties (thin coatings) and possibility for the HA of partly dissolving (up to 15-20 μm). However, possible dissolution depends on the exact nature of the deposit (such as HA or TCP). De Groot et al. chose a thickness of $\sim 50\mu\text{m}$, assuming some resorption would occur. They obtained shear stress values of up to 62 MPa for HA-coated Ti-6Al-4V substrate plugs implanted in dogs while non-coated plugs had no measurable adhesion to bone. In comparison, the only way to achieve retention of uncoated titanium implants is mechanical, by means of undercuts, while coated plugs achieved bonding strength close to the shear strength of bone.

Geesink (1989)^[82] provides clinical results for 100 HA-coated total hip replacements in humans. These human implantations followed his long term animal study (up to three years). He demonstrated that HA-coated implants had better histologic behavior in comparison with non-coated controls. One advantage of the HA coating is the rapidity of the bond formation with bone. The implant fixation around the bony envelope allows the prosthesis to withstand high shear and tensile forces, providing superior physiological stress transfer around the implant. Rapid functional recovery of patients after surgery indicated that results comparable to and competitive with cemented hip replacement can be obtained. Absence of postoperative discomfort adds significantly to a rapid functional recovery after the operation. However the follow up is still short (almost 2 years).

Following their crystallographic study (see ^[83] and ^[85]), Klein et al.(1990)^[86] performed in vitro solubility tests with the same three powders, HA, β -TCP, and tetra-CaP, in various solutions (lactate, citrate, Gomoris or Michaelis buffer with pH 6.2 or 7.2, and distilled water). It was previously shown that β -TCP gives rise to extensive bone remodeling around an implant, probably due to its Ca/P ratio of 1.5 leading to higher degradability. In contrast, both HA and tetra-CaP develop very intimate bone contact. Coatings are usually very thin (50 μm or less), such that even slight solubilities might lead to dissolution of these coatings. This possibility prompted the evaluation of the solubility of different calcium phosphate materials. In all cases, HA was the least soluble of the three materials.

In aqueous solutions, only 3 thermodynamically stable calcium phosphates are known (according to Driessens (1982) as reported by Klein et al.(1990)^[86]): monocalcium phosphate monohydrate ($\text{pH} < 2.5$), brushite ($1.5 < \text{pH} < 3.2$), and HA ($\text{pH} > 4.2$). TCP and

Tetra-CaP will dissolve and, if the calcium and phosphate ions reach a sufficiently high concentration, they will reprecipitate as HA. Their study showed that HA was the least soluble in vitro. However, they also showed that the specific buffer used had a much larger effect than either pH or even the specific calcium phosphate salt tested. This indicates that in vitro solubilities of calcium phosphate are at least as much dependent on buffering conditions as on the calcium phosphate themselves. But "in vitro solubility measurements may have little or no relevance with respect to in vivo degradability"^[86] leading to the need of in vivo evaluation.

The same powders studied above (HA, β -TCP, Tetra-CaP) were sprayed by Klein et al.(1991)^[25] onto cylindrical titanium (Ti-6Al-4V) substrates and implanted into femora of adult dogs. The materials were deposited to a thickness of 50 μ m. As indicated before, β -TCP transforms to α -TCP during spraying. Non-coated titanium plug implants were used as controls. Bone bonding and bone formation were evaluated by mechanical push-out tests and histological observations, after 3 months of implantation (because normal bone healing following bone fracture is expected to have been completed after that time (6 to 12 weeks)). The objective is to relate the in vivo biodegradation behavior of the coatings (histology observation) to their bonding properties and their interaction to bone formation.

Results showed that in vivo data did not correspond to the previous in vitro observations on solubility. In the in vivo study tetra-CaP showed a very good bone bonding and a shear strength similar to HA. The values of ~30 MPa were higher than with α -TCP or uncoated titanium (~10 MPa). Histological observations revealed an excellent bone contact with HA or Tetra-CaP, while α -TCP and titanium gave rise to more bone remodeling lacunae and/or connective tissue along the implant surface. They suggested that coating reprecipitation of HA on the surface of Tetra-CaP may be the reason that Tetra-CaP shows good bone contact.

Wolke et al.(1991)^[87] then compared the properties of HA coatings obtained by spraying with various systems, air plasma spraying (APS), vacuum plasma spraying (VPS), and high velocity oxygen fuel (HVOF) spraying. X-ray diffraction patterns showed for HA-APS and HA-VPS the presence of both a crystalline and an amorphous phase while HA-HVOF retained its crystalline structure. SEM investigations of the surface showed that HA-HVOF gave the most porosity, with the highest density for the HA-APS coating. The in vitro studies showed that HA-HVOF was the least soluble, probably due to the

crystalline structure, as compared to the solubility of HA-APS which had a higher percentage of amorphous structure. However, the authors warned against predicting in vivo behavior based on in vitro tests.

Wolke et al.(1992)^[88] performed a comparative study of HA and FA materials. Both powders were air plasma sprayed on titanium alloy cylindrical substrates in 2 particle size distributions (1-45 μm and 1-125 μm). In addition to the discussion on the coatings, the authors showed that different adhesives exhibit different failure modes and tensile strengths when used in the standard tensile test ASTM C-633^[89].

A very hot flame produces an amorphous coating with the formation of calcium oxide. After incubation in vivo or in vitro, the amorphous phase is either resorbed through physico-chemical dissolution or changed via a phase transition from an amorphous to a crystalline structure. The HA coating sprayed with a particle distribution of 1-45 μm produced an entirely amorphous phase, and this coating dissolved faster. Heat treatment after plasma spraying increased crystallinity and decreased the solubility of the coating. The thermal stability of fluorapatite at elevated temperatures is superior to that of HA, and, therefore, a FA coating has a higher degree of crystallinity than a HA coating. Push-out studies, however, showed that the high strengths of the HA coating did not change after gradual dissolution of the coating. Furthermore, because uncoated (and unloaded) titanium implants become bonded to bone after about 1 year, the conclusion is that apatite coatings are most important during the healing phase.

In parallel to this specific work on implantation, results with these new materials led to the development^[72] of strain gauges with a HA backing. Such strain gauges while implanted at a bone site can provide accurate strain measurements during in vivo bending load application. They can also be useful in the measurement of in situ strain occurring during remodeling processes after implantation. The HA backed strain gauge was developed as an alternate mean of attaching strain gauges in vivo. The objective was to replace cyanoacrylate adhesives which often biodegrade within one week exposure (implantation). Measurements obtained with these strain gauges help to improve the design of new implant models.

Various types of biocompatibility studies follow the successful preparation of materials considered "mechanically suitable". Examples include cytotoxicity evaluation of solid HA

materials sintered at various temperatures, using cultured cells^[44] or comparison of the growth-rate of animal cells on substrates with various HA/TCP ratios^[56]. One such study^[71] suggests that bone attachment may be the result of both physical chemical growth of apatite on the surface of the HA ceramic from body fluids (physico-chemical activity) and cellular formation (biological activity) and mineralization of osteoid (living cells) at the implant surface.

Some studies were more specifically related to the medical domain. Van Blitterswijk et al.(1990)^[84] evaluated the behavior of both macroporous and dense HA for ear prostheses as related to chronic infection. Others studied the behavior of cells (cytology)^[95, 112] and tissues (histology)^[111] in relation to biomaterial implantation.

A variety of other subjects discussed in the literature, in addition to all the work reviewed above, includes the following: solubility studies^[122, 123]; mineralization kinetics^[129 to 133]; preparation (chemistry) of various calcium phosphate-based materials^[99-101, 118], porous HA^[109, 110], hot isostatically pressed HA^[119], electrochemically deposited materials^[120], and Si-doped HA^[136]; transformation of materials after implantation^[108, 117]; other HA coating studies^[97], HA/FA coatings^[113], and TCP coatings^[106]; clinical studies of Ti coatings in humans^[104] and in dogs^[107]; specimen preparation^[105, 121, 137]; and various electron microscopy techniques^[96, 98], and / or chemical investigation techniques such as infrared spectroscopy (IR) techniques^[101], solid state NMR spectroscopy^[125], and x-ray diffraction evaluation^[135].

3. MATERIALS AND METHODS

Powder characterization results will be given in this section together with a description of all materials and methods used. Results of the coatings' characterization will be provided in the next chapter.

3.1 Powder Characterization

3.1.1 Particle Size and Size Distribution

A Horiba CAPA-700 Particle Analyzer was used to determine the particle size and size distribution of the various powders sprayed during the project. Two types of hydroxylapatite powder were evaluated. The first one was fabricated at the University of Toronto (HA-Toronto). The second HA powder was a commercial powder fabricated by Bioland from Toulouse, France (HA-Bioland). The powder used as a bond coat material was a Ca_2SiO_4 compound fabricated by Onoda Cement Co. Ltd from Japan.

A distribution table and the corresponding distribution graph (in volume %) of the HA-Toronto are given in Table 3.1 and Figure 3.1, respectively. The particle size limit measured was chosen after a few preliminary trials to determine the most appropriate range. Most particles are grouped either in the 50 μm range or 0-14 μm (for particle size 50 μm and smaller), indicating a bimodal distribution. This type of distribution is characteristic of very small particles which form agglomerates. This HA powder tended to plug the feeder hose to the spray gun, as experienced during preliminary spraying trials, and was not used in the final spraying program.

Table 3.1 Particle size distribution table (by volume) for HA-Toronto.

D(μm)	%	Cumulative %
0.00-12.0	35.2	35.2
12.0-14.0	9.8	45.0
14.0-16.0	0.0	45.0
16.0-48.0	0.0	45.0
48.0-50.0	55.0	100.0

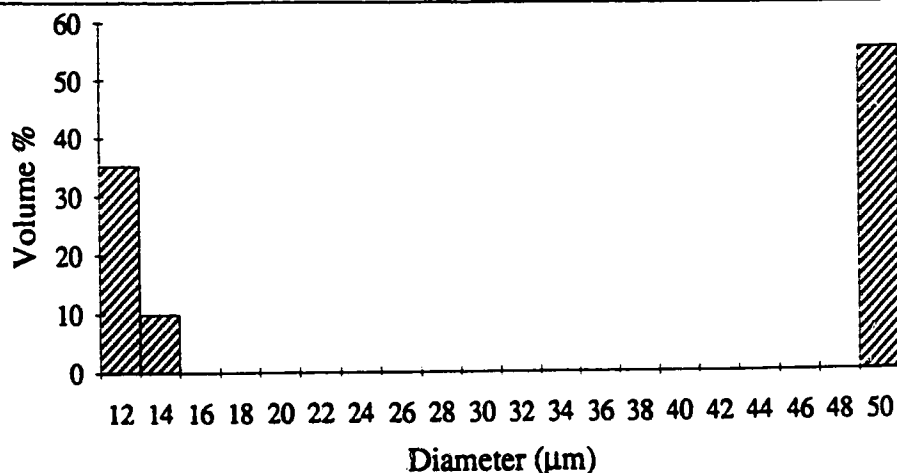


Figure 3.1 Particle size distribution for HA-Toronto.

The distribution table and corresponding graph for the HA-Bioland are provided in Table 3.2 and Figure 3.2, respectively. The particle size measured was 200 μm and smaller. This powder, with a median of 48.8 μm particle size, had a better flowing behavior during the spraying process as compared to the previous HA and was chosen for further work.

Table 3.2 Particle size distribution table (by volume) for HA-Bioland.

D(μm)	%	Cumulative %
0.00-60.0	61.5	61.5
60.0-80.0	27.6	89.1
80.0-100.	8.3	97.4
100.-120.	2.6	100.0
120.-200.	0.0	100.0

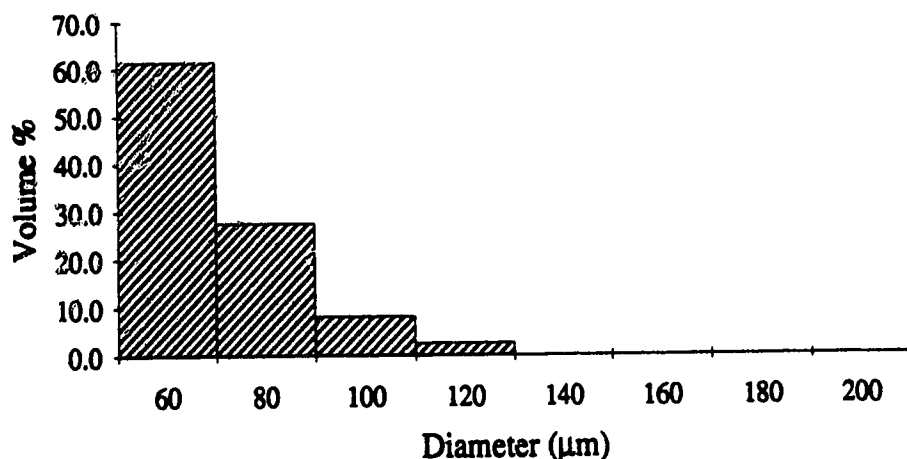


Figure 3.2 Particle size distribution for HA-Bioland.

The distribution table and corresponding graph for Ca_2SiO_4 are provided in Table 3.3 and Figure 3.3, respectively. The particle size measured was 50 μm and smaller, with a median of 13.55 μm and with up to 20.3% of the particles 4 μm and smaller.

Table 3.3 Particle size distribution table (by volume) for Ca_2SiO_4 -Japan.

D(μm)	%	Cumulative %
0.00-4.00	20.3	20.3
4.00-6.00	4.0	24.3
6.00-8.00	6.6	30.9
8.00-10.0	7.6	38.5
10.0-12.0	6.4	44.9
12.0-14.0	6.6	51.5
14.0-16.0	7.8	59.3
16.0-18.0	6.9	66.2
18.0-20.0	4.4	70.6
20.0-22.0	5.4	76.0
22.0-24.0	6.1	82.1
24.0-26.0	2.3	84.4
26.0-28.0	3.8	88.2
28.0-30.0	5.1	93.3
30.0-32.0	2.9	96.2
32.0-34.0	3.8	100.0
34.0-50.0	0.0	100.0

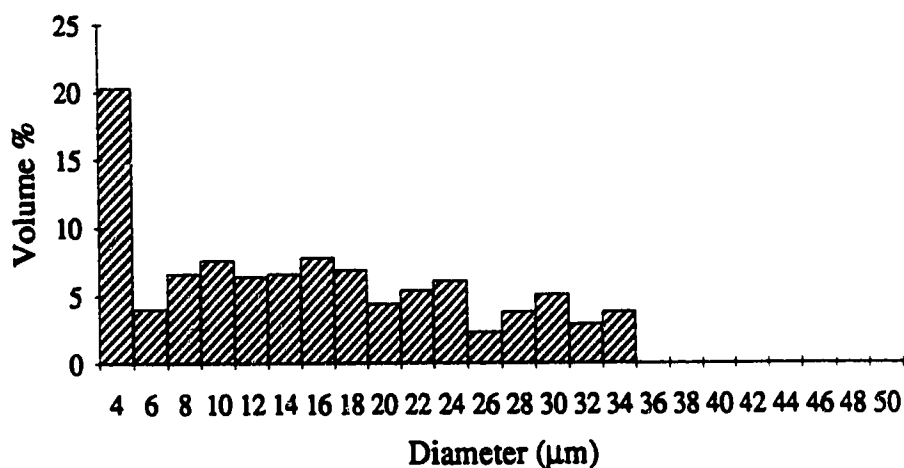


Figure 3.3 Particle size distribution for Ca_2SiO_4 -Japan.

3.1.2 Chemical Composition

Bioland provided the chemical composition of HA-Bioland. In addition to the stoichiometric composition, the following trace elements can be present up to the maximum indicated:

As: < 3 ppm
Cd: < 5 ppm
Hg: < 5 ppm
Pb: < 30 ppm

Additional qualitative EDX analyses were performed on the HA powders and on the Ca_2SiO_4 powder. In both HA powders, only Ca and P were detected (a beryllium window detector was used). In the calcium silicate powder, traces of Al and Fe were identified in addition to the main constituents of Ca and Si. This confirmed earlier comments by the manufacturer that the powder was not prepared in a pure form. A Hitachi S 2700 scanning electron microscope was used for observation of the powders. The elements were analyzed with a Link Analytical eXL energy dispersive x-ray analysis system. The spectra of the powders analyzed are provided in Figure 3.4 for the Ca_2SiO_4 and in Figures 3.5 and 3.6 respectively for HA.

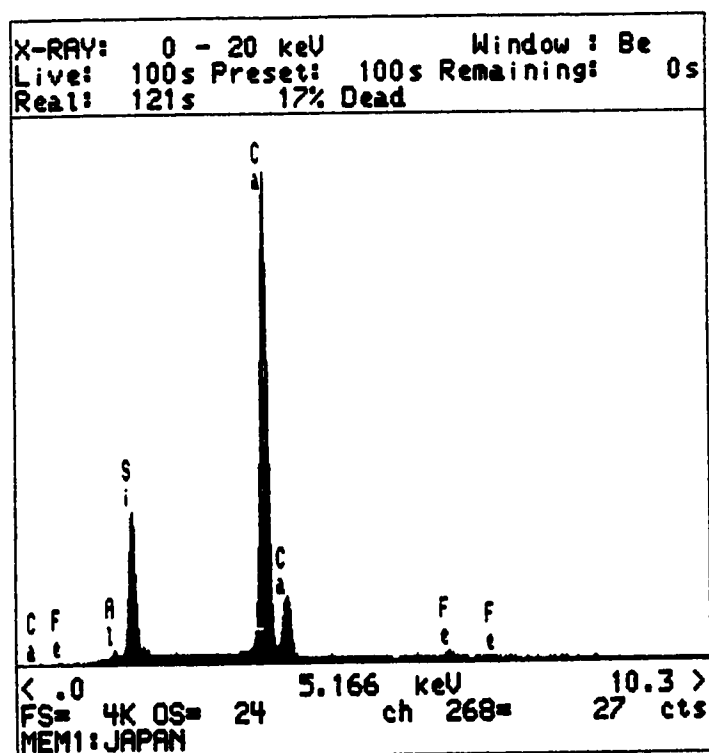


Figure 3.4 EDAX analysis for the Ca_2SiO_4 powder.

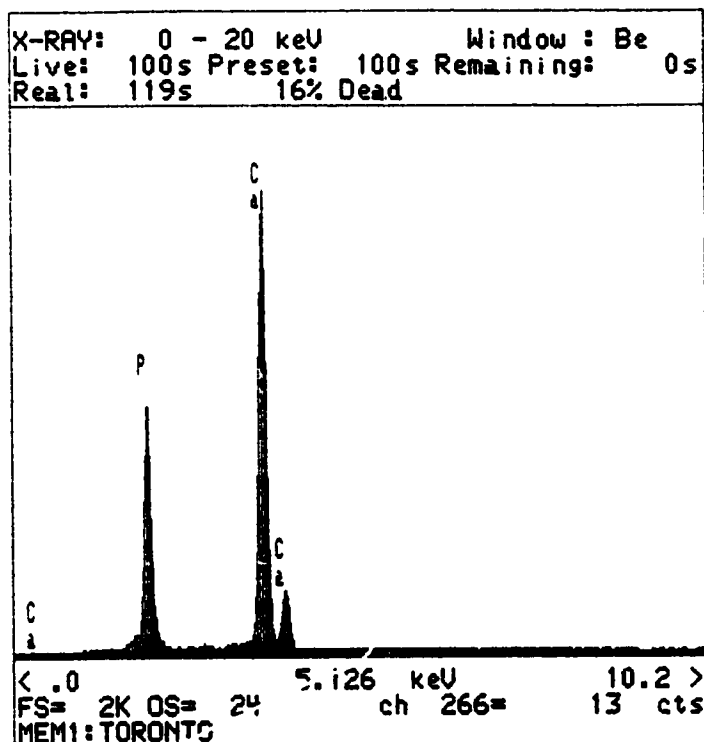


Figure 3.5 EDAX analysis for HA-Toronto.

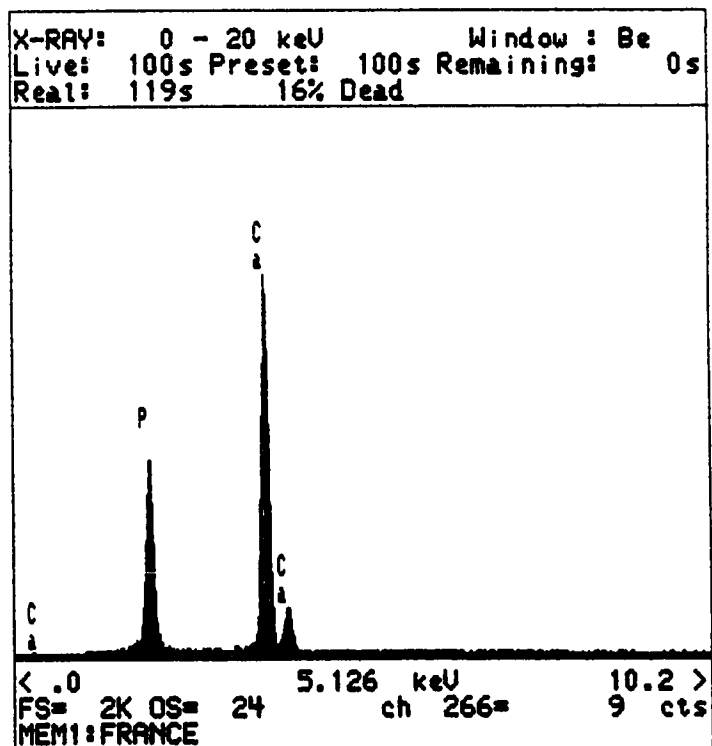


Figure 3.6 EDAX analysis for HA-Bioland.

3.1.3 Phase Identification

X-ray diffraction was performed on the powders, before plasma-spraying, to identify the state in which the raw materials were prepared. A Philips x-ray diffraction instrument was used, with a Cu target, and the intensity vs. 2θ curves was recorded. The counting rate was set at 400 counts per second for all powders. Phases were identified based on data from the JCPDS Powder Diffraction Files. Figure 3.7 shows the x-ray diffraction pattern for the Ca_2SiO_4 powder. The strong lines for $\gamma\text{-Ca}_2\text{SiO}_4$, file #31-297, are as follows: 2.73, 3.01, 2.75, 1.91, 3.82, 4.32, 1.69, and 1.80. These lines were identified on the spectrum below as the γ -phase, confirming the γ -crystal structure of the Ca_2SiO_4 powder.

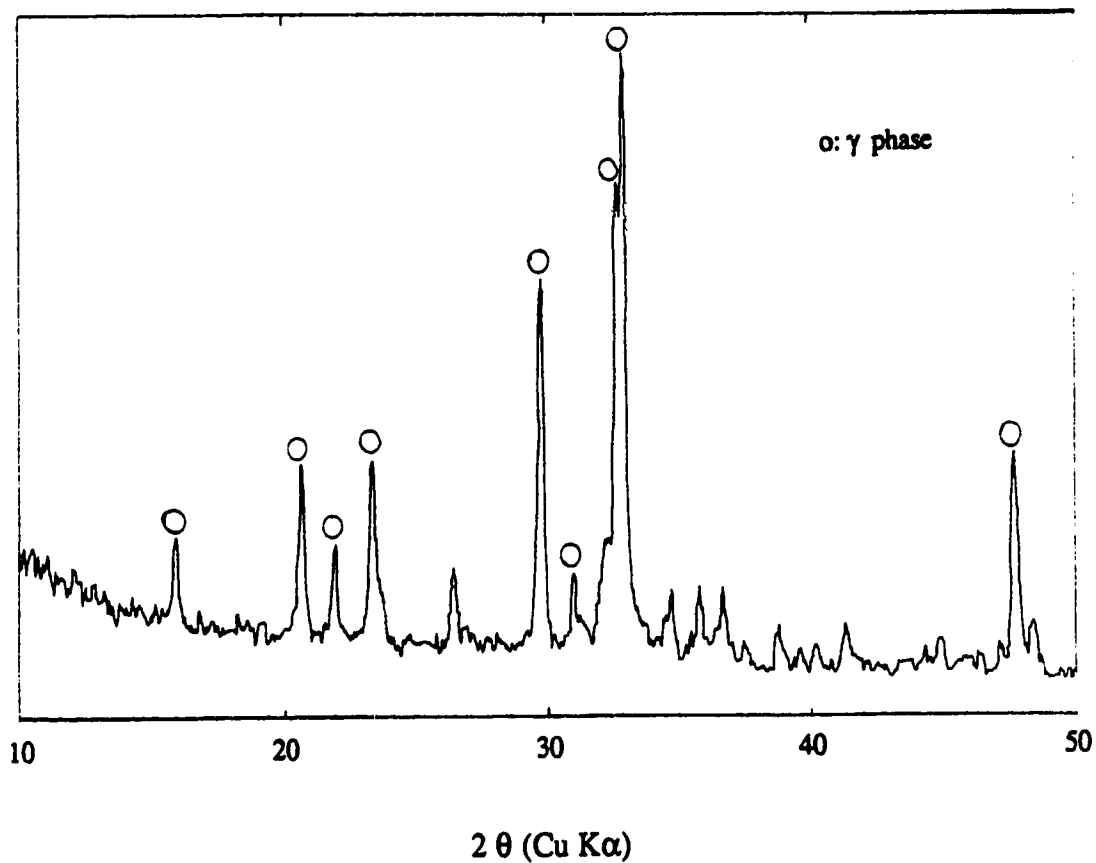


Figure 3.7 X-ray diffraction pattern for Ca_2SiO_4 .

Figure 3.8 shows the patterns for the two HA powders. All main peaks for HA-Bioland were identified as HA, according to file #9-432. The strong lines, indicated on the spectrum, are as follows: 2.81, 2.78, 2.72, 3.44, 1.84, 1.94, 2.63, and 2.26. However, the main constituent of HA-Toronto was β -TCP, together with some HA. The strong lines for β -TCP, according to file #9-169 are as follows: 2.88, 2.61, 3.21, 3.45, 1.73, 5.21, 2.75, and 1.93. In any cases, HA-Toronto was discarded due to its poor flowability.

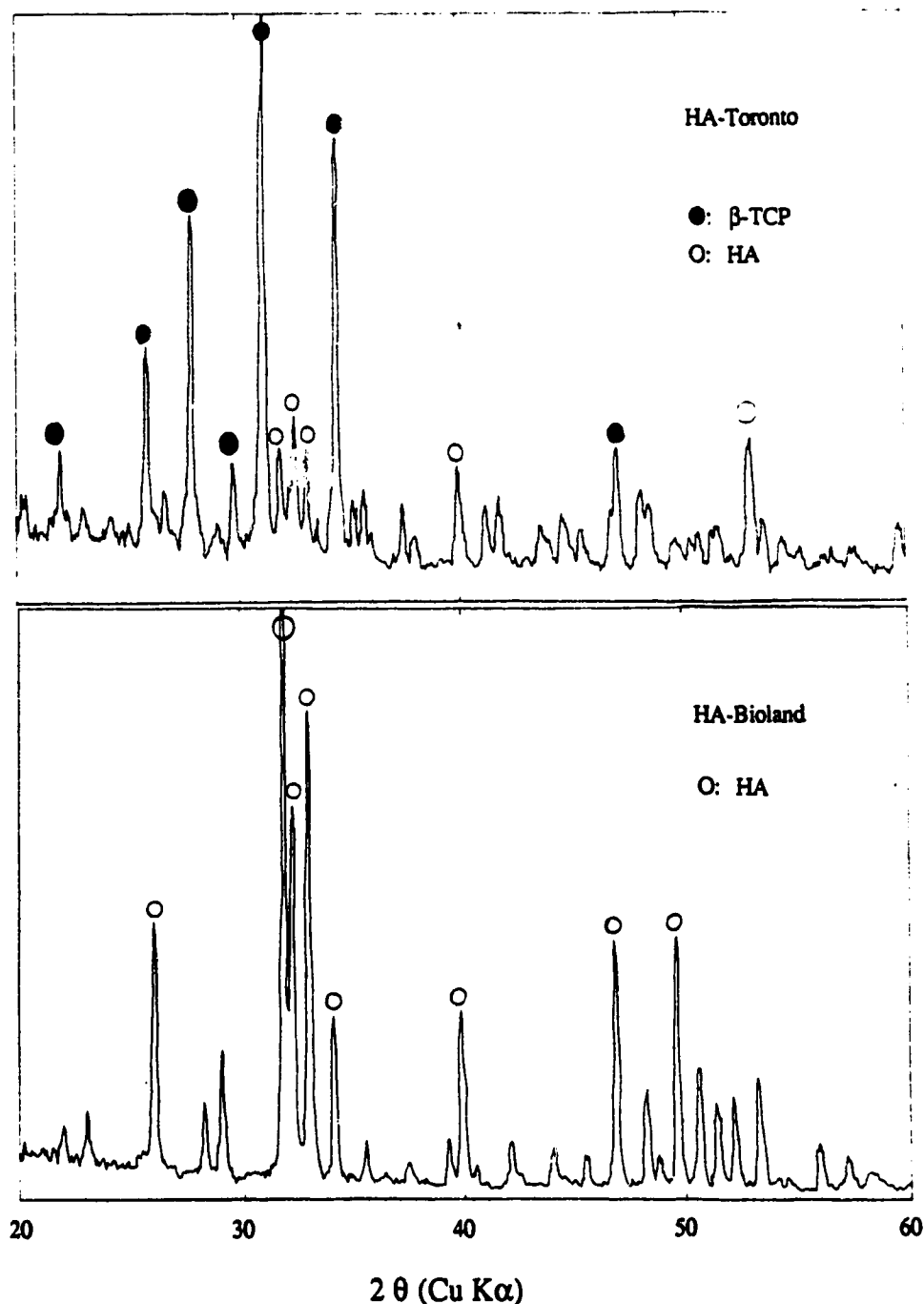


Figure 3.8 X-ray diffraction patterns for HA-Toronto (top) and HA-Bioland (bottom).

3.1.4 Particle Morphology

Photomicrographs of the raw powders were taken with a Reichert-Jung MeF3 optical metallograph. Although the metallograph is not ideal for examination of powder particles, it provided a comparison of the morphology of the powders. The pictures of the three powders, all taken at the same magnification, illustrate the differences. Raw HA-Toronto powder, as seen in Figure 3.9, are very small particles (rather spherical in shape, as seen later at higher magnification). Some agglomerates are also seen on this picture, explaining the bimodal particle size distribution observed in Figure 3.1. By contrast, the HA-Bioland raw powder, shown in Figure 3.10, had very coarse grains, with a blocky shape. Finally, the Ca_2SiO_4 powder, shown in Figure 3.11, had particles of intermediate size and mostly rounded in shape.

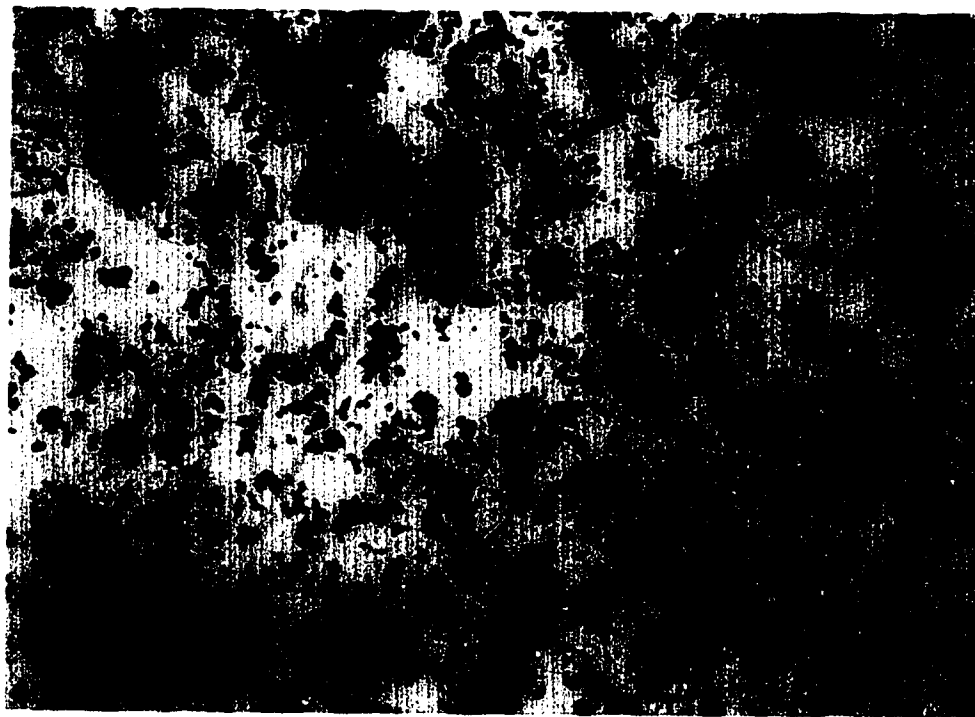


Figure 3.9 Raw HA-Toronto powder. 112 X. 100 μm



Figure 3.10 Raw HA-Bioland powder. 112 X. 100 μm

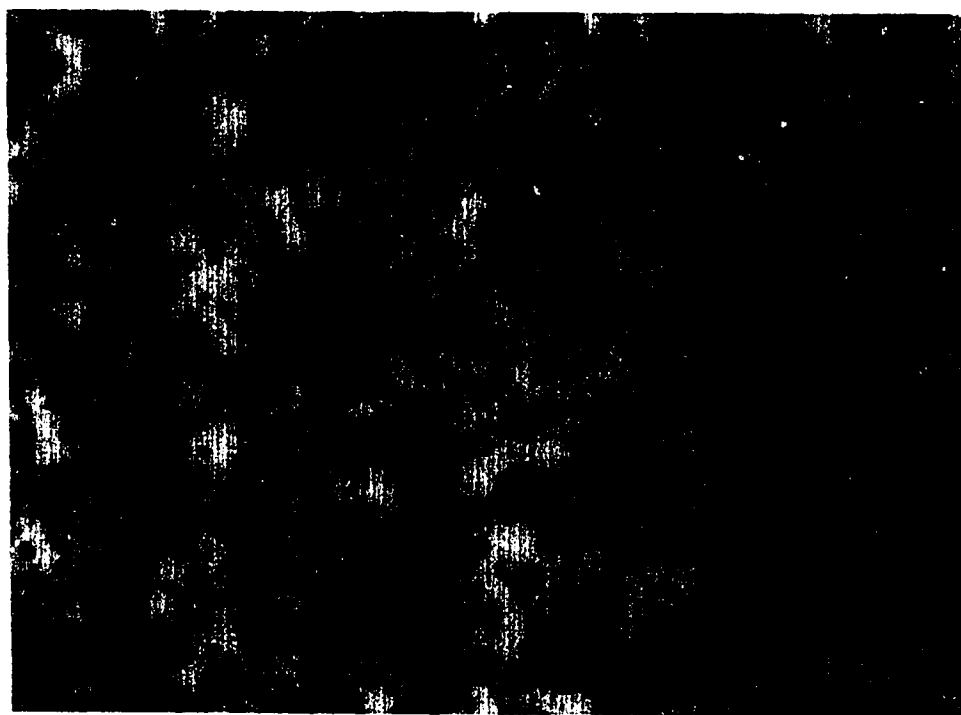


Figure 3.11 Ca₂SiO₄ raw powder. 112 X. 100 μm

3.2 Plasma Spraying

3.2.1 Spraying Parameters

The plasma spraying process requires optimizing many parameters, as shown by Heimann et al.(1990-a)[138] and (1990-b)[139], to obtain suitable coatings. In this project, the parameters studied were as follows:

- amperage
- arc gas pressure,
- auxiliary arc gas pressure
- carrier gas pressure
- powder flow rate
- spray distance.

Amperage was varied from 700 to 900 amperes. Argon, the arc gas, was the main gas used to produce a plasma (dissociation of a gas into ions and electrons). An auxiliary gas, helium, was used to augment the energy obtained in the plasma. A power source provided the energy to dissociate the gases. The heat produced when the gas particles recombine was used to melt the powder. The carrier gas transported the powder into the plasma. Further discussion of the spraying process and the particular spraying system used is found in Appendix.

A new set of spraying parameters was established for each powder. There are no patterns or rules that give optimized parameters since the values will vary for each particle size, size distribution, and morphology. The work related to spraying parameters consisted in optimizing the above six parameters.

The plasma spraying system used in this experiment, a Plasmadyne model 3610-D, requires a minimum of 45-50 psi argon arc pressure. With the argon gas set at this value, a few trials were performed to establish the sprayability of all powders. Two types of HA were available. The HA-Toronto powder was not appropriate as it did not flow properly through the hose leading to the gun, causing plugging of the system in addition to containing a large amount of TCP. This powder was not used further. The powder from Bioland had good flowing properties, as did the Ca_2SiO_4 powder, and was used for all sprayed specimens.

3.2.2 Specimen Preparation

Conditioning the substrate is essential to the plasma spraying process. The coating adheres to the substrate's roughened surface by a mechanical interlocking of individual particles. The specimens were sandblasted manually in a Pro-Finish™ sandblaster (Empire Abrasive Equipment Corporation) with a coarse alumina/silica mixture until the whole surface was conditioned (*roughened*). An air jet of ~80 psi compressed air removed remaining alumina/silica particles from the specimens' surface. The titanium or titanium alloy specimens were then passivated in 30 vol% nitric acid at room temperature for 1 hour. The purpose of passivation was to restore the oxide layer that might have been altered during the sandblasting operation. The presence of the oxide layer is essential for the future development of the layered coating.

The specimens were rinsed in water and air dried. Surface roughness of each specimen was measured with a Mitutoyo 402 Surftest Series 178 Surface Roughness Tester coupled with a Mitutoyo 402 Surftest Analyzer. Immediately before coating, the specimens were cleaned with a 1,1,1-trichloroethane vapor degreasing process. The specimens were handled with latex gloves until they were removed from the holder, after deposition of the coating. The thickness of the specimens was measured to the nearest 0.01 mm with a Mitutoyo No 2024 digital caliper immediately before installation in the holder. The thickness was measured again after deposition of each coating layer (Ca_2SiO_4 and/or HA) in order to quickly determine the overall thickness of the coating. More accurate measurements of the thickness were obtained by measuring the specimen's cross-section with the scale incorporated into the optical microscope.

3.2.3 Wipe Tests

Preliminary work was performed on roughened steel coupons to determine some possible spraying parameters. These are listed in Table 4.1. First, parameters for Ca_2SiO_4 were investigated. Following visual observation of the substrate and the fact that a large amount of powder was transported without melting into the spray chamber with the first two (out of three) sets of parameters, only the last set was chosen for a wipe test.

When a preliminary set of parameters is established, a "wipe test" is performed with a specimen holder carrying microscope glass slides, using the selected parameters. A total of 6 slides are staged in front of the gun, at a distance of 2.54 cm (1 inch) from each other and the gun is quickly moved in front of the specimen holder, in a rapid movement (the "wipe test"), to produce individual splat particles on the slides. The objective is to determine the best spraying distance for the parameters set, by looking at the shape of individual splats under the microscope. Best splats are well flattened and spread, but not cracked. Two more parameters sets, in particular with an increased amperage and with a lower auxiliary gas content, were evaluated in a wipe test. The three sets of parameters evaluated are given in Table 4.4. The same process was performed with the HA-Bioland powder. Some parameters were first established by spraying roughened steel coupons. These parameters are listed in Table 4.3. The work was continued with microscope glass slides (wipe tests), evaluating a series of parameters sets, as listed in Table 4.5.

3.2.4 Final Spray Parameters

Two sets of spraying parameters were chosen for the Ca_2SiO_4 and for the HA, based on the results of the wipe tests. Pure titanium coupons of 7.7 cm x 2.54 cm x 0.3 cm (3 inches x 1 inch x 0.125) were prepared as described above. Ten coupons were sprayed using the first set of parameters for Ca_2SiO_4 and ten coupons with the second set. The first set of parameters for HA was used to spray five coupons with the first base coat and five coupons with the second base coat. The spraying schedule was as follows:

10 coupons - set #1: Ca_2SiO_4 (#1 to #10)	5 coupons HA set #1 (#1 to #5)
	5 coupons HA set #2 (#6 to #10)
10 coupons - set #2: Ca_2SiO_4 (#11 to #20)	5 coupons HA set #1 (#11 to #15)
	5 coupons HA set #2 (#16 to #20)

One cross-section from each group of specimens was prepared for microscopic examination. A 5-minute epoxy was applied on top of the coating to prevent cracking of the thin coating while cutting the specimen. A Buehler® Isomet™ Plus precision saw was

used to cut all specimens. The cross-sections were prepared for final examination first by mounting in resin with a Buehler Pneumat[®]I mounting press and polishing with an automated Buehler polishing system (Ecomet[®]IV Grinder/Polisher equipped with an Euromet[™]I Power Head). Based on the observation of the microstructure of the four types of coating obtained, one coating system was selected and a variety of coupons were sprayed using the corresponding spraying parameters. The coatings were later characterized.

3.3 Coatings Characterization

3.3.1 Morphology

Coatings microstructure were observed and photographed on a Reichert-Jung MeF3 optical metallograph. The optical metallograph confirmed the coating features such as layering of the two sprayed materials (Ca_2SiO_4 and HA), the degree of porosity and the presence or absence of unmelted particles.

3.3.2 Thickness

The specimens were measured before spraying and after the deposition of each material to determine "by difference" the thickness of each coating layer. In addition to these measurements, selected specimens with mounted and polished cross-sections were also measured with a scale incorporated into the optical metallograph. The objective was to compare the two types of measurement systems.

3.3.3 Phase Identification

A x-ray diffraction spectrum of one of the coated specimens was taken directly from the flat specimen, as deposited, another spectrum was taken after exposing the specimen to 330 °C for 24 hours. The objective was to see if the various peaks would become more defined (less amorphous material) after the heat treatment. Otherwise, the procedure was similar to the raw powder measurements.

3.3.4 Chemical Analyses of Interfaces

Observation of the interfaces was performed on the same cross-sections used for phase identification (x-ray). Two cross-sections were observed: one was observed in the as-sprayed condition, and the second in the heat-treated condition. In the observation of the coating systems, the Hitachi S 2700 scanning electron microscope at 20 kV was used in combination with a Link Analytical eXL EDAX system with an ultrathin window detector. For this evaluation, P from the top coat (HA) was measured in the bond coat field and Ti from the substrate was measured in the bond coat field, to detect the possibility of chemical bonding between the layers.

3.3.5 Surface Roughness

The surface roughness of some specimens, sprayed with the parameters used for adhesion strength testing, was measured to provide a general characterization of the obtained coatings. In addition, measurements were also used to help in the selection of spraying parameters for the Ca_2SiO_4 material. The two selected sets of parameters and the effects of preheating were evaluated in terms of the coating build up.

3.3.6 Mechanical Evaluation

A tensile (bond strength) adhesion test completed the characterization of the obtained coatings. This test was based on ASTM C 633 Standard Test Method for Adhesion or Cohesive Strength of Flame Sprayed Coatings^[89], but with some modifications, as developed by Dr.R.Pilliar, from Toronto^[115, 116]. Variations to the test include using a smaller specimen size ("test buttons"), 12.57 mm (0.495 inch) diameter instead of the traditional 25.4 mm (1 inch) and the choice of the adhesive, Concise[®]-3M, which is a high viscosity dental bonding agent, chosen to prevent adhesive penetration through the porous coating.

The test specimens were bonded, with the adhesive, to a roughened titanium alloy substrate similar to the sprayed substrates. After curing, the specimens were loaded axially in tension at a crosshead speed of 0.1 cm/min. One set of test buttons (thin HA coating, with no bond coat) is shown in Figure 3.12, and Figure 3.13 shows a schematic of the bonded test buttons. Figure 3.14 shows all tensile specimens used in this project, with specimens having thick coatings on the left and specimens having thin coatings on the right.

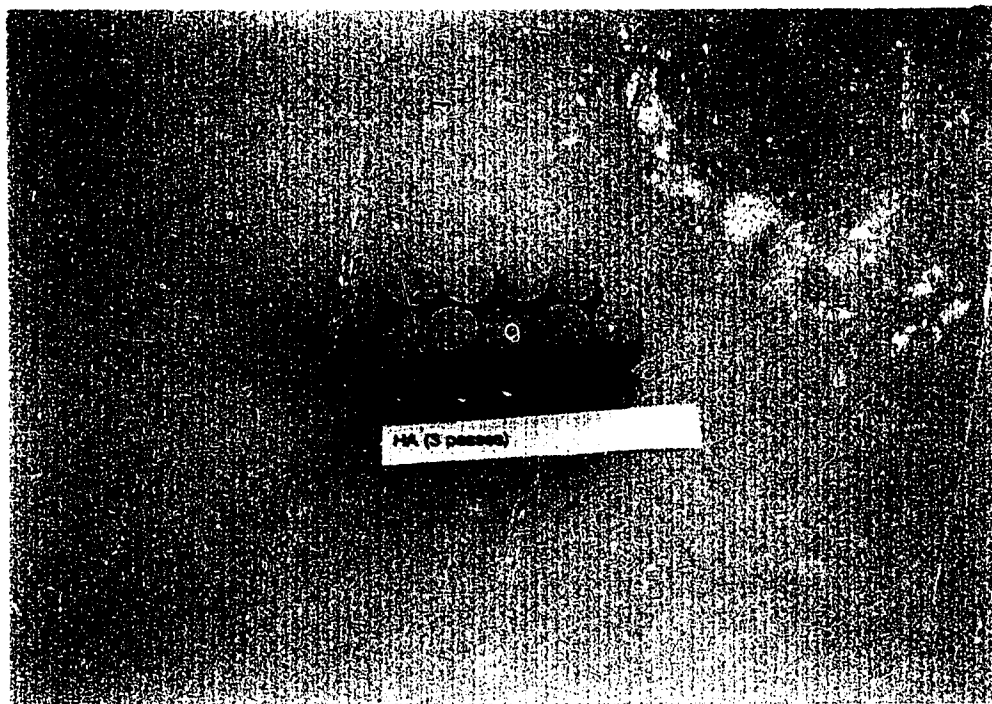


Figure 3.12 Specimens with thin HA coating used for bond strength evaluation.

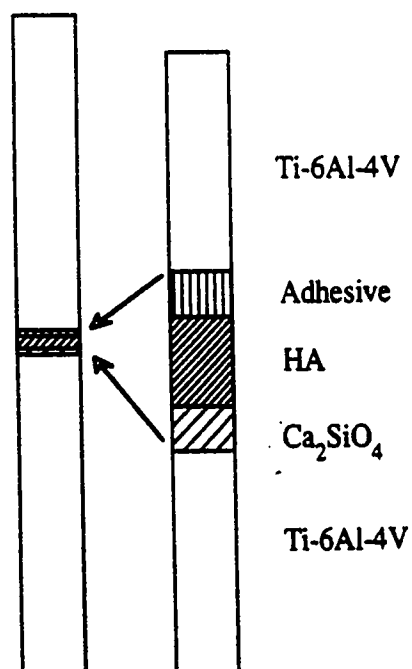


Figure 3.13 Schematic of the bonded structure used to evaluate the bond strength of plasma sprayed coatings.

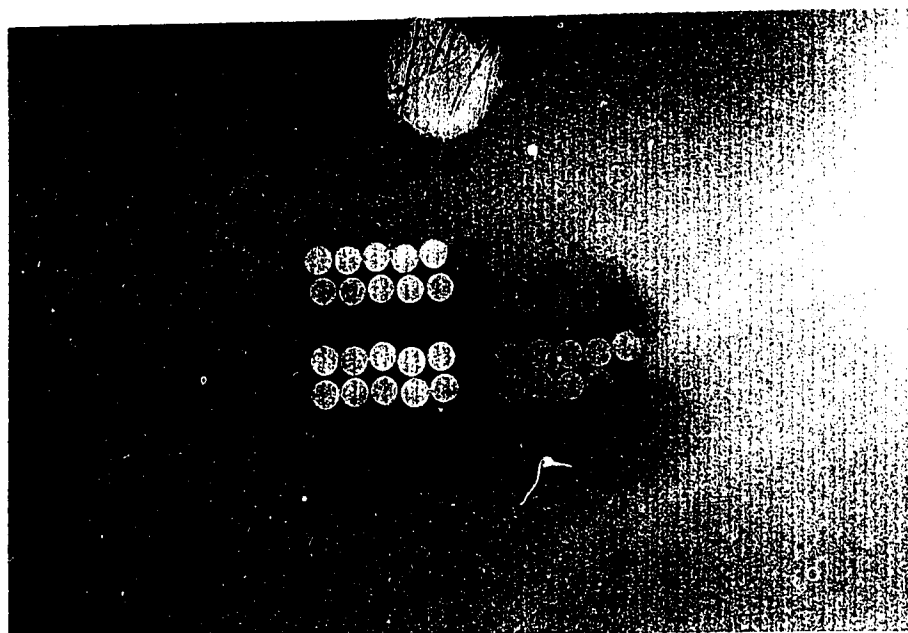


Figure 3.14 Tensile specimens with thick coatings (left) and thin coatings (right).

4. RESULTS AND DISCUSSION

4.1 Preliminary Work

4.1.1 Steel Substrate

Carbon steel coupons were used to investigate the spraying parameters of the first trials with Ca_2SiO_4 powder. The surface of the coupons was prepared by sandblasting before applying the coating. Three sets of parameters were used, as shown in Table 4.1

Table 4.1 Parameters for Ca_2SiO_4 on steel.

Parameters	Set 1	Set 2	Set 3
Amperage (A)	700	750	750
Arc gas/Ar, in l/min (psi)	47.2 (60)	45.8 (58)	45 (58)
Aux gas/He, in l/min (psi)	17 (76)	10 (45)	15.7
Carrier gas/Ar, in l/min (psi)	4.5 (33)	3.5	3.5
Powder flow rate (rpm)	2.00	2.02	2.02
Spray distance (cm)	18.42	19.05	19.05
Voltage (volts)	37.0	37.1	37.1

No visible coating was produced on the first coupon (spraying parameters set #1). After varying some parameters, a very thin coating was observed on coupon #2. An increase in the auxiliary gas produced a thicker coating. Figure 4.1 shows a cross-section of the obtained coating, as observed on coupon #3. These preliminary trials were necessary to help identify suitable parameters.

Using the spraying parameters from set # 3, cylindrical Ti-6Al-4V alloy specimens were used to compare the effect of surface preparation on the quality of the deposit. Three types of surface preparation were compared: sand-blasting with a coarse alumina/silica sand, polishing with a 600 grit ($\sim 40 \mu\text{m}$) finish, and surface blasting with glass beads. Spraying parameters set #3 produced a coating on both the steel coupon and the Ti-6Al-4V coupon sandblasted with the coarse alumina/silica mixture. However, the coating peeled off as successive layers were deposited on the two other types of surface preparation, with the same spraying parameters. The surface roughness of each type of substrate was measured prior to the deposition. Values are provided in Table 4.2, with an average surface roughness of $0.095 \pm 0.014 \mu\text{m}$ for 600 grit polishing, $0.72 \pm 0.04 \mu\text{m}$ for glass beads and $3.11 \pm 0.49 \mu\text{m}$ for coarse alumina/silica. These results confirm observations of the plasma spraying process: the bonding is first of all of a mechanical nature, with each

individual splat interlocking with the asperities of the roughened surface of the substrate. Polishing and glass beads produced a surface too smooth, with less than 1 μm surface roughness, as indicated in Table 4.2, for the splats to remain attached.



Figure 4.1 Ca_2SiO_4 sprayed with parameters set #3. 225 X. 50 μm

Table 4.2 Surface roughness (R_a , in μm) according to surface preparation.

600 Grit	Glass Beads	Coarse Alumina/Silica
0.100	0.71	3.60
0.085	0.77	3.77
0.085	0.70	3.25
0.122	0.75	2.82
0.090	0.67	3.22
0.090	-	2.40
		3.30
		2.50
Aver: 0.095 \pm 0.014	0.72 \pm 0.04	3.11 \pm 0.49

Several spraying parameters were tried for the commercial HA powder using carbon steel coupons. Values are provided in Table 4.3.

Table 4.3 Parameters for HA on steel.

Parameters	Set 1	Set 2	Set 3	Set 4	Set 5	Set 6&7
Amperage (A)	750	750	800	800	850	850
Arc gas/Ar, in l/min (psi)	47.6	47.6	45.1	45	45	45
Aux gas/He, in l/min (psi)	20.3	20.3	19.8	20	20	20
Carrier gas/Ar, in l/min (psi)	4.8	4.8	4.8	4.8	4.8	4.8
Powder flow rate (rpm)	2.0	2.0	2.0	2.0	2.0	2.0
Spray distance (cm)	17.8	14.8	14.8	12.5	12.5	10.5

Note: In the Plasmadyne spraying system, voltage is not an adjustable parameter.

Parameters set #1 did not produce a coating. Parameters set #2, with the coupon closer to the gun, had a thin deposit, as shown in Figure 4.2. The next coupon was sprayed at the same distance (14.8 cm), but with a higher energy, increasing the current from 750 to 800 amperes (set #3). The coating, shown in figure 4.3, was thicker and had fewer cracks running through the thickness, an indication that the particles were in a softer state while reaching the surface. Coupon from set #4 was sprayed with the same parameters as set #3, but closer to the gun (12.5 cm versus 14.8 cm for set #3). Cracks were observed through the coating together with porosity and unmelted particles, as seen in Figure 4.4. Increase in the amperage, from 800 to 850 amperes (set #5) produced a thick coating and, overall, the coating appeared smoother, with fewer cracks: higher energy contributed to the softening of the particles. A cross-section of this coating is shown in Figure 4.5. Coupons from sets #6 and #7 are shown in Figure 4.6 and 4.7 respectively. The coatings were both obtained with the parameters used for set #5, but both were sprayed closer to the gun, at 10.5 cm (versus 12.5 cm for set #5). The obtained coatings were thick with a good spreading of the particles, although some bigger particles did not melt properly, as seen in Figure 4.6, coupon #6 (from set #6).

The above preliminary spraying tests demonstrated "sprayability" of the powders. These tests indicated the adjustment range of the parameters that would yield an acceptable coating. High energy levels were required to melt large particles. This overheated smaller particles causing them to either spread too much on the coupon or vaporize.

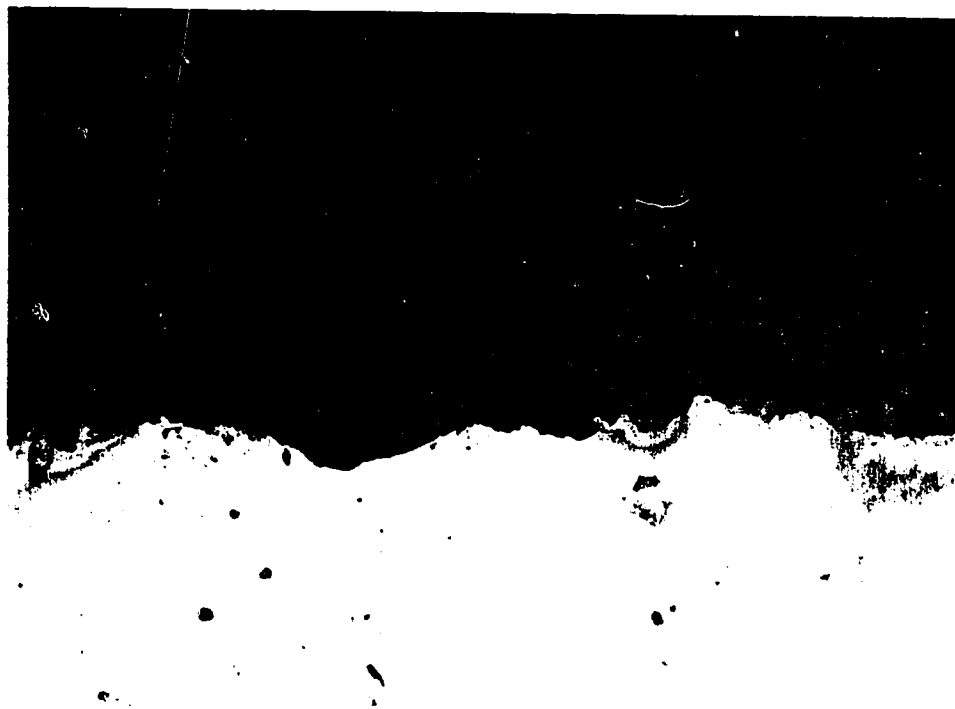


Figure 4.2 HA sprayed with conditions #2. 225 X. 50 μ m

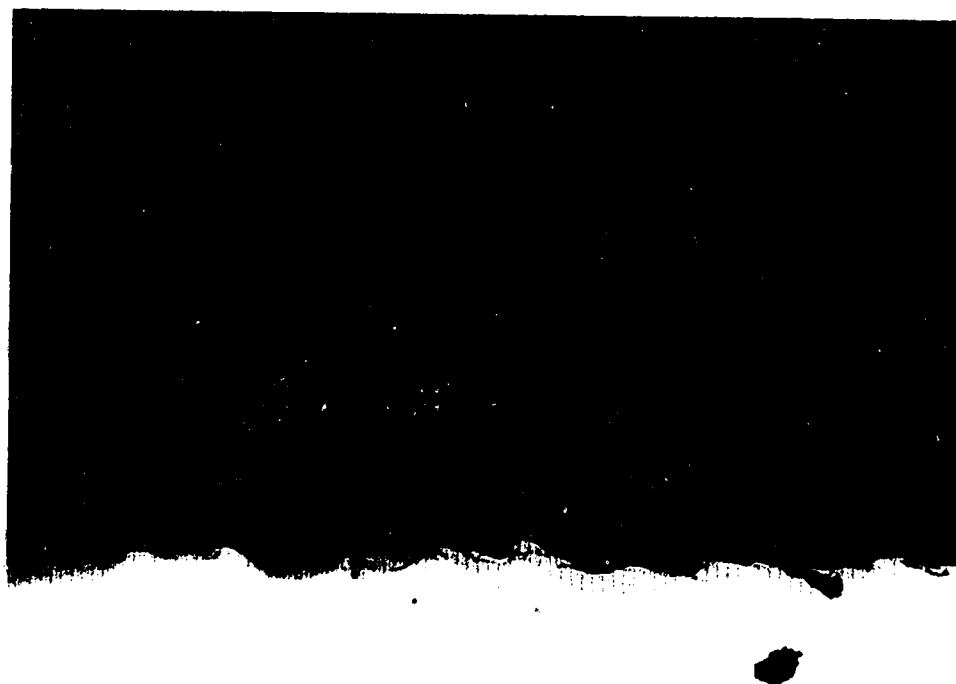


Figure 4.3 HA sprayed with conditions #3. 225 X. 50 μ m

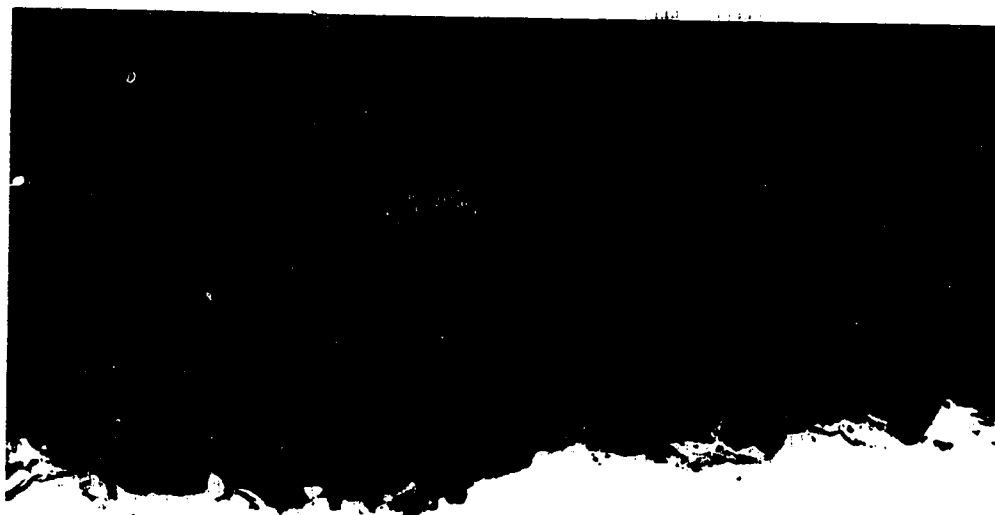


Figure 4.4 HA sprayed with conditions #4. 225 X. 50 μ m



Figure 4.5 HA sprayed with conditions #5. 225 X. 50 μ m

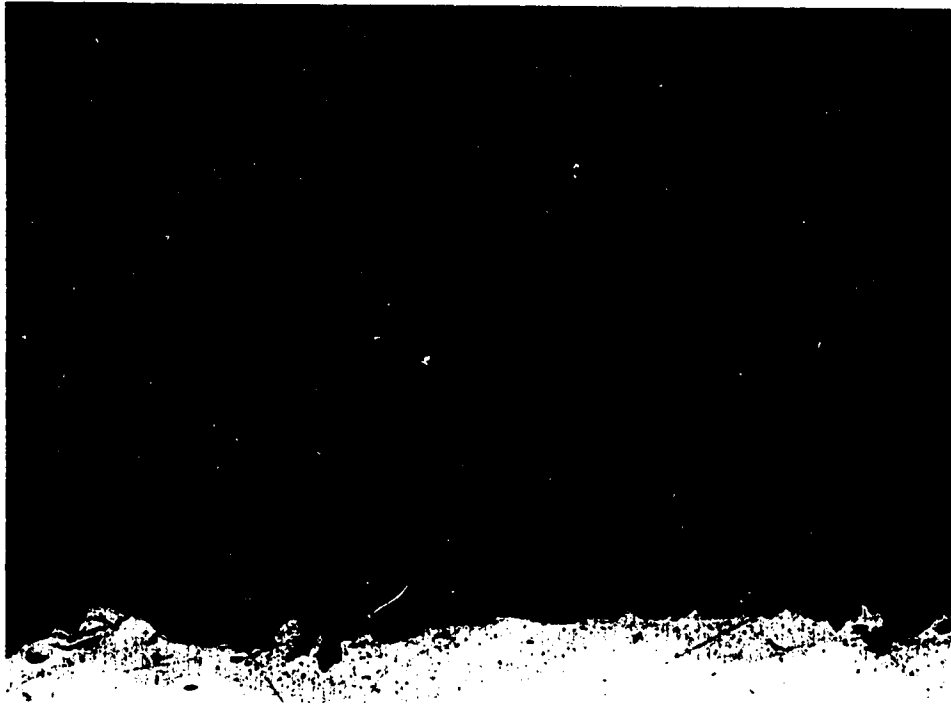


Figure 4.6 HA sprayed with conditions #6. 225 X. 50 μ m



Figure 4.7 HA sprayed with conditions #7. 225 X. 50 μ m

4.1.2 Wipe Tests

The wipe tests were first performed with the Ca_2SiO_4 powder. Using results from the preliminary work on steel coupons, a first set of spraying parameters was selected based on conditions from the previous parameters set sprayed on steel, with some modifications. The carrier gas flow rate was increased and the auxiliary gas flow rate was decreased. The spray distance was varied from 9.52 to 22.2 cm. Only the first three slides (closest to the gun) had a deposit. Further tests were performed with the specimen holder closer to the gun, with slides spread from 5.72 cm to 18.4 cm. In parameters sets II and III the amperage was increased to 900 amperes, to insure a proper particle melting. Table 4.4 lists the spraying parameters for the three conditions investigated. Figure 4.8 shows glass slides used for the wipe tests of the Ca_2SiO_4 powder, grouping the slides according to their spraying conditions. Slides were identified by two numbers, the first number representing the spraying set and the second number representing the position in the specimen holder, with 1 being closest to the gun and 6, farthest.

Table 4.4 Wipe tests for Ca_2SiO_4 parameters.

Parameters	Set I	Set II	Set III
Amperage (A)	750	850	900
Arc gas/Ar, in l/min (psi)	45(60)	39.8(50)	39.8(50)
Aux gas/He, in l/min (psi)	10(42)	10	10
Carrier gas/Ar, in l/min (psi)	4.6(32)	4.5	4.5
Powder flow rate (rpm)	2.0	2.0	2.0
Spray distance (cm)	9.52	5.72	5.72
	to	to	to
	22.2	18.4	18.4

A similar process was used for the HA powder. Several parameters sets were investigated. In the case of HA, the powder flow rate was decreased, because of the larger average particle size compared to Ca_2SiO_4 . The objective was to make sure that each particle softened before reaching the substrate. Spraying conditions are provided in Table 4.5 and Figure 4.9 shows all glass slides used for the HA wipe tests. The HA glass slides were identified in the same manner as the Ca_2SiO_4 slides. All glass slides were carefully examined under an optical microscope to determine the best spraying conditions, based on

the appearance of individual splats. Production of single splats was possible because of the rapid movement of the gun as it sprayed the slides in a single pass.

Table 4.5 Wipe tests for HA parameters.

Parameters	Set I	Set II	Set III	Set IV	Set V
Amperage (A)	900	900	850	850	900
Arc gas/Ar, in l/min (psi)	39.7(50)	39.4	39.4	39.4	40.6
Aux gas/He, in l/min (psi)	20(90)	1.5	20.79	17.7	20.45
Carrier gas/Ar, in l/min (psi)	4.5(33)	4.1	4.12	3.1	4.44
Powder flow rate (rpm)	0.89	0.71	0.95	1.35	1.35
Spray distance (cm)	5.08	5.08	5.08	5.08	10.16
	to	to	to	to	to
	17.8	17.8	17.8	17.8	22.86
Voltage (volts)	35.4	35.0	35.5	34.9	35.8

Two sets of parameters were selected for the Ca_2SiO_4 powder and two sets for the HA powder. Examples of individual splats for each spraying condition selected are provided. For comparison purpose, examples of splats for rejected conditions are also shown. Figure 4.10 gives an example of splats for the first Ca_2SiO_4 parameters set selected (conditions "2.3", set II sprayed at 10.8 cm from the gun). Splats for the other parameters set selected, (conditions "3.3", set III sprayed at 10.8 cm from the gun) are shown in Figure 4.11. In both cases, long arms project from the periphery of the particle. This is a desirable phenomenon observed when softened particles hit the substrate. In comparison, rejected conditions are shown by splats from conditions "1.1", Figure 4.12 and conditions "3.6", Figure 4.13. In Figure 4.12, the central particle had a low viscosity when it hit the substrate and did not form a continuous splat. In contrast, particles shown in Figure 4.13 were too hard and did not spread sufficiently and cracked, as shown by the particle at the top of the picture.

In the case of HA, spraying conditions "5.3" (set V, sprayed at 15.24 cm), shown in Figure 4.14, and spraying conditions "1.2" (set I, sprayed at 7.62 cm), shown in Figure 4.15, were selected. In both cases, arms spread from the periphery of the particles. In comparison, Figures 4.16 and 4.17 show examples of conditions that were rejected. In Figure 4.16, particles remained well formed, with little spreading, indicating a lack of heat (not enough energy). In contrast, in Figure 4.17, the centers of the splats were missing. This happens when a particle is not hot enough or has cooled down before hitting the substrate and the hard center bounces away, producing a porous coating.

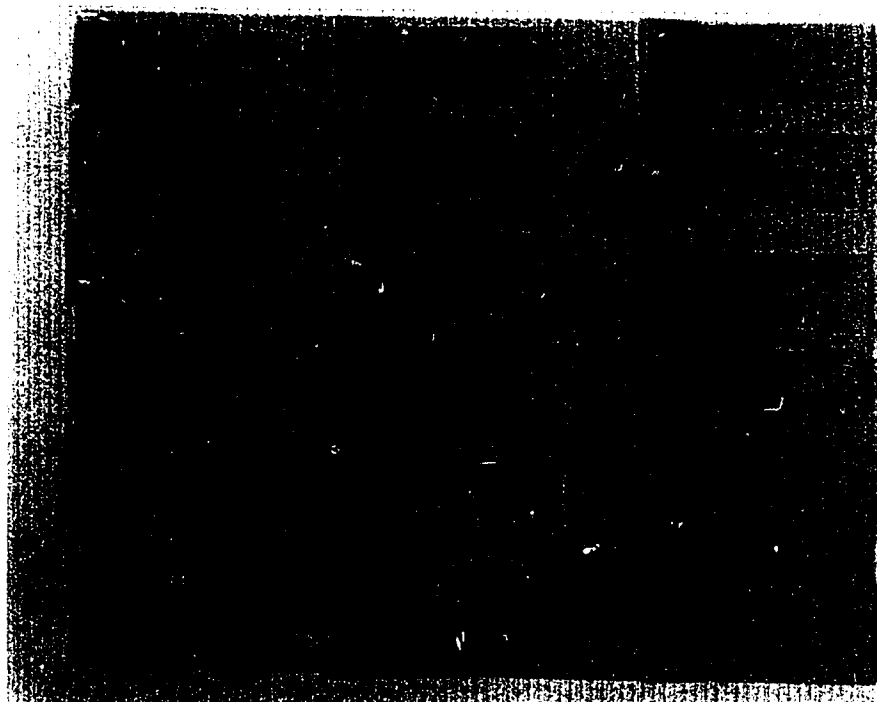


Figure 4.8 Glass slides for Ca_2SiO_4 wipe tests. (Slides are 2.54 cm X 7.62 cm).

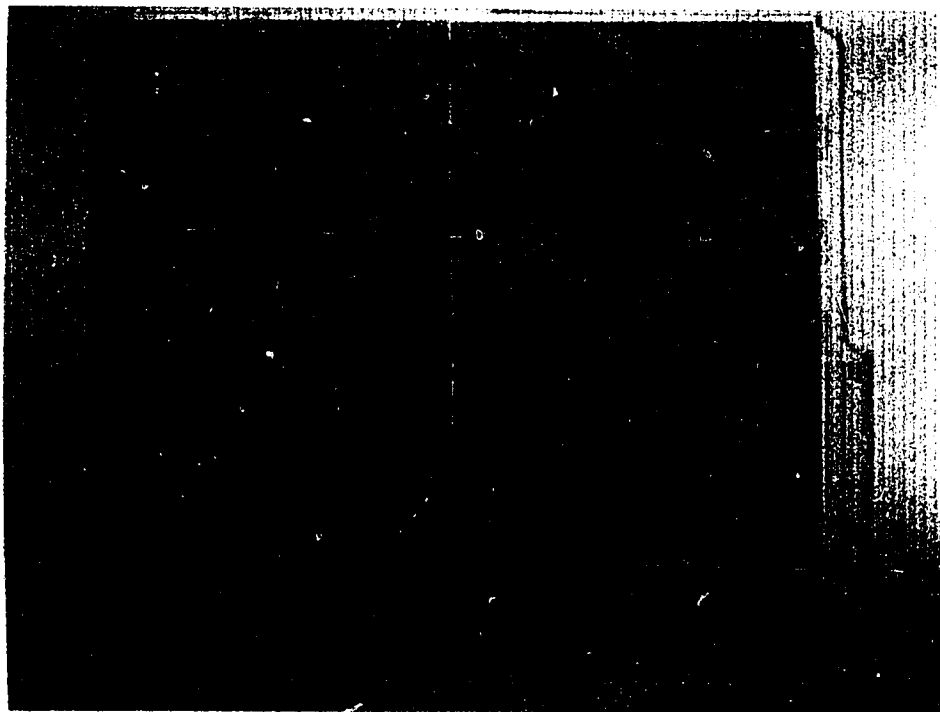


Figure 4.9 Glass slides for HA wipe tests. (Slides are 2.54 cm X 7.62 cm).

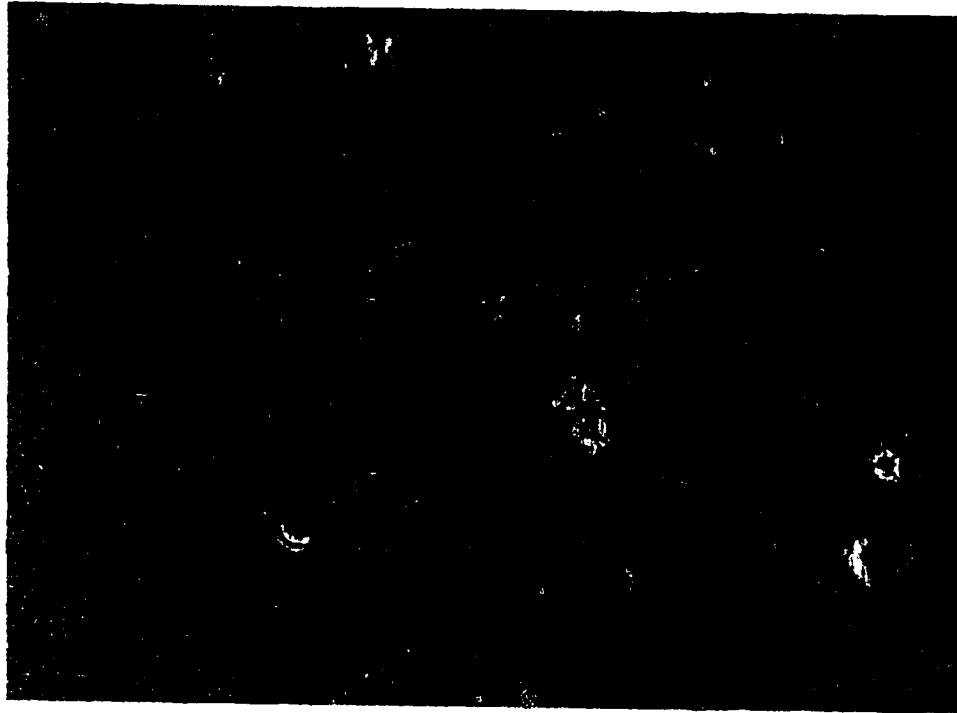


Figure 4.10 Example of a good splat for Ca_2SiO_4 sprayed with conditions "2.3". 340 X.
50 μm

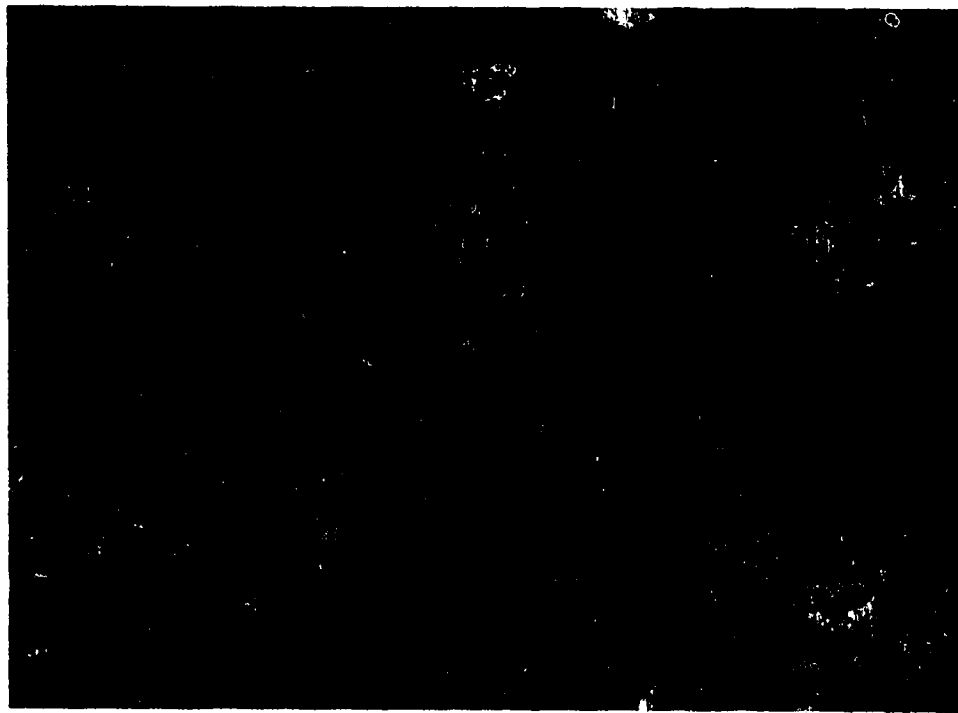


Figure 4.11 Example of a good splat for Ca_2SiO_4 sprayed with conditions "3.3". 340 X.
50 μm

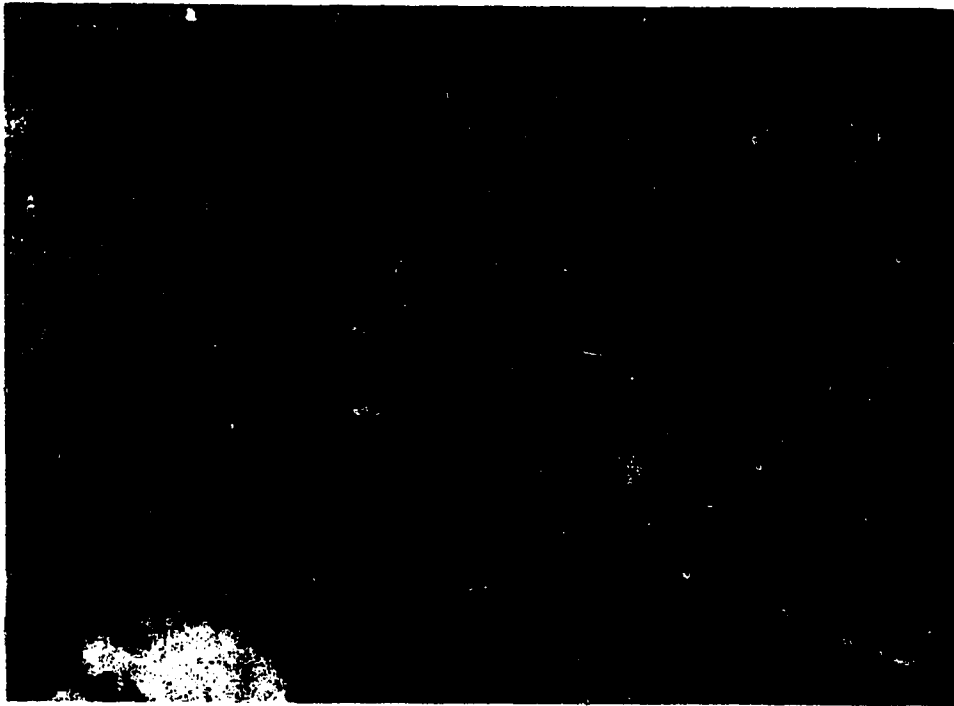


Figure 4.12 Example of splats for Ca_2SiO_4 sprayed with conditions "1.1", which were considered inappropriate. 340 X. 50 μm

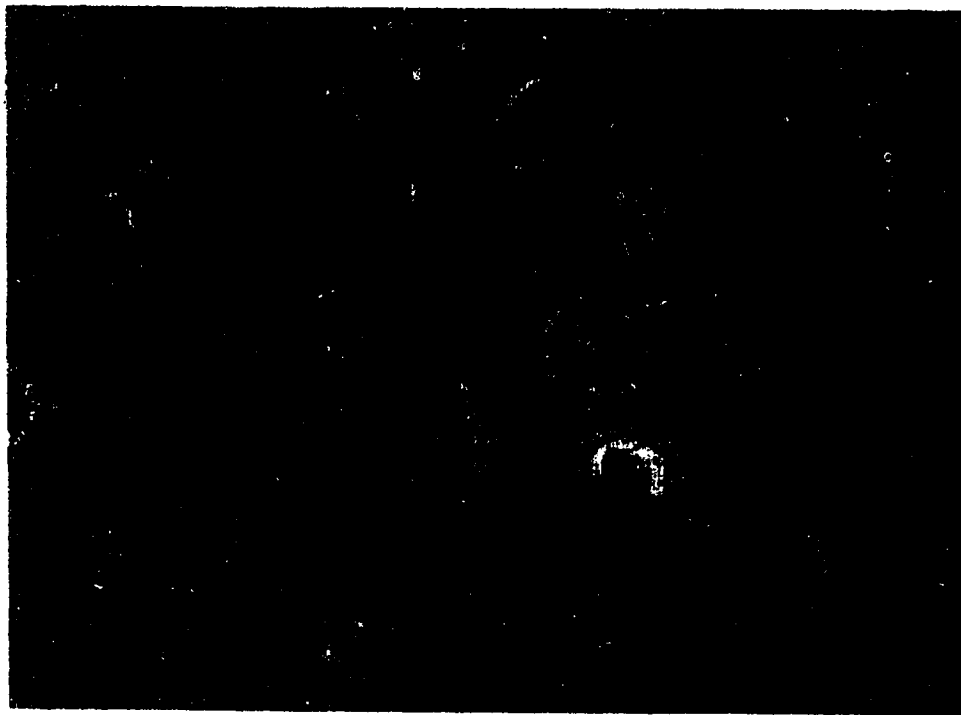


Figure 4.13 Example of splats for Ca_2SiO_4 sprayed with conditions "3.6", which were considered inappropriate. 340 X. 50 μm

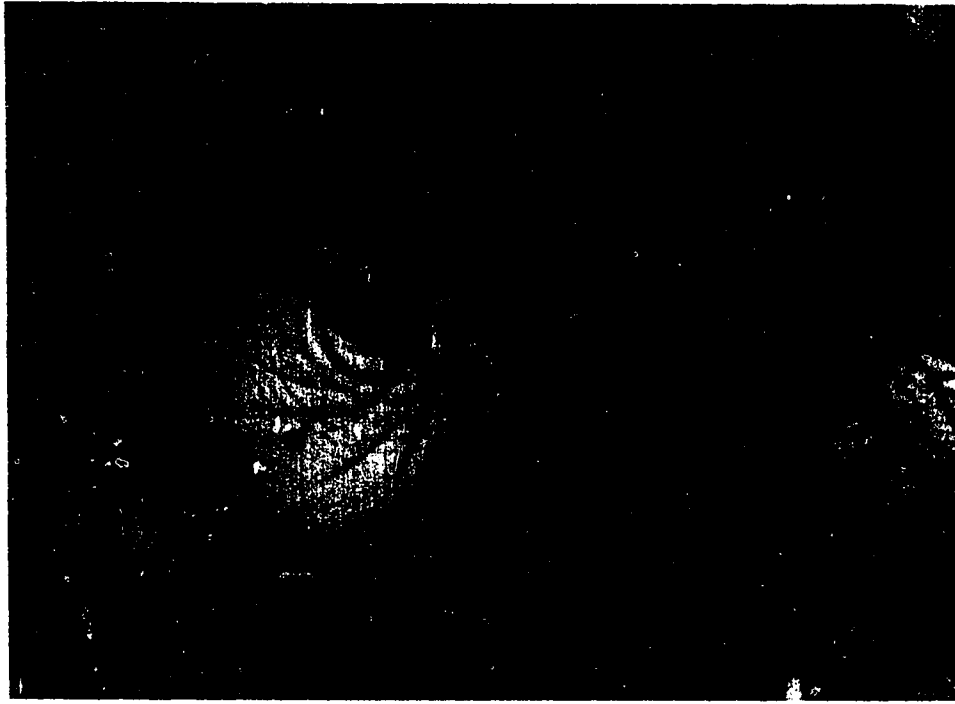


Figure 4.14 Example of a good splot for HA sprayed with conditions "5.3". 340 X.
50 μm



Figure 4.15 Example of a good splot for HA sprayed with conditions "1.2". 340 X.
50 μm

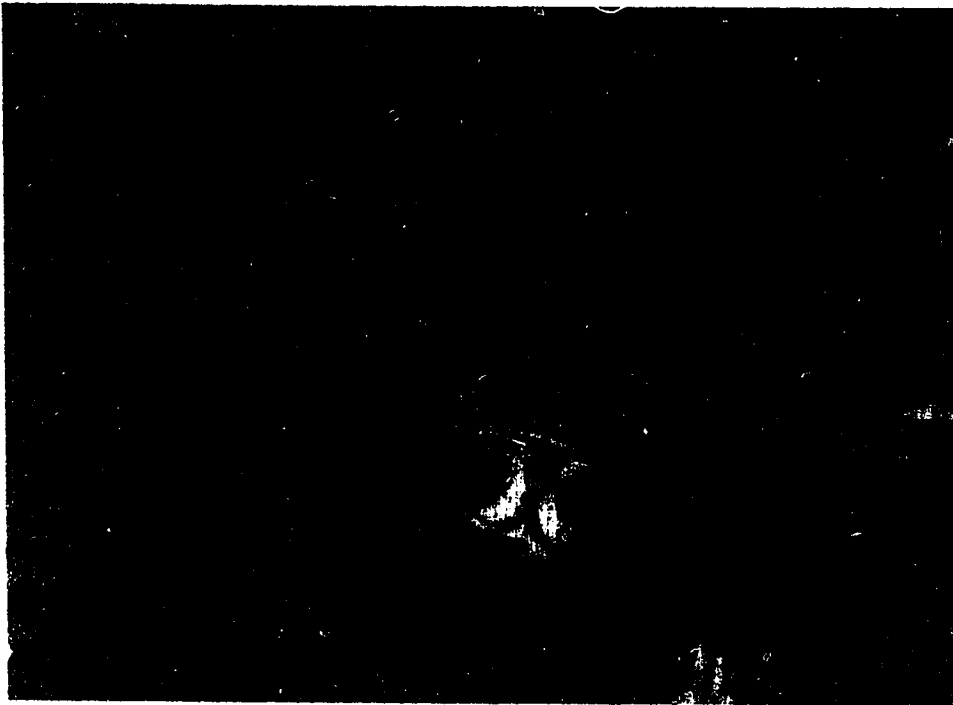


Figure 4.16 Example of splats for HA sprayed with conditions "3.6", which were considered inappropriate. 340 X. 50 μ m



Figure 4.17 Example of splats for HA sprayed with conditions "4.6", which were considered inappropriate. 340 X. 50 μ m

4.1.3 Pure Titanium Substrate

Parameters retained for spraying both the Ca_2SiO_4 powder and the HA powder, two sets for each powder, are provided in Table 4.6. Parameters' sets were selected with the wipe tests based on the splats appearance, which depended on the characteristics of the plasma combined with the characteristics of the powder.

Table 4.6 Parameters selected for spraying on titanium substrate.

Parameters	Ca ₂ SiO ₄ Powder		HA Powder	
	Set "2.3"	Set "3.3"	Set "5.3"	Set "1.2"
Amperage (A)	850	900	900	900
Arc gas/Ar, in l/min (psi)	40.6	39.8	40.6	39.7
Aux gas/He, in l/min (psi)	10.2	10	20.45	20.0
Carrier gas/Ar, in l/min (psi)	4.5	4.5	4.44	4.5
Powder flow rate (rpm)	1.97	2.0	1.35	0.89
Spray distance (cm)	10.8	10.8	15.24	7.62

Twenty pure titanium coupons of 7.7 cm x 2.54 cm x 0.3 cm (3" x 1" x 0.125") were prepared for spraying, as described in section 3.2.2. Ten coupons (#1 to #10) were sprayed with the bond coat material, Ca_2SiO_4 , conditions set "2.3". Of those ten coupons, #1 to #5 were sprayed with the HA coating with conditions set "1.2" while #6 to #10 were sprayed with the HA coating with conditions set "5.3". Ten other coupons (#11 to #20) were sprayed with the bond coat, Ca_2SiO_4 , with conditions set "3.3". Among the latter ten coupons, #11 to #15 were sprayed with the HA coating with conditions set "1.2" and #16 to #20, with conditions set "5.3". One coupon of each coating system was cut and a cross-section prepared for examination of the microstructure. Figure 4.18 shows remaining coupons having a top coat of HA sprayed with conditions set "1.2". Coupon #14 (second top right) was caught in front of the gun while spraying due to a problem with the specimen carrier. This caused local overheating and breakage of the coating system. Figure 4.19 shows the other coupons with a top coat of HA sprayed with conditions set "5.3". Surface roughness of all coupons was measured (R_a , in μm) before spraying. Values are given in Table 4.7, together with the thickness (in μm) of each layer of the coating system. Thickness of the coupons was measured before and after spraying and the thickness of the coating was determined by difference. With the exception of a few coupons prepared with glass beads or polished with a 600 grit, all coupons in the study were surface roughened with a coarse alumina/silica mixture, resulting in a similar surface roughness in the range of 3.0 to 5.0 μm .

1 15
2 14
3 12
4 11

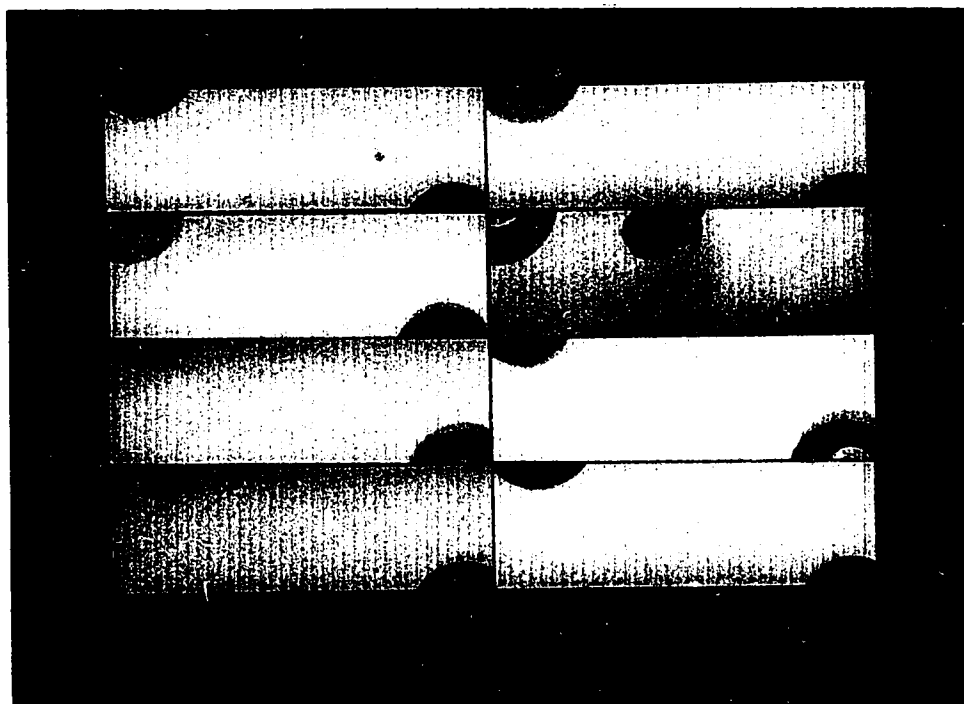


Figure 4.18 Top coat of HA sprayed with conditions set "1.2". Numbers on the side identify the coupons. Coupons are 2.54 cm X 7.62 cm.

16 7
17 8
18 9
19 10

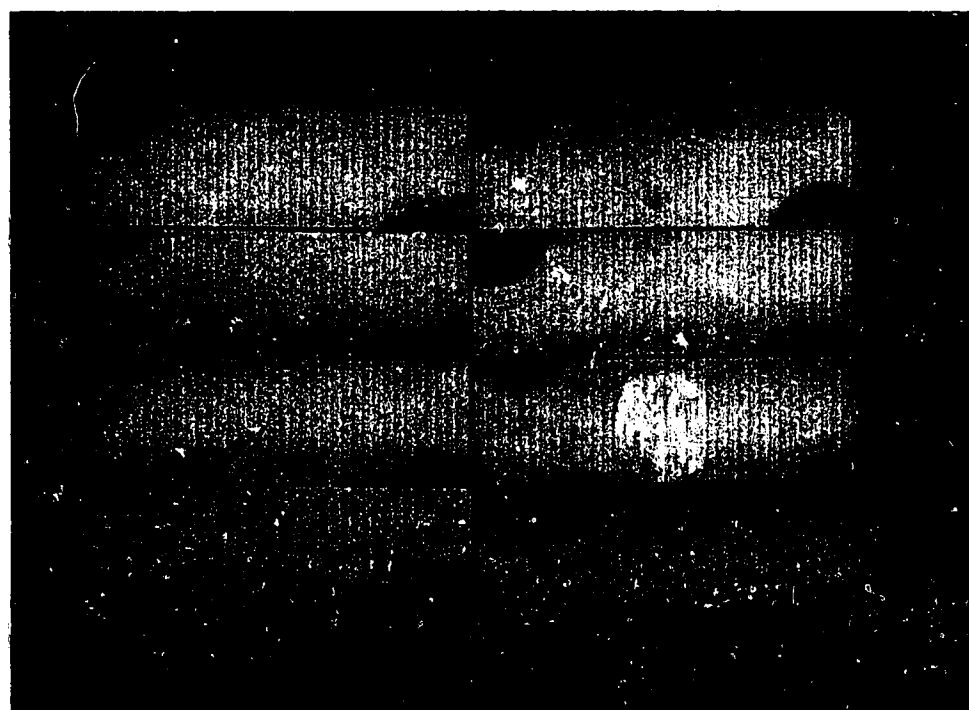


Figure 4.19 Top coat of HA sprayed with conditions set "5.3". Numbers on the side identify the coupons. Coupons are 2.54 cm X 7.62 cm.

Table 4.7 Surface roughness and coating thickness for first series of titanium coupons.

Specimen I.D.	Surface roughness (Ra μm)	Bond coat (μm)	HA (μm)	Specimen I.D.	Surface roughness (Ra μm)	Bond coat (μm)	HA (μm)
1	3.9	101.6	102	11	4.2	88.9	267
2	3.8	101.6	178	12	3.8	152.4	229
3	3.8	38.1	216	13	3.8	254	203
4	3.4	101.6	178	14	3	215.9	-
5	3.5	139.7	140	15	4.1	50.8	165
6	3.6	203.2	203	16	3.8	203.2	254
7	4.3	254	152	17	3.7	203.2	254
8	3.6	165.1	292	18	3.5	152.4	356
9	4	127	241	19	4.1	215.9	229
10	4.8	152.4	267	20	3.7	177.8	279

The coating structure is shown in Figures 4.20 to 4.23. In all figures, the titanium substrate is at the bottom, followed by the Ca_2SiO_4 bond coat and then, the HA coating at the top. In some cases, a gap is seen between the top coat and the mounting resin. The final spraying parameters for HA were selected based on the overall appearance of these cross-sections. Spraying conditions "5.3", as shown with coupon #20 in Figure 4.23, were considered best. The top coating was well developed (good spreading of the splats) with few large cracks, as compared to the HA layer from the three other coupons. In addition, surface roughness of these four coupons (top coating) was measured. Values are given in Table 4.8. For a medical application, a rough surface is most effective in preventing micromotion of the implanted device it covers. Coupons #13 and #20 had a rough surface (table 4.8), but coupon #20 was chosen for its overall appearance.

Table 4.8 Surface roughness of HA for the four coupons.
(all values in μm)

#5:	8.9, 8.8, 8.7	avg.: 8.8 ± 0.1
#13:	10.0, 9.3, 9.3	avg.: 9.5 ± 0.4
#6:	8.5, 8.7, 8.4	avg.: 8.5 ± 0.2
#20:	9.1, 9.7, 10.0	avg.: 9.6 ± 0.5



Figure 4.20 Coupon #5, coated with "Ca 2.3" and "HA 1.2". 225 X.
50 μ m

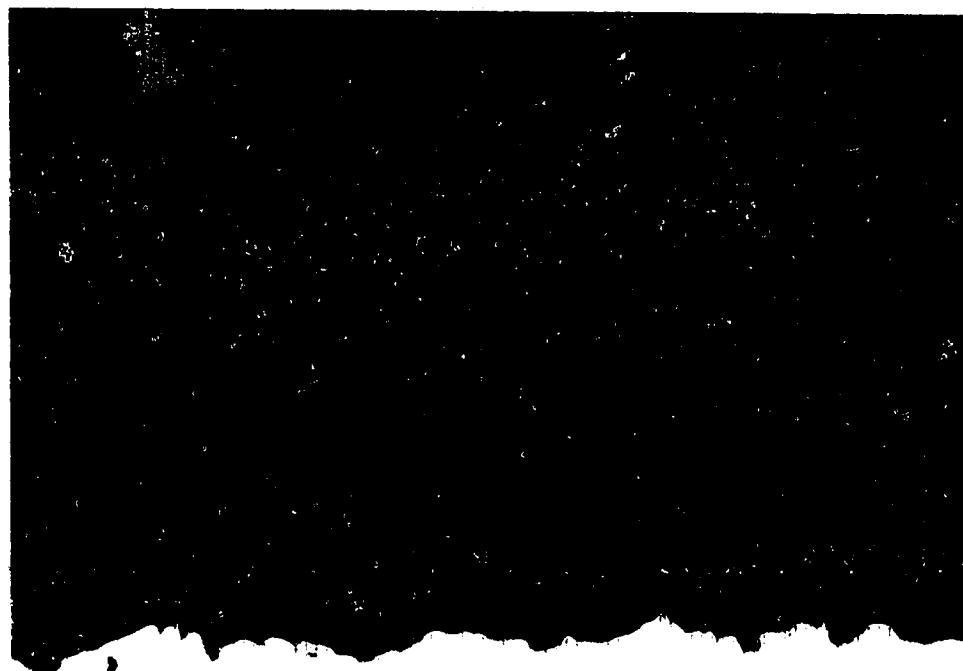


Figure 4.21 Coupon #13, coated with "Ca 3.3" and "HA 1.2". 225 X.
50 μ m

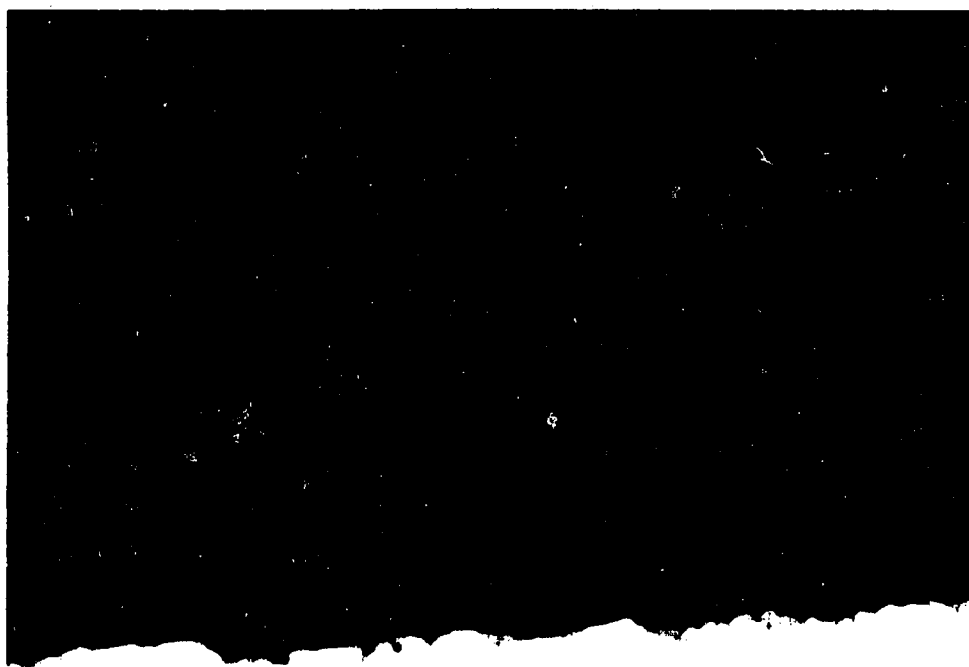


Figure 4.22 Coupon #6, coated with "Ca 2.3" and "HA 5.3". 225 X.
50 μ m

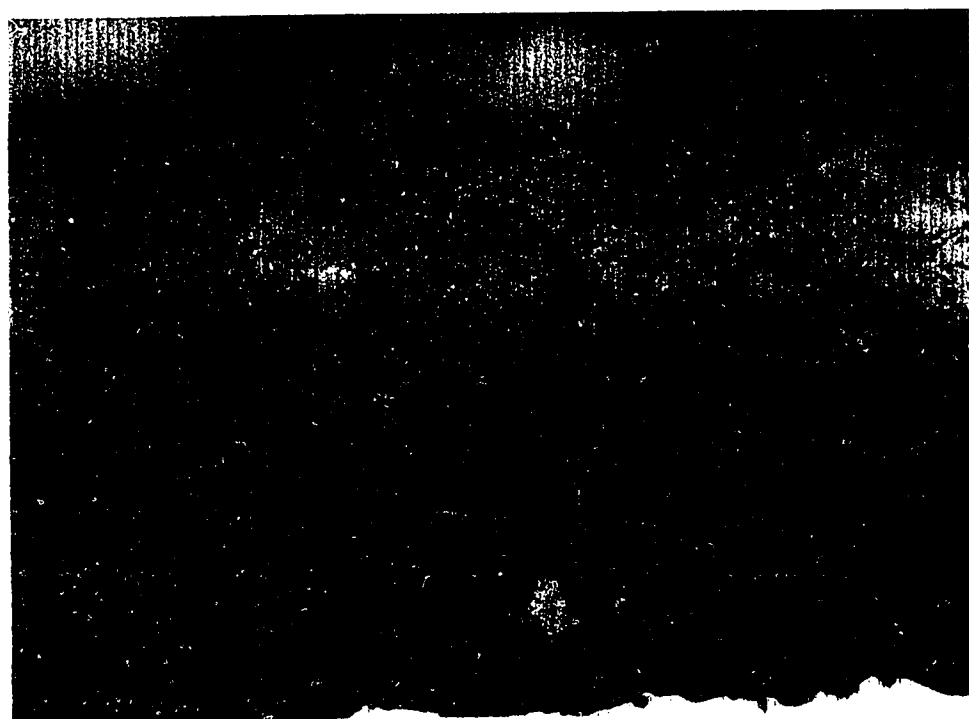


Figure 4.23 Coupon #20, coated with "Ca 3.3" and "HA 5.3". 225 X.
50 μ m

New titanium coupons were sprayed to help optimizing the parameters for the Ca_2SiO_4 bond coat material. Both sets of parameters previously selected ("2.3" and "3.3") were used. Some coupons were sprayed as previously described while other coupons were sprayed only after preheating their surface with the spray gun. One coupon from each set (coupons #82, #84, #87, and #89) was evaluated by measuring the surface roughness of the coatings. The spraying schedule together with the results of surface roughness measurements is provided in Table 4.9.

Based on the results, spraying conditions with preheat were eliminated. Preheat might have caused the surface of the coatings to become smooth by excessive spreading of the individual splats, preventing the next coat (HA) from becoming well attached to the substrate. For example, coupons #84 and #89, sprayed after preheating the surface, had a somewhat smoother surface than non-preheated coupons, as indicated in Table 4.9. Of the remaining two coupons examined, coupon #82 sprayed with conditions "3.3" had a higher roughness value with $7.8\ \mu\text{m}$ versus $7.0\ \mu\text{m}$ for coupon #87 sprayed with conditions "2.3". The final spraying conditions set "3.3" was chosen based on the roughest surface criterion.

Table 4.9 Spraying schedule and surface roughness for Ca_2SiO_4 coatings.

Specimen #(1)	Conditions	Surface Roughness (Ra, in μm)
81 82 83	"Ca 3.3"	7.8
84 85	"Ca 3.3" with preheat of the coupon	6.4
86 87 88	"Ca 2.3"	7.0
89 90	"Ca 2.3" with preheat of the coupon	6.3

(1) Numbers in bold indicate which coupons were further examined

Spraying conditions for the HA powder, set "5.3", were chosen based on the good spreading of the individual splats and on the overall appearance of the deposited coating. Spraying conditions for the Ca_2SiO_4 powder, set "3.3", were chosen because they provided a coating with good splats spreading and because they produced the rough surface required for the next coating layer.

Optimizing the spraying parameters for the two powders was halted at this point. Therefore, all remaining coupons in the project were sprayed with these two sets of parameters. However, it is possible to push further this activity and to perform a statistical multifactorial design matrix for further refining the spraying parameters. In such optimization work, a central point is chosen for each parameter evaluated around which a low value and a high value of the parameter are selected. A series of coupons are sprayed with the central point and the various combinations of high and low values for all parameters. In the present study, the central point would be the two parameters sets identified above, set "3.3" for the Ca_2SiO_4 powder and set "5.3" for the HA powder.

The key to multiple parameter optimization (of plasma sprayed coatings) is the choice of one easily measured variable that reflects the required performance of the coatings. In the oil and gas industry, where plasma sprayed coatings are extensively used for wear and corrosion protection, variables frequently measured for optimization include hardness, wear resistance (as evaluated with test ASTM G-65), toughness, AC impedance measurement (before and after soaking in corrosive fluids), etc. These easily measured characteristics do not reflect the performance requirements of implanted HA coatings. The strength of attachment of the HA coating to the metallic substrate was selected for measurement as an indication of the behavior of the implanted coatings. This will be further discussed in section 4.2.3. However, a true optimization was not performed due to the number of specimens required.

The flow rate of each powder was measured by weighing the amount of powder sprayed into a container at the scheduled carrier gas flow rate for a determined period of time. This allowed the conversion of the "rpm" values of the dial into "grams per minute" units. In the case of Ca_2SiO_4 , the flow rate of 2.0 rpm corresponded to 4.7 g per minute and the HA flow rate of 1.35 rpm corresponded to 12.8 g per minute.

4.2 Coating Systems Characterization

4.2.1 Thick Coatings Morphology

Flat titanium coupons were sprayed with the parameters selected: conditions set "3.3" for the Ca_2SiO_4 bond coat and conditions set "5.3" for the HA top coat. Ten coupons were sprayed with these parameters (#21 to #30) and ten other coupons (#31 to #40) were sprayed with only the HA top coat. Table 4.10 provides the surface roughness measurements of the coupons and the thickness of each coating layer. The layers were obtained by passing the spray gun ten times in front of each coupon in order to get a thick coating. Figures 4.24 and 4.25 respectively show the sprayed coupons. Missing coupons have been used for cross-section examination. Coupon #21 was used to study the effect of heat treatment on the phases of the coating.

Table 4.10 Flat titanium coupons sprayed with "thick" coating layers.

Specimen I.D.	Surface roughness (R_a , μm)	Bond coat (μm)	HA (μm)	Total thickness (μm)
21	3.8	170	200	370
22	4.2	140	190	330
23	3.2	160	200	360
24	3.8	150	190	340
25	4	130	170	300
26	4.2	110	160	270
27	3.2	180	160	340
28	3.8	150	170	320
29	3.9	140	260	400
30	3.5	130	180	310
31	3.4	-	170	
32	3.7	-	170	
33	4.3	-	240	
34	4.2	-	210	
35	3.2	-	240	
36	4.2	-	210	
37	3.7	-	180	
38	3.7	-	200	
39	3.6	-	190	
40	4.2	-	170	

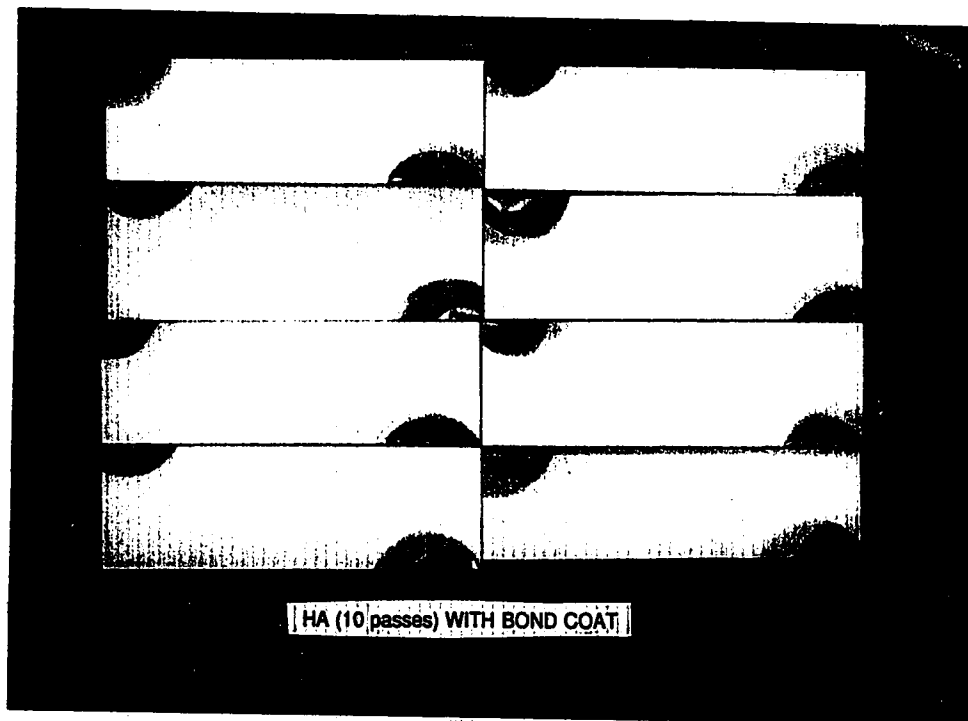


Figure 4.24 Flat titanium coupons with thick HA coating and a thick bond coat.
Coupons are 2.54 cm X 7.62 cm.

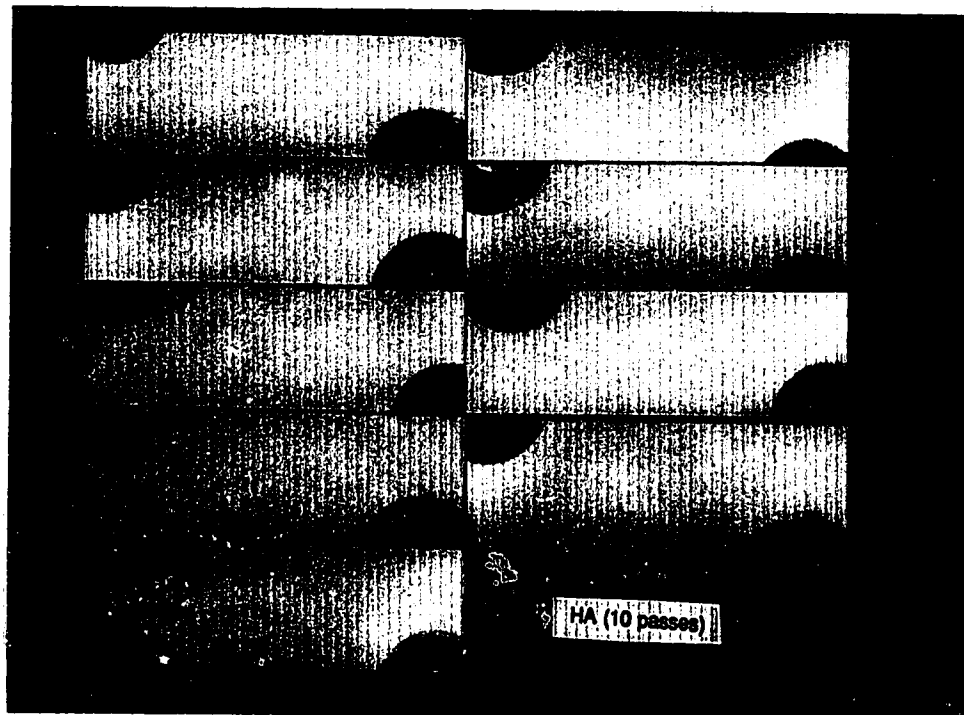


Figure 4.25 Flat titanium coupons with only a thick HA coating.
Coupons are 2.54 cm X 7.62 cm.

One coupon with a bond coat and one coupon without the bond coat was sectioned and examined under an optical microscope. Figures 4.26 and 4.27 show a cross-section of specimen #23. The titanium substrate is located at the bottom, followed by the Ca_2SiO_4 layer, the HA layer and a protective epoxy layer used while cutting the specimen. Figure 4.26 shows the layers of the coating system. In Figure 4.27, the Ca_2SiO_4 layer appears as a single mass. However, the build-up of the individual particles is better defined in the HA top coating, with the occasional presence of unmelted round particles. The complexity of the coating system is illustrated in that picture.

It is of value to note that photomicrographs of polished cross-sections of such coating systems are difficult to obtain as they involve five different materials: titanium metal (substrate), Ca_2SiO_4 , HA, epoxy, and mounting resin, which are all polished simultaneously. In most cases, the camera was focused on the HA layer.

Figures 4.28 and 4.29 show a cross-section of specimen #40, sprayed without a bond coat. General appearance of the HA coating is similar in both coupon #23 and coupon #40, as seen in Figures 4.27 and 4.29.

Coupons #21 to #40 had thick coatings, varying from 170 μm to 400 μm (Table 4.10). Such thick coatings were deliberately produced to facilitate the observation of the cross-sections. Thinner coatings were produced next with the same spraying parameters, in order to satisfy the requirements for medical applications (Pilliar, oral communication).



Figure 4.26 Coupon #23, with thick Ca_2SiO_4 and thick HA layers. 112 X. 100 μm



Figure 4.27 Same cross-section from coupon #23. 225 X. 50 μm



Figure 4.28 Coupon #40, with only a thick HA coating. 112 X. 100 μ m

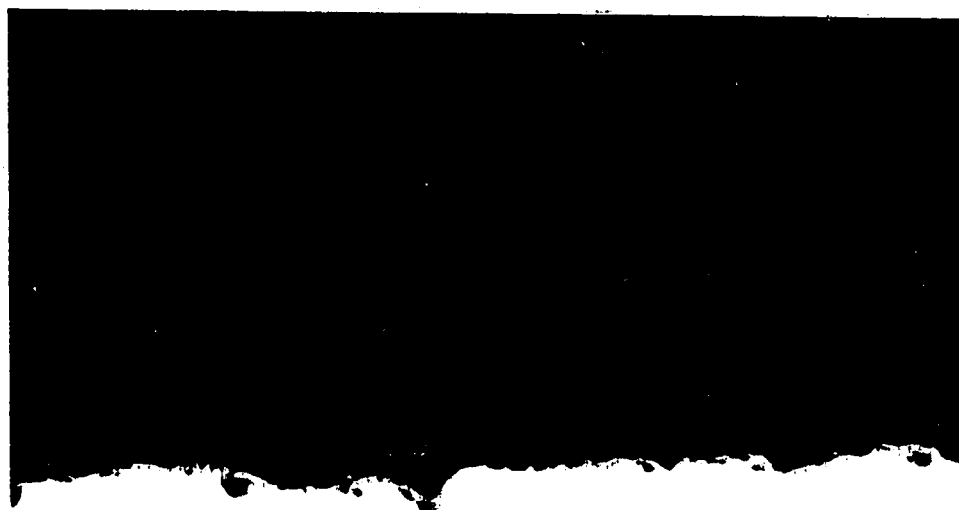


Figure 4.29 Same cross-section from coupon #40. 225 X. 50 μ m

4.2.2 Thin Coatings Morphology

Flat titanium coupons were sprayed with the same parameters used to spray thick coatings (section 4.2.1), conditions set "3.3" for Ca_2SiO_4 bond coat and conditions set "5.3" for the HA top coat. Five coupons (#41 to #45) were sprayed with the parameters and five other coupons (#46 to #50) were sprayed with only the HA top coat. Table 4.11 provides the surface roughness measurements of the coupons and the thickness of each coating layer. The thickness of the coating layers was obtained by the difference in measurements. Thin coatings were obtained by passing the spray gun two times to build up the bond coat followed by two passes with the HA powder. Coatings without a bond coat were built up with three passes of HA powder, since the raw powder contained larger particles, less material was required to produce a specific thickness. Sprayed coupons are shown in Figure 4.30. Missing specimens were used for cross-section examination.

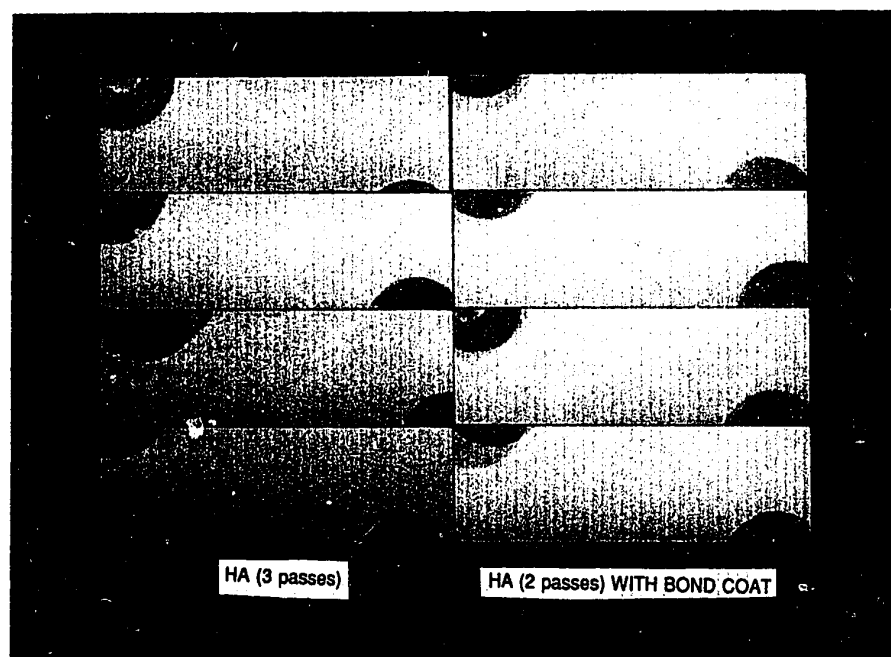


Figure 4.30 Coupons sprayed with a thin coating system: coupons on the left had only the HA coating (3 passes) while coupons on the right had a Ca_2SiO_4 bond coat (2 passes) and the HA top coat (2 passes). Coupons are 2.54 cm X 7.62 cm.

Table 4.11 Flat titanium coupons sprayed with "thin" coating layers.

Specimen I.D.	Surface roughness (Ra, μm)	Bond coat (μm)	HA (μm)	Total thickness (μm)
41	3.5	20	60	80
42	3.8	30	60	90
43	3.9	30	60	90
44	3.9	10	60	70
45	4.0	30	50	80
46	4.0	-	80	80
47	4.1	-	80	80
48	4.0	-	60	60
49	3.7	-	70	70
50	4.1	-	70	70

As seen in Table 4.11, the overall coating thickness was substantially decreased by reducing the number of gun passes. Coating thickness varied from 60 to 90 μm , for the thin coating system, with an average value of $77 \pm 9.0 \mu\text{m}$.

One coupon with a bond coat and one coupon without the bond coat were cut and the cross-sections examined under an optical microscope. Figures 4.31 and 4.32 show a cross-section of coupon #45. The titanium substrate is located at the bottom of the picture, followed by the Ca_2SiO_4 layer, the HA layer, and a protective epoxy layer used while cutting the specimen. Although the coatings are quite thin in this series (coupons #41 to #50) with an average of $77 \pm 9.0 \mu\text{m}$, the coating on coupon #45 appears dense, especially Figure 4.32. There is no evidence of gross porosity, but some rounded unmelted particles are seen (in the HA coating).

Figures 4.33 and 4.34 show a cross-section of specimen #47, sprayed without a bond coat. Again, the coating appears dense with low porosity, as seen with the optical microscope. Some unmelted round particles are also observed.

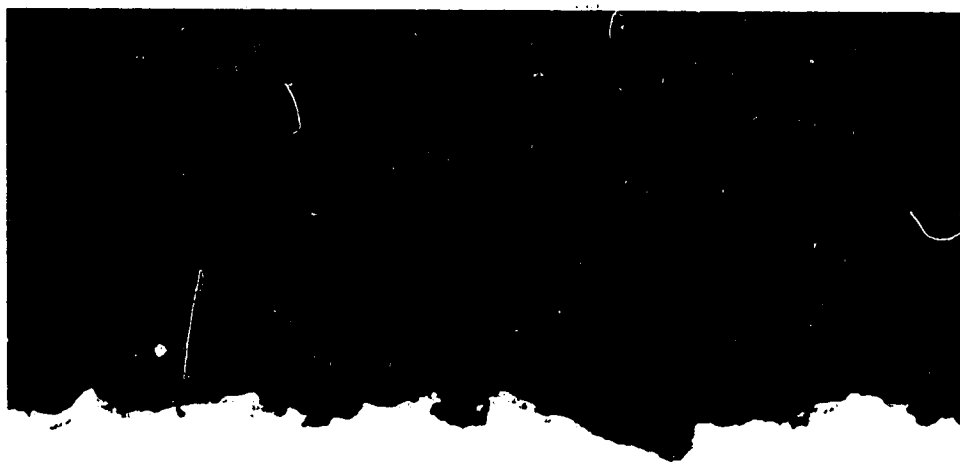


Figure 4.31 Coupon #45, with thin Ca_2SiO_4 and thin HA layers. 112 X.
100 μm

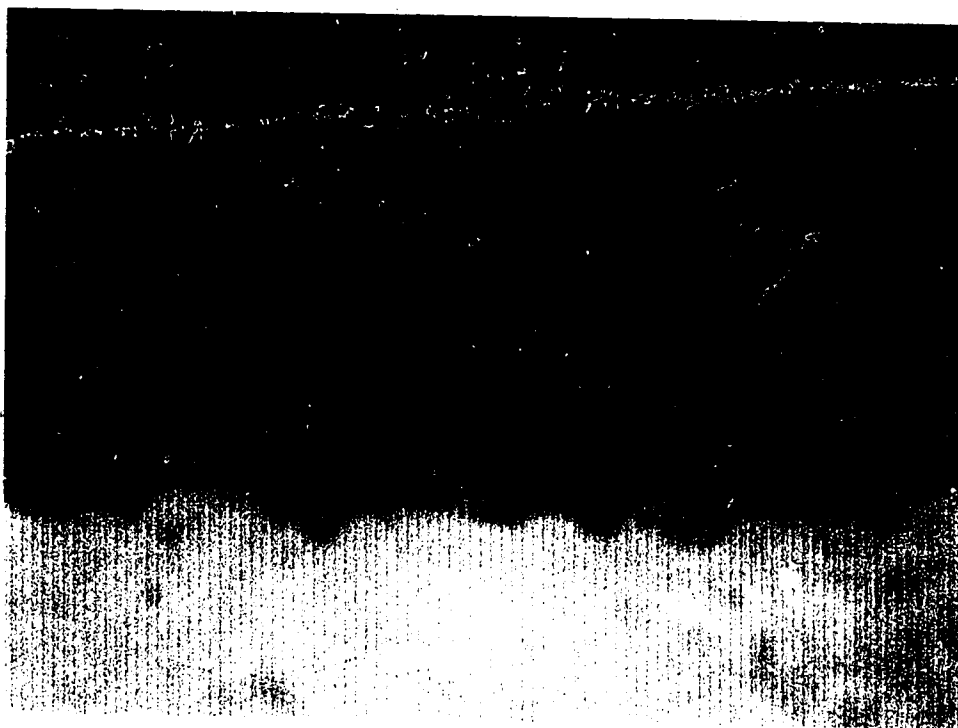


Figure 4.32 Same coupon #45. 360 X. 25 μm

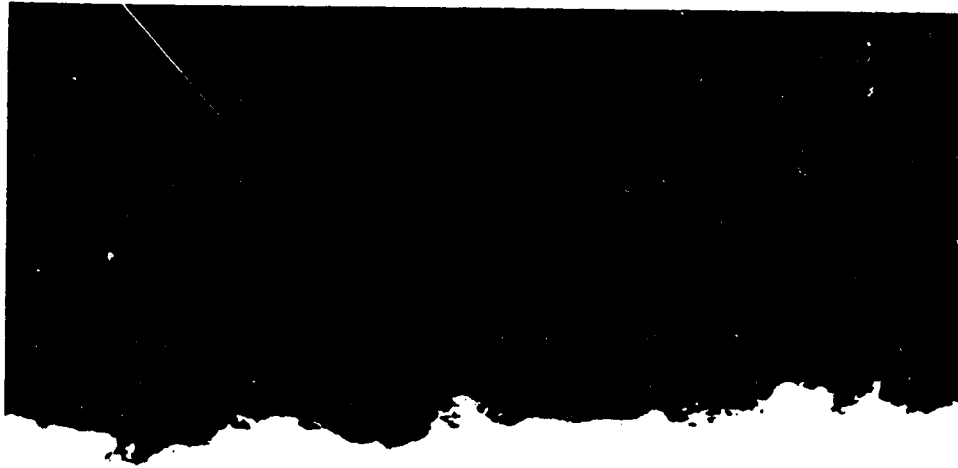


Figure 4.33 Coupon #47, with only a thin HA layer. 225 X. 50 μm



Figure 4.34 Same cross-section from coupon #47. 360 X. 25 μm

4.2.3 Adhesion Test

Using the same spraying conditions used on the flat coupons (sections 4.2.1 and 4.2.2), the buttons (shown in Figures 3.12 and 3.14) were prepared and sprayed to measure the adhesion strength of the coating systems. Surface roughness of the coupons, coating thickness, and tensile strength values are provided in Table 4.12 for thick coatings and in Table 4.13 for thin coatings. In medical applications such as dental implants and in orthopaedics, the value of interest is the shear strength. For example, in the case of a hip implant coated with HA, the shear strength value of the coating / bone interface will control the eventuality of micro movement of the prostheses. Many researchers, as discussed in section 2, have measured this value. They have already demonstrated the positive effect of HA coatings on bone bonding (HA / bone interface). The objective of the present project was to improve the attachment of the HA coating to the metal substrate (substrate / HA interface). Therefore, medical implantations were not required. Adhesion strengths of plasma sprayed coatings have been extensively discussed, in particular by Berndt^[140] and Pilliar^[115, 116].

Table 4.12 Adhesion strength for thick coatings.

Specimen I.D.	Surface roughness (Ra, μm)	Bond coat (μm)	HA (μm)	Tensile Strength (MPa)	Failure Mode
E2	4.9	100	240	15.02	M/HA & (HA/A)
No I.D.	3.7	120	160	5.38	HA/A
3 (open)	4.4	40	170	6.64	A/M & (HA/A)
3 (closed)	4	140	220	6.72	HA/A
15	4.1	180	150	13.12	A/M
B15	4.6	210	110	13.12	A/M
B18	1.6	180	150	9.17	A/M
B19	4.1	100	260	15.49	A/M
Z36	4.4	110	200	15.02	A/M
C37	3.7	140	140	10.67	A/M
E36	2.7	-	230	6.72	HA/A
E38	3.6	-	210	13.91	A/M
E43	4.8	-	360	11.23	HA/A & (A/M)
E45	3.7	-	280	9.8	HA/A & (A/M)
E49	3.6	-	180	3.56	HA/A & (M/HA)
E56	4.2	-	220	11.3	HA/A & (A/M)
E61	3.2	-	120	11.3	M/HA & (HA/A)
E62	3.6	-	210	8.85	A/M
E66	3.9	-	170	7.51	HA/A
E70	5	-	330	9.64	HA/A

Table 4.13 Adhesion strength for thin coatings.

Specimen I.D.	Surface roughness (Ra, μm)	Bond coat (μm)	HA (μm)	Tensile Strength (MPa)	Failure Mode
E21	3.7	10	50	14.23	M/HA & (HA/A&A/M)
#2	3.9	10	30	11.07	HA/A & (M/BC)
E44	3.9	30	70	15.02	M/HA
B29	3.6	50	30	14.47	HA/A+A/M & (M/HA)
D19	3.7	40	80	11.07	M/HA
E3	3.6	20	60	13.6	M/HA & (HA/A +A/M)
B14	3.8	50	80	14.47	M/HA & (HA/A +A/M)
A15	3.6	30	50	15.02	M/HA & (HA/A +A/M)
E39	4.4	10	30	13.99	M/HA & (HA/A)&(HA/A+A/M)
Z34	4.1	-	130	11.3	M/HA
C32	3.3	-	50	14.39	M/HA & (M/HA + HA/A) *
No I.D.	4.2	-	110	9.49	M/HA
A14	3.4	-	90	9.64	M/HA
E24	3.5	-	70	2.21	ERROR IN TESTING
E63	3.7	-	60	11.62	M/HA
E50	3.6	-	80	11.38	M/HA
B20	3.5	-	70	12.49	M/HA
#1	3.9	-	110	10.75	M/HA

Note: *: adhesive penetration

Pilliar et al.(1991)^[115] discussed the importance of choosing a high viscosity adhesive for preventing penetration within the coating during mechanical testing. A standard tensile adhesion test was chosen to characterize the substrate / HA interface. The objective was to obtain comparative values for the strength of adhesion to the substrate with and without the presence of the bond coat. Values obtained with this test are far from absolute since they depend on so many parameters such as the nature of the adhesive used, specimen preparation, specimen alignment, speed of testing, etc. The test specimens consisted of several interfaces: metal (M) / HA, HA / adhesive (A), adhesive (A) / metal (M) when no bond coat was used, or with the presence of a bond coat: metal (M) / bond coat (BC), bond coat (BC) / HA, HA / adhesive (A), and adhesive (A) / metal (M).

Failure modes provided in Tables 4.12 and 4.13 indicate the location within the layers where separation occurred. In some cases it was not possible to distinguish between the bond coat and the HA and, therefore, the failure location was also identified as M / HA. A failure interface in brackets indicates partial failure through this interface. Ideal failure mode would occur at the M / HA, the M / BC, or the BC / HA interfaces for true characterization of the strength of adhesion. In the case of thick coatings, Table 4.12, failures occurred more frequently at an interface with the adhesive itself indicating the modulus of the coating layers was higher than the modulus of the adhesive. This does not reflect on the strength behavior of the coating itself. Because all samples did not break only in the M / HA interface, no estimate can be given for the average M / HA interface strength. Only lower bounds can be provided, that is the M / HA interface strength for thick coatings is $>11.04 \pm 3.86$ MPa with bond coat and $>9.38 \pm 2.91$ MPa without bond coat.

Failure modes for thin coatings, Table 4.13, occurred more frequently at a "proper" interface, M / HA or M / BC. The average adhesion strength was calculated at 13.66 ± 1.54 MPa with the presence of the bond coat and at 10.95 ± 1.08 MPa without the bond coat. This second value does not include two of the specimens, as indicated in the table. One was rejected because of adhesive penetration and the other because of an error in performing the test. It is noticeable that with thinner coatings less spread is observed in the data and that values are higher with a bond coat, which is expected, if chemical reaction has occurred between the titanium substrate and the Ca_2SiO_4 bond coat and between the bond coat and the HA. However, one must remain cautious in the interpretation of these results as the failure mode was frequently of a mixed nature (failure occurred through several interfaces) in presence of the bond coat. No statistical analysis of the results was performed for this reason. Selection of a higher modulus adhesive could help in producing results more appropriate for further statistical evaluation. Berndt^[140] discussed the occurrence of what he calls "cohesive" or "adhesive" failure in term of modulus, but he did not explain why mixed mode failures occur. Results showed the complexity of the layers present during an adhesion test: titanium substrate, Ca_2SiO_4 bond coat (present or not), HA, adhesive, and titanium substrate. During the test, deformation (tensile strain) is applied to the adhesive layer as well as to the other layers, yet they have a different modulus. Therefore, failure is more likely to occur in the material with the lowest modulus, which did often happened in failures where an interface with the adhesive was involved. Filiaggi et al.^[116] have indicated that fracture toughness testing of a similar interface produced less scatter in the data than a corresponding tensile strength test.

4.2.4 Thickness on Cross-Sections

The thickness of each layer was determined by measuring the coupons at a specific location before and after spraying. Even though each series of coupons was sprayed with similar parameters, the coating thickness varied from one coupon to the next. This variation is explained by the way the coupons are sprayed: coupons are moved horizontally in front of the gun with a specimen holder activated with a worm gear. Because the coupon is wider than the spray jet, several passes were required to cover the whole width (up to 4 passes): this was achieved by moving the gun up or down, by steps, after completion of one spray width. Installation of coupons in the holder can vary, resulting in different degree of overlapping of the spraying passes. Coatings thicknesses are found in Table 4.10 (flat coupons, thick), Table 4.11 (flat coupons, thin), Table 4.12 (tensile buttons, thick), and Table 4.13 (tensile buttons, thin).

Coating thickness on flat coupons was also measured using an optical microscope. Measurements were performed for a binotube magnification of 250 X (with a 10 X eyepiece, a 20 X objective, and a microscope "q" factor of 1.25). One example from each of the four coating groups was used, in addition to coupon #21. Results are provided in Table 4.14. Values were the average of five measurements along the specimen width. Results obtained by difference (see Table 4.14) were within the range of the values measured using the optical microscope.

Table 4.14 Coating thickness with optical microscope.

Specimen I.D.	Thickness (μm) (difference)	Thickness Measurements (μm)
23-Ca	160	153 ± 11
23-HA	200	194 ± 13
40-HA	170	174 ± 21
45-Ca	30	38 ± 5
45-HA	50	29 ± 6
47-HA	80	82 ± 18
21-CA	170	162 ± 14
21-HA	200	184 ± 21
21 HT-Ca	170	156 ± 17
21 HT-HA	200	193 ± 26

4.2.5 Phase Identification

One of the specimens with a thick coating, specimen #21, was used to study the effect of the spraying process on the HA powder. Some authors have indicated that phase change sometimes occurs and also that some of the material becomes amorphous after the spraying process. Harris^[73] has indicated that heat treating between 300 and 400 °C for several hours can transform back the amorphous (or microcrystalline) material into a crystalline one. Flat specimen #21 was cut in two and one piece was kept aside while the other half was exposed to a heat treatment (330 °C for 24 hours). The x-ray diffraction spectrum from the HA-Bioland powder, shown in Figure 3.8 (bottom), was compared with a spectrum of the HA coating as deposited and to the spectrum from the heat-treated piece.

In this case, the two x-ray diffraction spectra from specimen #21 indicate that the heat treatment provided was not sufficient to revert the so-called amorphous material into a more crystalline structure. However, although broadening of the peaks was observed, major peaks identifying the HA material are still well recognized in both the as-sprayed and the heat-treated specimen. Figure 4.35 provides the spectra, in a) for the HA-Bioland raw powder, in b) for the HA coating (specimen #21) as-sprayed, and in c) for the HA coating (specimen #21) after 24 hours at 330 °C.

All characteristic peaks for the HA phase structure in HA-Bioland raw powder have been identified. Wolke et al.^[83] indicated that a cooler plasma keeps the HA material in a crystalline phase, as compared to the stability of the various calcium phosphate-based materials. Koch et al.^[85] discussed the behavior of these same materials after exposure to the plasma spraying process. They observed that HA did not change (phase), although the "crystallite" sizes decreased 10- to 100-fold compared to the raw powder. Berndt et al.(1992)^[141] claim that heat treatment of amorphous coatings at 800 °C for 2 hours produces a rise in peak height, suggesting an increase in crystallinity. Most likely the temperature for the heat treatment performed in the present work (330 °C) was not high enough to allow for the growth of the crystallites.

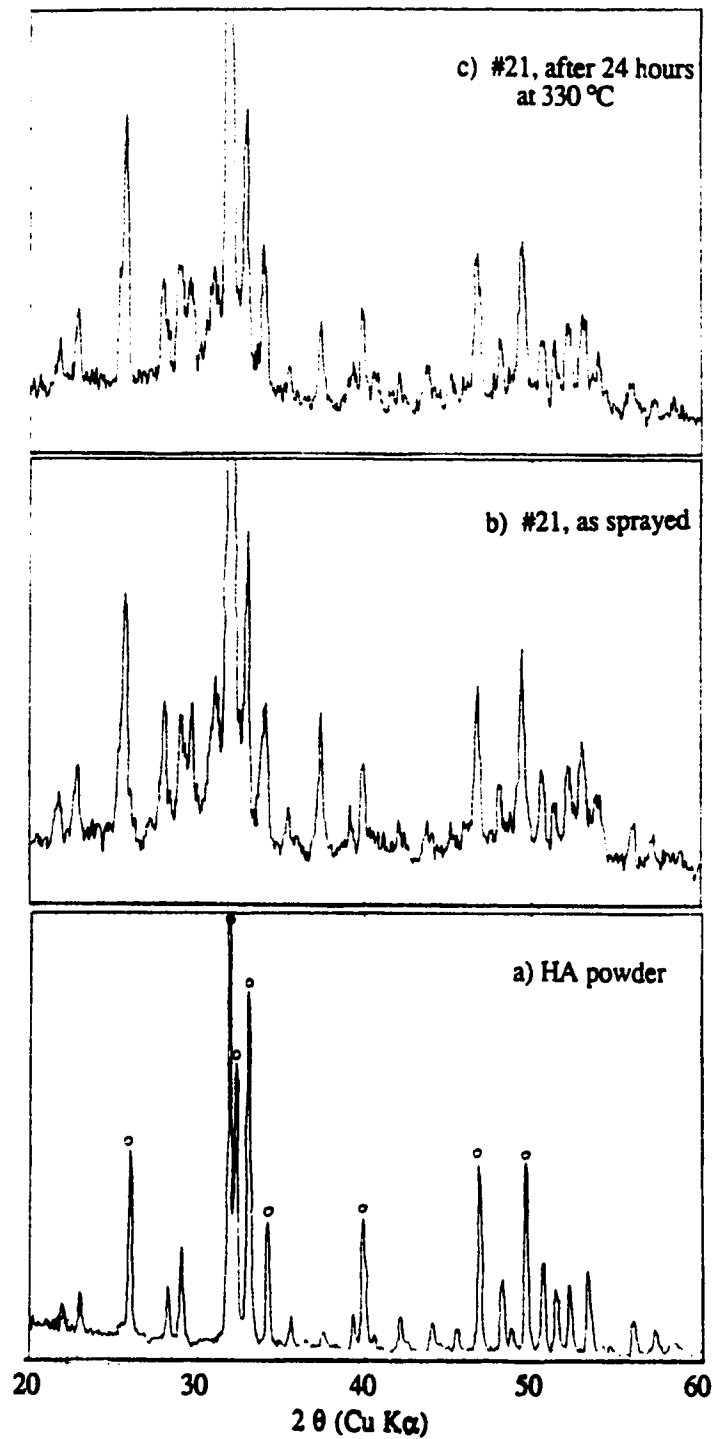


Figure 4.35 X-ray diffraction spectra. a) HA powder; b) HA as sprayed; c) HA after 24 hours at 330°C.

4.2.6 Chemical Analyses of Interfaces

Specimen #21 (with a thick coating) was used to study the possible formation of intermediate materials at the interfaces. Both an as-sprayed piece and a heat-treated piece were examined. One cross-section of each type was observed with the scanning electron microscope, linked to the energy dispersive x-ray analysis system. Point counts, expressed in weight % of the element of interest, were performed on the other side of the critical interfaces: Phosphorus was measured within the Ca_2SiO_4 bond coat layer, below the HA layer, and titanium was counted in the Ca_2SiO_4 layer, above the titanium substrate. The objective was to detect the formation of the intermediate substances such as silico-carnotite, $\text{Ca}_5[(\text{PO}_4)_2\text{SiO}_4]$, between the HA layer and the bond coat layer, or titanite (sphene), $\text{CaTi}[\text{O}(\text{SiO}_4)]$, between the bond coat layer and the substrate (titanium dioxide).

Results for the as-sprayed specimen #21 were as follows:

P:	0.6 μm into bond coat	:0.54 wt%	Ti:	0.5 μm above substrate:	23.06
	1.2	0.42		1.0	14.42
	1.8	0.45		1.5	09.46
				2.0	05.91
				2.5	03.63
				8.0	04.50
				20.0	00.50

The amount of phosphorus measured in the bond coat layer was small but the amount of titanium appeared more significant. It was difficult to conclude on the presence of the intermediate substances based only on these measurements since specimen preparation could produce some smearing of the materials between the layers. Two optical photomicrographs of specimen #21, as-sprayed, are shown in Figures 4.36 and 4.37. Figure 4.38 shows line scans of several elements (O, Si, P, Ca, and Ti) performed on the cross-section of this specimen. A more detailed line scan for Ti and P is provided in Figure 4.39 and Figure 4.40, respectively.

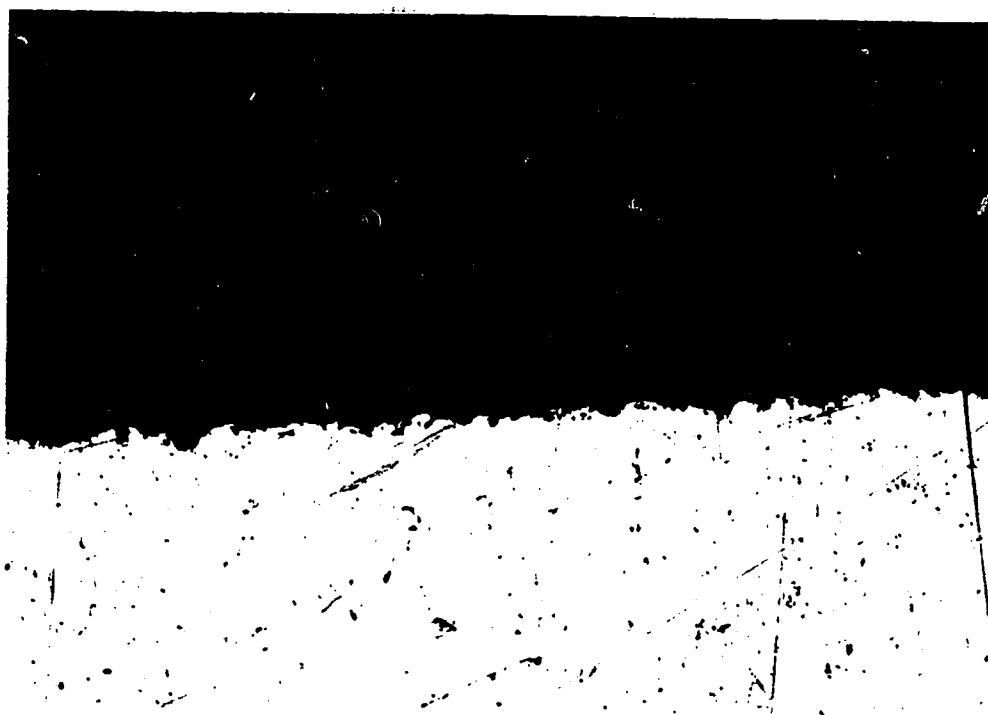


Figure 4.36 Flat coupon #21, as sprayed. 112 X. 100 μ m

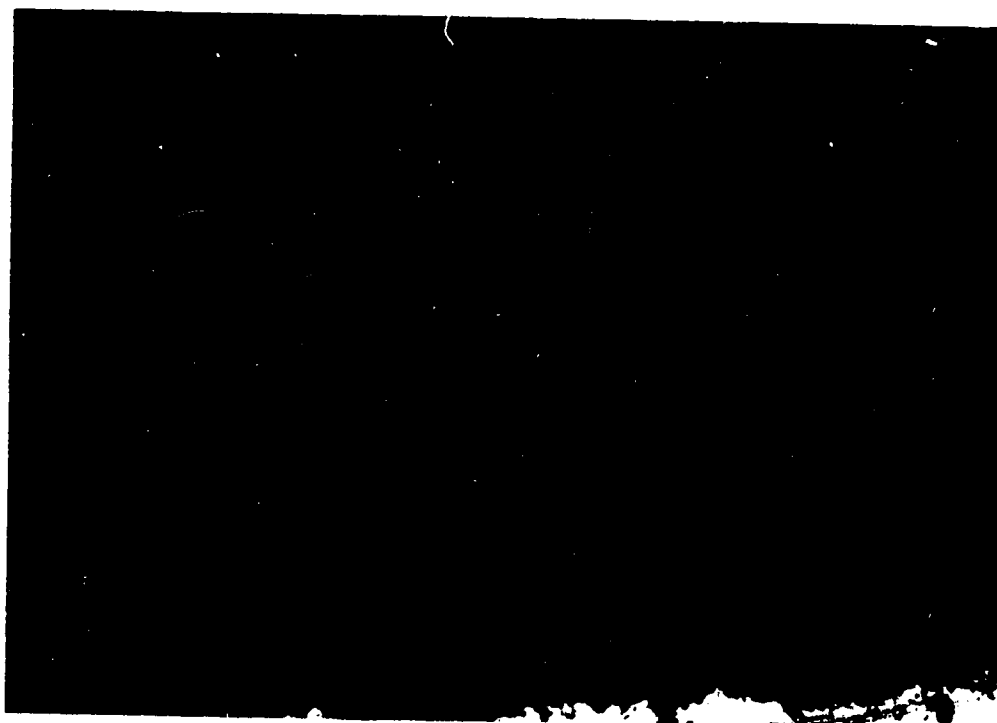


Figure 4.37 Flat coupon #21, as sprayed. 225 X. 50 μ m



Figure 4.38 Flat coupon #21, as sprayed: digital line scans through the cross-section.

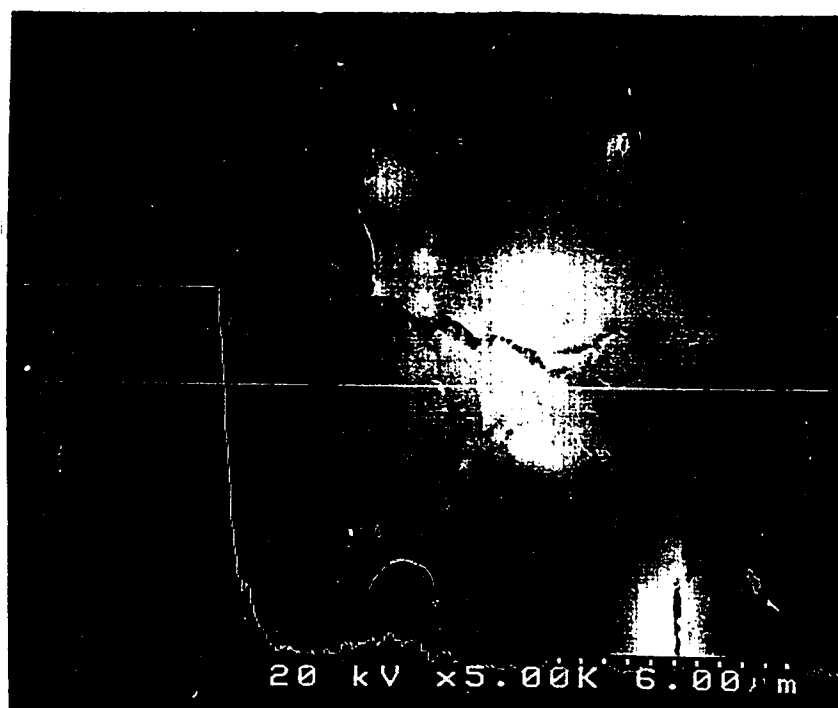


Figure 4.39 Flat coupon #21, as sprayed: digital line scan for Ti.

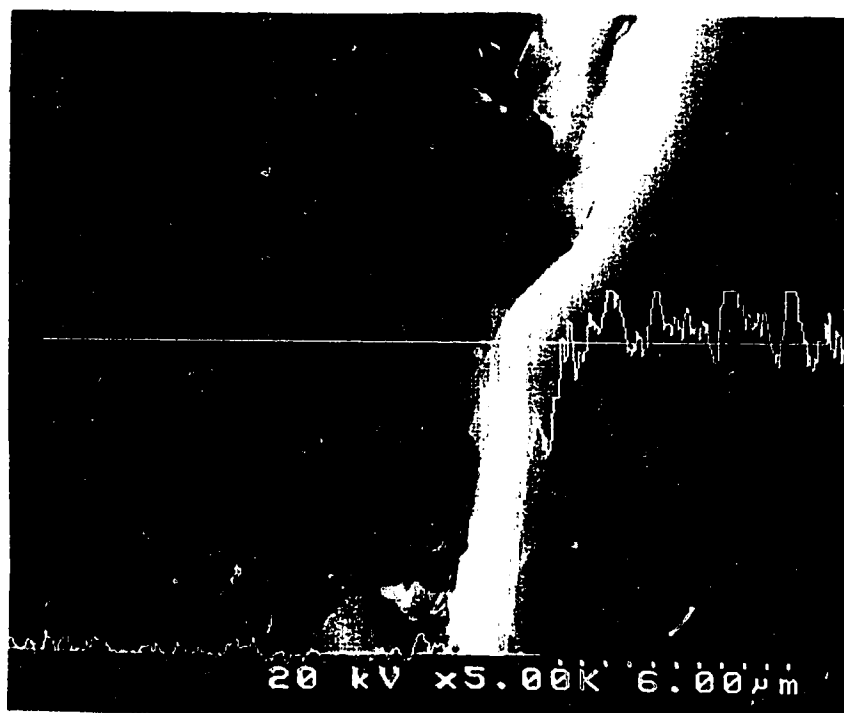


Figure 4.40 Flat coupon #21, as sprayed: digital line scan for P.

Results for the heat treated specimen #21 are provided below. The first objective of the heat treatment was to allow the amorphous, or micro-crystalline, material to develop a more crystalline structure. A second objective of this treatment was to allow more time for the formation of intermediate materials. The kinetics of the formation of intermediate compounds has not been investigated.

P: 0.6 μm into bond coat: 5.14 wt/%		Ti: 0.6 μm above substrate: 16.01	
1.2	3.94	1.2	14.56
1.8	2.84	1.8	10.95
6.0	0.79	2.4	07.16
in HA field	21.26	3.0	04.56
		8.0	00.67
		in Ti field	69.46

The amount of phosphorus measured in the bond coat layer was larger than in the as-sprayed condition while the amount of titanium appeared somewhat less. Again, it was difficult to conclude on the presence of the intermediate compounds based only on these measurements since the specimen preparation could smear the materials between the layers. Two optical photomicrographs of specimen #21, after heat-treatment, are shown in Figures 4.41 and 4.42. No obvious difference was seen between the two sets of optical photomicrographs. Figure 4.43 shows line scans of several elements (O, Si, P, Ca, and Ti) performed on the cross-section of the heat-treated specimen. A more detailed line scan for Ti and P is provided in Figure 4.44 and Figure 4.45, respectively.

Bredig (1943)^[126] discussed the occurrence of intermediate ternary compounds in the system calcium orthosilicate-orthophosphate such as $5\text{CaO} \cdot \text{P}_2\text{O}_5 \cdot \text{SiO}_2$ (silico-carnotite) or $\text{Ca}_5[(\text{PO}_4)_2|\text{SiO}_4]$. From his experimental work, he claims that such ternary compounds are in reality solid solutions of $\text{Ca}_3(\text{PO}_4)_2$ in Ca_2SiO_4 . Nurse et al.(1959)^[127] further investigated the system dicalcium silicate-tricalcium phosphate, looking at high temperatures phase equilibria. They found that silico-carnotite exists as a homogeneous solid solution over a range of composition that varies with temperature and remains stable at room temperature. Dickens and Brown (1971)^[128] observed that there is a resemblance between the unit cell dimensions of HA and $\text{Ca}_5[(\text{PO}_4)_2|\text{SiO}_4]$. However, further work is required to confirm the occurrence of such a substance in the coatings studied here.

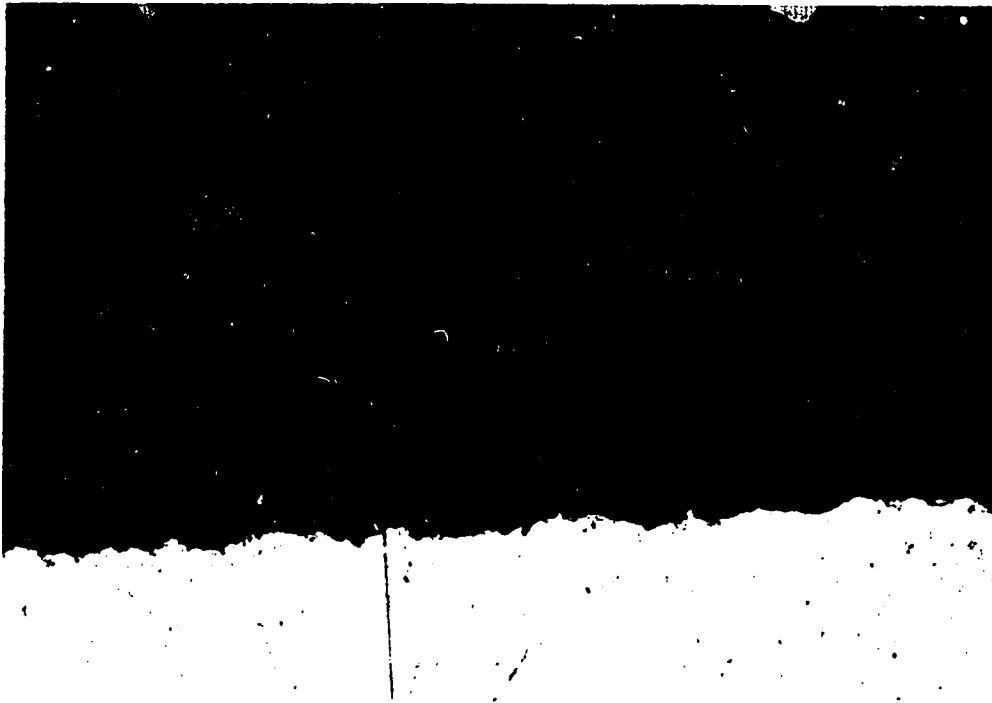


Figure 4.41 Flat coupon #21, after heat treatment. 112 X. 100 μ m

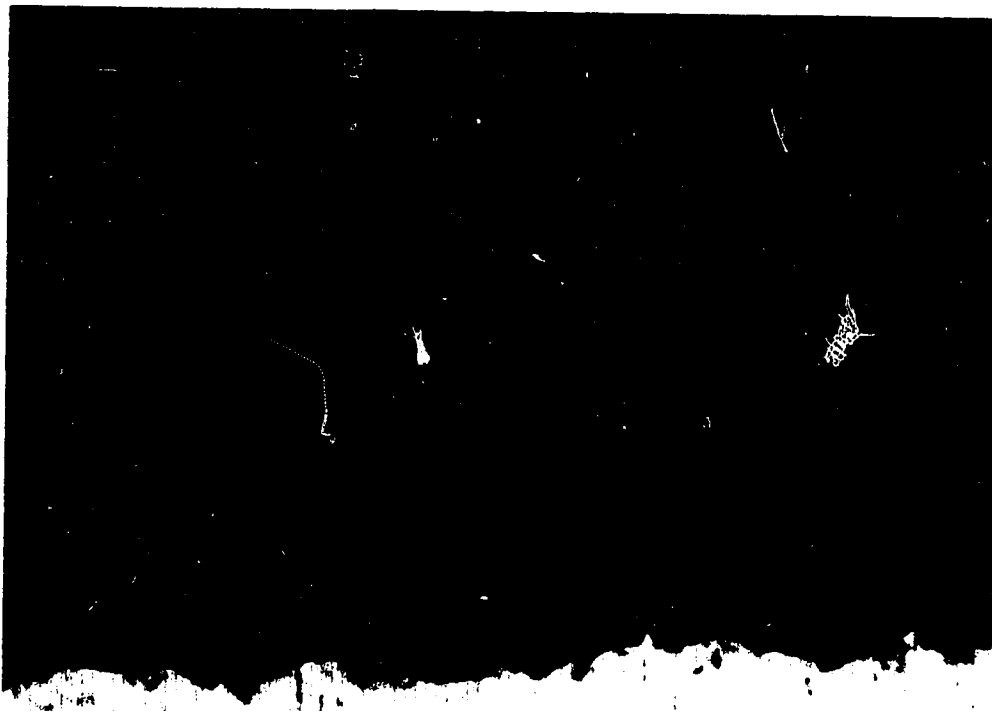


Figure 4.42 Flat coupon #21, after heat treatment. 225 X. 50 μ m

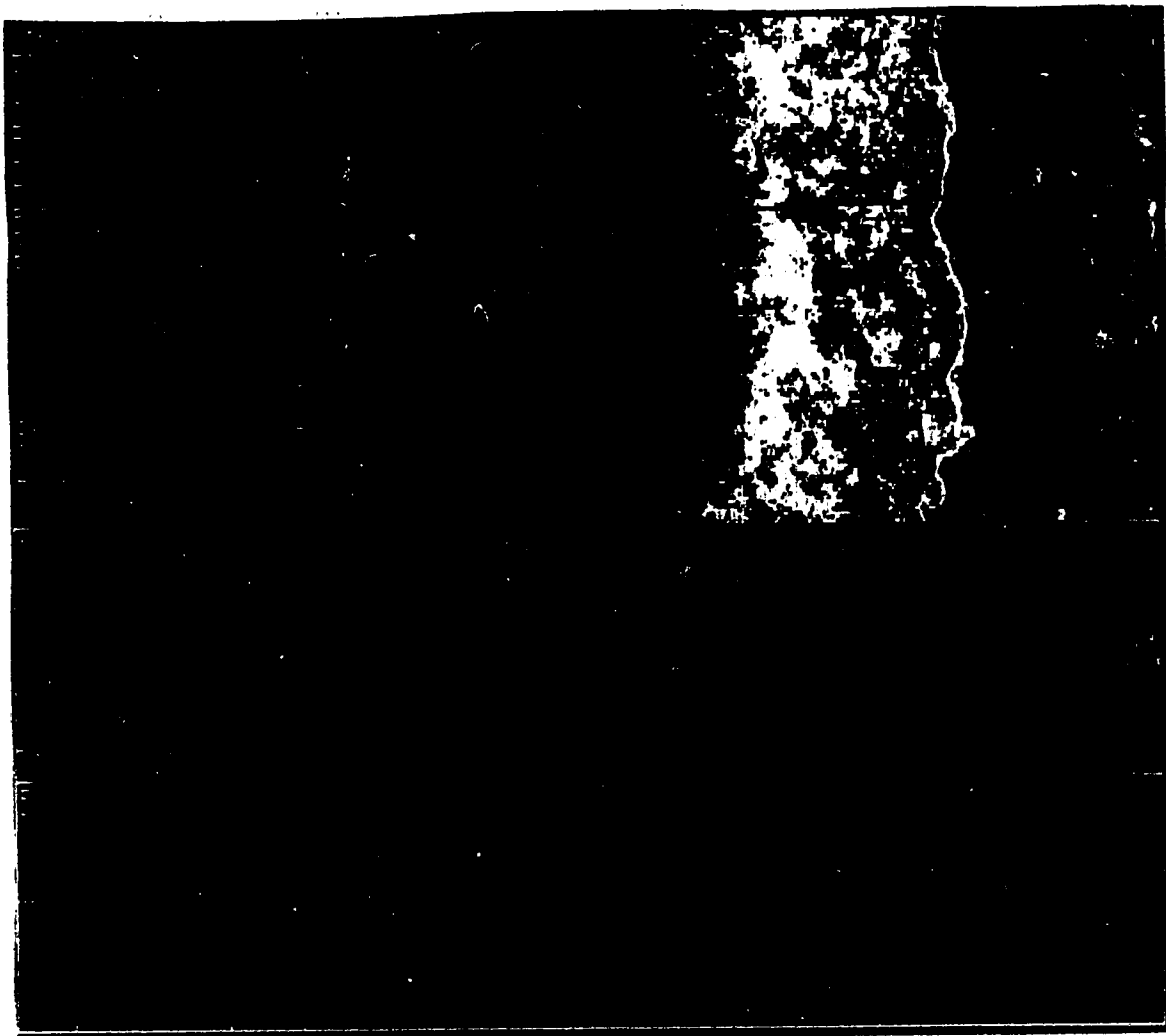


Figure 4.43 Flat coupon #21, after heat treatment: digital line scans through the cross-section.

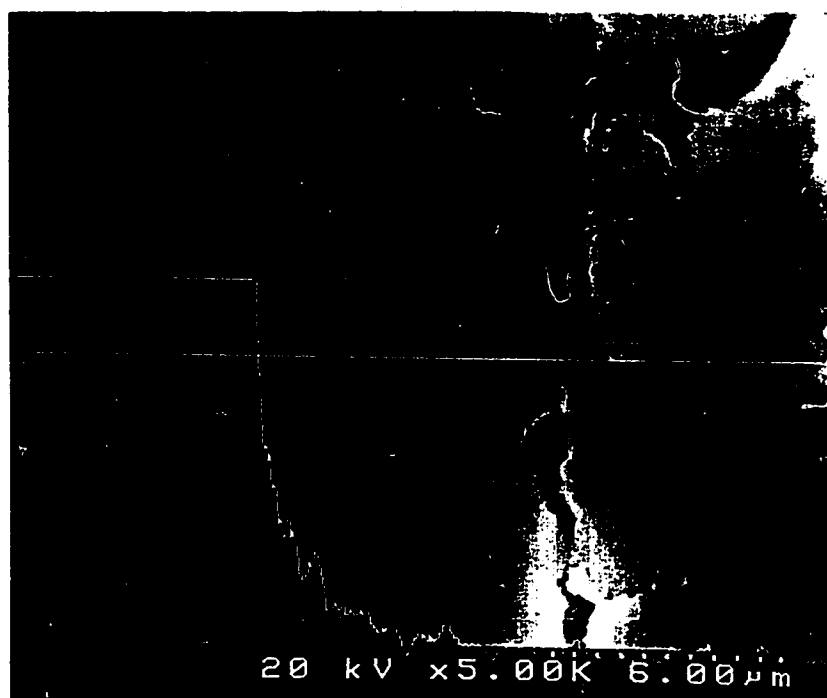


Figure 4.44 Flat coupon #21, after heat treatment: digital line scan for Ti.

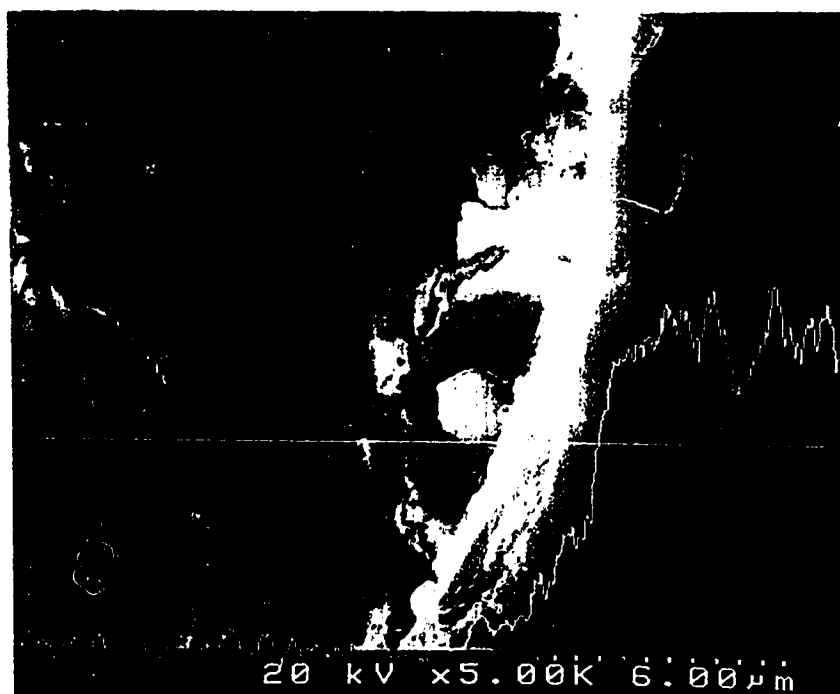


Figure 4.45 Flat coupon #21, after heat treatment: digital line scan for P.

4.2.7 Surface Roughness

The surface roughness of some coupons sprayed with the selected parameters sets was measured. Coupons #21, #23, and #40 had a thick overall coating while coupons #45 and #47 had a thin overall coating. Values are provided in Table 4.15. No consistent trends were observed because several variables were distributed within a very small number of specimens: presence or absence of a bond coat, effect of heat treatment, thick or thin overall coating, and wide variation in thickness within a category. All values are larger than for a polished metal surface. This characteristic is expected to contribute to the attachment of bone to the coating surface.

Table 4.15 Surface roughness measurements on flat coupons.

Specimen ID.	Surface roughness (Ra, μm)
# 23	8.40 ± 0.56
# 40	8.90 ± 0.36
# 45	5.57 ± 0.67
# 47	7.16 ± 0.58
# 21	7.70 ± 2.42
# 21 HT	8.23 ± 0.71

A few bone screws made of pure titanium were sprayed using the selected parameters sets, "3.3" for Ca_2SiO_4 and "5.3" for HA. Three screws were sprayed with only the HA while three other screws were sprayed with the bond coat and the HA. In addition, in each group, only two screws were roughened (sandblasted) before deposition of the coating. All pieces, shown in Figure 4.46, have been implanted in a sheep for evaluation by a Ste-Justine Hospital researcher, but the experiment has not yet been completed. More sprayed specimens are shown in Figure 4.47. Color varies with thickness of the deposit as well as with the presence or absence of a bond coat.

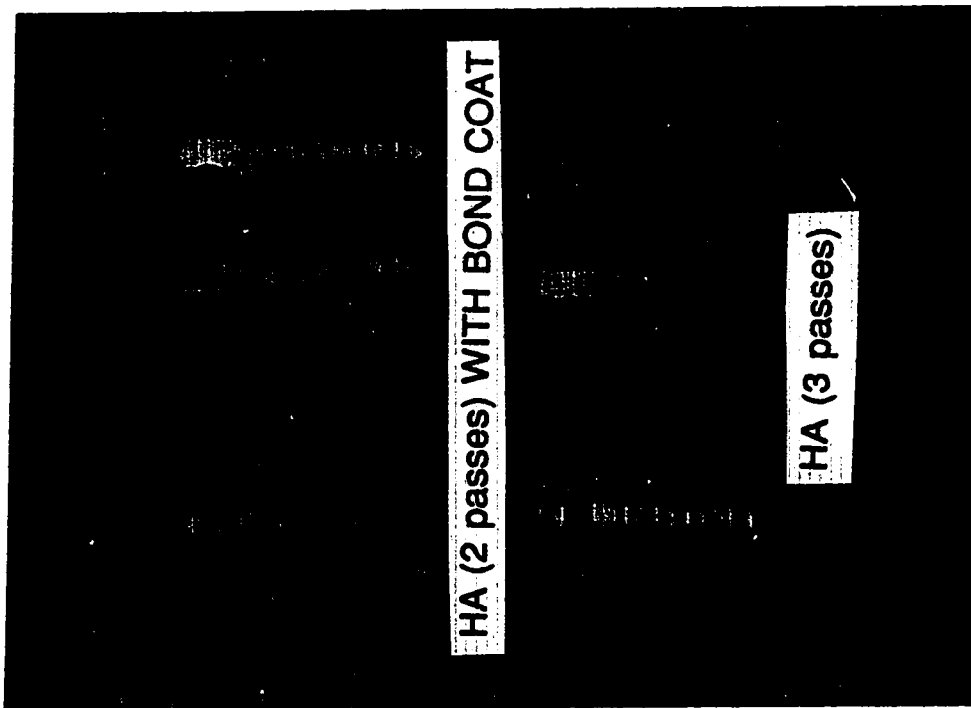


Figure 4.46 Pure titanium bone screws with a bond coat, left, and with only HA, right.

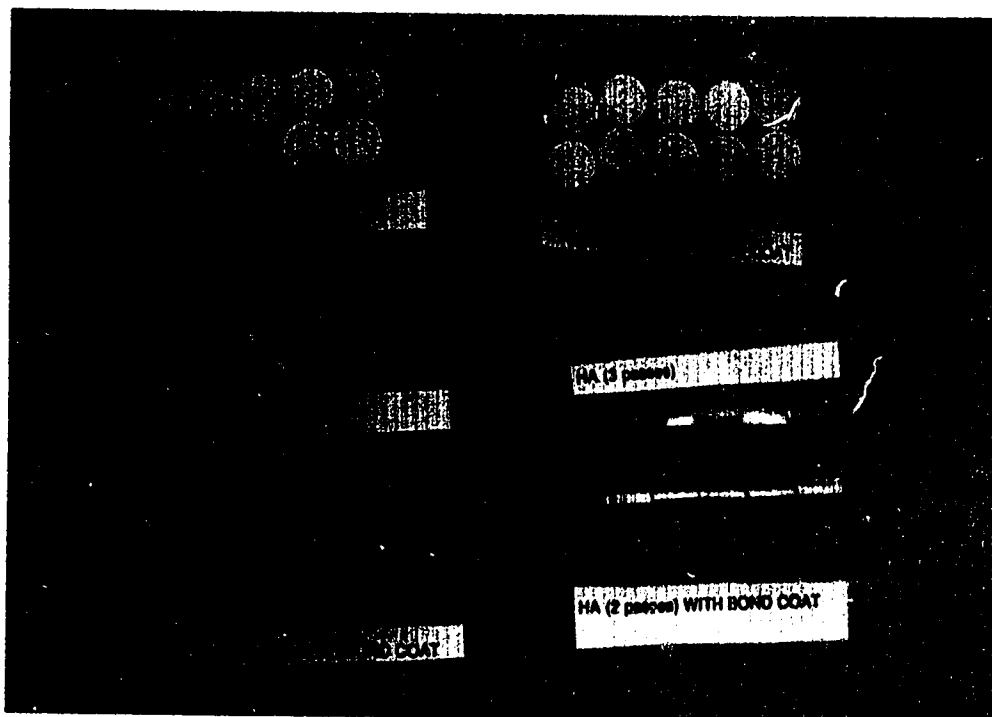


Figure 4.47 Sets of specimens sprayed with a variety of coating systems.

5. CONCLUSIONS

The work completed during this project resulted in the development of a set of spray parameters for each of the two powders. Both powders were deposited onto the substrate as built-up layers by the air plasma spray coating technique. The wipe test was useful for selecting appropriate spray parameters.

Surface preparation improved the attachment of the first layer of the coating to the substrate. A sand-blasted (roughened) surface provided the primary mechanical attachment of the particles, while the coating peeled away from a similar substrate with a polished surface, as successive layers were deposited.

Thickness of the coating depended on the number of gun passes used to deposit the materials. The thickness for one pass is related to the particle size of the raw powders. Hence, the Ca_2SiO_4 powder had small particle size ($< 50 \mu\text{m}$, with a median of $13.55 \mu\text{m}$) producing a thinner coating with the same number of gun passes than the HA powder which had larger particles (up to $120 \mu\text{m}$, with a median of $48.8 \mu\text{m}$). The average thickness value was $13.3 \mu\text{m}$ per pass for the Ca_2SiO_4 powder and $22.0 \mu\text{m}$ per pass for the HA powder.

Heat treatment (24 hours at 330°C) of a coated specimen was not sufficient to affect the crystallinity of the top HA coating. X-ray diffraction spectra were similar for both the heat treated and the as-sprayed specimens. The spectrum for the raw powder had much sharper and better defined peaks than the sprayed material. The spraying process produced a somewhat less crystalline material as observed with the broadening of the peaks. However, no phase change had occurred.

The mechanical test used in the characterization of the adhesion strength of the coatings was not conclusive. Variations in failure location within the coating layers prevented a proper statistical analysis. In the case of thin coatings, the average value was $13.66 \pm 1.54 \text{ MPa}$ in the presence of a bond coat, with most failures of a mixed nature. The adhesion strength was $10.95 \pm 1.08 \text{ MPa}$ without the bond coat. In the case of thick coatings, failure occurred at the interface with the test adhesive rather than within the coatings.

Some elements were identified across their own interfaces: Ti was identified in the Ca_2SiO_4 layer and P was also found in the Ca_2SiO_4 layer. Observation of these elements was used as an indication of the possible formation of intermediate materials. However, more work is required to confirm whether the presence of these elements results from new substances and to clarify the phenomena involved.

6. FUTURE WORK

The work of developing spraying parameters for the two powders has been completed. Coatings can be produced as required, thick or thin and with or without a bond coat. The presence of a bond coat appeared preferable to improve the attachment of the HA material to the substrate. However, the use of a different type of adhesive would help in confirming this. More work is now required to verify the existence of the expected substances at the interfaces.

- 1) Identification of the presence of $\text{CaTi}[\text{O}|\text{SiO}_4]$, titanite (or sphene) at the interface between the titanium-based substrate and the Ca_2SiO_4 (dicalcium silicate) bond coat.
- 2) Identification of the presence of $\text{Ca}_5[(\text{PO}_4)_2|\text{SiO}_4]$, silico-carnotite, at the interface between the Ca_2SiO_4 bond coat and the top hydroxylapatite or $\text{Ca}_{10}(\text{PO}_4)_6(\text{OH})_2$ layer.

Transmission electron microscopy could be used in this work. However, delicate specimen preparation techniques are required to expose the thin interfaces. Diagonal sectioning could increase the exposed surfaces of the areas of interest. Electron spectroscopic imaging (ESI), an extension of elemental mapping techniques to electron energy loss spectroscopic analysis has also been used for such work. SIMS and cathodoluminescence techniques have been proposed.

More fundamental work is also required in the understanding of the kinetics of formation of the new materials and in understanding the transport phenomena contributing to the presence of the elements across their respective interfaces.

A second field of interest for further work involves the clinical evaluation of the new coating system, on a long term basis. Adhesion tests after implantation in bone, both in static and dynamic conditions, are required to confirm the laboratory observations.

REFERENCES

1. R.L. Sutherby, "Corrosion Behavior of Surgical Implants Materials", M.Sc. Thesis, University of Alberta, 149 p., 1984.
2. T. Kokubo, S. Yoshikawa, N. Nishimura, T. Yamamuro, and T. Nakamura, "Bioactive Bone Cement Based on CaO-SiO₂-P₂O₅ Glass". J. Am. Ceram. Soc., Vol. 74, No. 7, p.1739-1774, 1991.
3. V. Sahay, P.J. Lare, and H. Hahn, "Physical and Mechanical Characterization of Porous Coatings for Medical and Dental Devices", in "Thermal Spray Research and Applications", p.425-430, Proceedings of the Third National Thermal Spray Conference, Long Beach, CA, USA, 20-25 May 1990.
4. H. Oonishi, S. Miyamoto, A. Kodha, H. Ishimaru, and E. Tsuji, "Hydroxyapatite Coating on Ti and Al₂O₃ - Studies on the Biological Fixation", in "Biomaterials and Clinical Applications", edited by A.Pizzoferrato, P.G.Marchetti, A.Raviglioli and A.J.C.Lee, Elseviers, Amsterdam, p.69-74, 1987.
5. R.B.Heimann, "Improving the Adherence of Plasma-Sprayed Bioceramic Calcium Phosphate Coatings Through a Silicate-Based Bond Coat". Preliminary Proposal to Onoda Cement Co., March 16, 1992.
6. H. Uchikawa, H. Hagiwara, M. Shirasaka, and H. Yamane, "Properties of the CaO-SiO₂ System Plasma-Sprayed Coatings", p.45-52, Proc. Surface Engineering Intern. Conf., Tokyo, Japan, Oct.18-22, 1988.
7. K. Ogawa, N. Nagata, and T. Yogoro, "Properties of Plasma-Sprayed Coating of the 2 CaO.SiO₂-CaO.ZrO₂ System", Onoda Research Report, Vol.43, No.125, p.45-54, 1991.
8. R.C. Eberhart, H-H. Huo, and K. Nelson, "Cardiovascular Materials". MRS Bulletin, No. 9, p.50-54, 1991.
9. K.J. Korane, "Replacing the Human Heart", Machine Design, p.100-105, Nov.7, 1991.
10. R. Langer, "Drug Delivery Systems". MRS Bulletin, No. 9, p.47-49, 1991.
11. Proceedings of a "Consensus Conference on Implantology", Oct. 18, 1989, Mainz, West Germany. The International Journal of Oral and Maxillofacial Implants, p.182-187, Vol.5, No.2, 1990.
12. E.P. Mueller and S.A. Barenberg, "Biomaterials in an Emerging National Materials Science Agenda". MRS Bulletin, No. 9, p.86-87, 1991.
13. E. Mueller, R. Kammula, and D. Marlowe, "Regulation of Biomaterials and Medical Devices". MRS Bulletin, No. 9, p.39-41, 1991.

14. C. Chopplet and J.P. Thierry, "Biomedical Materials". *Int. J. of Materials and Product Technology*, Vol. 5, No.3, p. 273-280, 1990.
15. W. Rieger, Medical Applications of Ceramics" in "High-Tech Ceramics. Viewpoints and Perspectives", Zurich, Switzerland, 10-11 Nov. 1988. Publ. Academic Press Limited, London, p.191-228, 1989.
16. H. Aoki, "Hydroxyapatite of Great Promise for Biomaterials", SIMAP '88, Osaka, Japan, 17-18 May 1988, *Trans. JWRI*, Vol.17, No.1, p.107-112, 1988.
17. M.N. Helmus, "Overview of Biomedical Materials". *MRS Bulletin*, No. 9, p.33-38, 1991.
18. R.M. Pilliar, J.E. Davies, and D.C. Smith, "The Bone-Biomaterial Interface for Load-Bearing Implants". *MRS Bulletin*, No. 9, p.55-61, 1991.
19. L.L. Hench and J. Wilson, "Bioceramics". *MRS Bulletin*, No. 9, p.62-74, 1991.
20. A.S. Hoffman, "Environmentally Sensitive Polymers and Hydrogels "Smart" Biomaterials". *MRS Bulletin*, No. 9, p.42-46, 1991.
21. J.M. Anderson and Q.H. Zhao, "Biostability of Biomedical Polymers". *MRS Bulletin*, No. 9, p.75-77, 1991.
22. N. Kossovsky and D. Millett, "Materials Biotechnology and Blood Substitutes". *MRS Bulletin*, No. 9, p.78-81, 1991.
23. B. Kasemo and J. Lausmaa, "Biomaterial and Implant Surfaces: A Surface Science Approach", *The International Journal of Oral and Maxillofacial Implants*, p.247-25, Vol 3, No.4, 1988.
24. C.C. Berndt, G.N. Haddad, A.J.D. Farmer and K.A. Gross, "Review Article - Thermal Spraying for Bioceramic Applications", *Materials Forum*, Vol.14, p.161-173, 1990.
25. C.P.A.T. Klein, P. Patka, H.B.M. van der Lubbe, J.G.C. Wolke, and K. de Groot, "Plasma-Sprayed Coatings of Tetracalcium Phosphate, Hydroxylapatite, and alpha-TCP on Titanium alloy: An Interface Study", *Journal of Biomedical Materials Research*, Vol. 25, p.53-65, 1991.
26. A. Cullison, "Plasma Spraying Technique Offers Possible Medical Breakthrough", *Welding Journal*, No. 2, p.51-53, 1987.
27. P.W. Brown and M. Fulmer, "Kinetics of Hydroxyapatite Formation at Low Temperature", *J. Am. Ceram. Soc.*, Vol. 74, No. 5, p.934-940, 1991.
28. C.J. Damien and J.R. Parsons, "Bone Graft and Bone Graft Substitutes: A Review of Current Technology and Applications", *Journal of Applied Biomaterials*, Vol. 2, p. 187-208, 1991.
29. N. Kossovsky, "It's a Great New Material, But Will the Body Accept It? *Research & Development*, No. 8, p.48-54, 1989.

-
30. L.L. Hench and E.G. Ethridge, "Biomaterials. An Interfacial Approach". Biophysics and Bioengineering Series. Academic Press, Inc. Chap. 5. "Ceramics", p.62-86, 1982.
 31. J.W. Boretos, "Bioceramics Come of Age". Chemtech, No. 4, p.224-231, 1987.
 32. L.L. Hench and J.Wilson, "Surface-Active Biomaterials". Science, vol. 226, No. 11, p. 630-636, 1984.
 33. P. Li, C. Ohtsuki, T. Kokubo, K. Nakanishi, N. Soga, T. Nakamura, and T. Yamamuro, "Apatite Formation Induced by Silica Gel in a Simulated Body Fluid", J. Am. Ceram. Soc., Vol. 75, No. 8, p. 2094-2097, 1992.
 34. L.L. Hench, "Bioceramics: From Concept to Clinic", Journal of the American Ceramic Society, Vol.74, No.7, p.1487-1510, 1991.
 35. L.L. Hench, C.G. Pantano Jr., P.J. Buscemi, and D.C. Greenspan, "Analysis of Bioglass Fixation of Hip Prostheses", Journal of Biomedical Materials Research, Vol. 11, p. 267-282, 1977.
 36. L.L. Hench, "Bioactive Ceramics", in Annals New York Academy of Sciences", p. 54-71, 1988.
 37. National Institutes of Health "Consensus Conference Statement: Dental Implants", 13-15 June 1988. The International Journal of Oral and Maxillofacial Implants, p.290-293, Vol.3, No.4, 1988.
 38. M. Jarcho, "Biomaterial Aspects of Calcium Phosphates. Properties and Applications", Dental Clinics of North America, Vol. 30, No. 1, p.25-47, 1986.
 39. K. de Groot, "Hydroxylapatite as Coating for Implants", Interceram No. 4, p.38-41, 1987.
 40. H.W. Denissen, K. de Groot, A.A. Driessen, J.G.C. Wolke, J.G.J. Peelen, H.J.A. van Dijk, A.P. Gehring, and P.J. Kloppe, "Hydroxyapatite Implants: Preparation, Properties and Use in Alveolar Ridge Preservation", Science of Ceramics, Vol.10, p.63-69, 1980.
 41. H. Monma, "Tricalcium Phosphate Ceramics Complexed with Hydroxyapatite", J. Ceram. Soc. Jpn., Vol.95, No.8, p.814-818, 1987.
 42. H. Oonishi, "Mechanical and Chemical Bonding of Artificial Joints", Clin. Mater., Vol.5, No.2-4, p.217-233, 1990.
 43. K. Yamashita, T. Kobayashi, M. Kitamura, T. Umegaki, and T. Kanazawa, "Effect of Water Vapor on the Solid-State Reaction Between Hydroxyapatite and Zirconia or CaO-PSZ", J. Ceramic Soc. Jpn., Vol.96, No. 5, p.616-619, 1988.
 44. K. Hyakuna, T. Yamamuro, Y. Kotoura, Y. Kakutani, T. Kitsugi, H. Takagi, M. Oka, and T. Kokubo, "The Influence of Calcium Phosphate Ceramics and Glass-

- Ceramics on Cultured Cells and Their Surrounding Media", *Journal of Biomedical Materials Research*, Vol. 23, p. 1049-1066, 1989.
45. S. Oki, S. Gohda, T. Shomura, T.H. Kimura, and T. Yoshioka, "Plasma Spraying of Titanium and Apatite to Biomedical Materials", in "Proceedings of the Fourth National Thermal Spray Conference", p. 491-495, Pittsburgh, PA, USA, 4-10 May, 1991.
 46. M. Toriyama, S. Kawamura, and S. Shiba, "Bending Strength of Hydroxyapatite Ceramics Containing α -Tricalcium Phosphate", *J. Ceram. Soc. Jpn. Inter. Ed.*, Vol.95, No.4, p.411-412, 1987.
 47. M. Toriyama and S. Kawamura, "Sinterable Powder of Mechanochemically Synthetic β -Tricalcium Phosphate", *J. Ceram. Soc. Jpn. Inter. Ed.*, Vol.95, No.7, p.698-702, 1987.
 48. M. Toriyama, S. Kawamura, H. Nagae, and K. Ishida, "Effect of MgO Addition on Bending Strength of Sintered β -Tricalcium Phosphate Prepared by Mechanochemical Synthesis", *J. Ceram. Soc. Jpn. Inter. Ed.*, Vol.95, No.8, p.772-774, 1987.
 49. M. Toriyama, S. Kawamura, Y. Ito, H. Nagae, and I. Toyama, "Effects of Mixed Addition of Al_2O_3 and SiO_2 on Mechanical Strength of Sintered β -Tricalcium Phosphate", *J. Ceram. Soc. Jpn. Inter. Ed.*, Vol.96, No. 8, p.815-819, 1988.
 50. M. Toriyama, S. Kawamura, Y. Ito, and H. Nagae, "Thermal Change of Calcium Deficient Apatite Obtained by Mechanochemical Treatment", *J. Ceram. Soc. Jpn. Inter. Ed.*, Vol.97, No. 5, p.545-549, 1989.
 51. M. Toriyama, S. Kawamura, Y. Kawamoto, T. Suzuki, Y. Yokogawa, and S. Ebihara, "Estimation of Biocompatibility of High Strength β -Tricalcium Phosphate Ceramics By a Tissue Culture Method", *J. Ceram. Soc. Jpn. Inter. Ed.*, Vol.98, No. 4, p.420-423, 1990.
 52. M. Toriyama, S. Kawamura, Y. Kawamoto, T. Suzuki, and Y. Yokogawa, " β -Tricalcium Phosphate Coating on Alumina Ceramic", *J. Ceram. Soc. Jpn. Inter. Ed.*, Vol.98, No.9, p.1061-1063, 1990.
 53. Y. Kawamoto, Y. Yokogawa, M. Toriyama, S. Kawamura, and T. Suzuki, "Coating of β -Tricalcium Phosphate on Yttria-Partially Stabilized Zirconia Using Magnesium Metaphosphate as an Interlayer", *J. Ceram. Soc. Jpn. Inter. Ed.*, Vol.99, No. 1, p.19-22, 1991.
 54. Y. Yokogawa, Y. Kawamoto, M. Toriyama, T. Suzuki and S. Kawamura, "Tricalcium Phosphate Coating on Zirconia Using Calcium Metaphosphate and Tetracalcium Phosphate", *J. Ceram. Soc. Jpn. Inter. Ed.*, Vol.99, No. 3, p.206-209, 1991.
 55. M. Toriyama, Y. Kawamoto, T. Suzuki, Y. Yokogawa, K. Nishizawa and H. Nagae, " β -Tricalcium Phosphate Coating on Titanium", *J. Ceram. Soc. Jpn. Inter. Ed.*, Vol.99, No. 12, p.1231-1233, 1991.
 56. T. Suzuki, M. Toriyama, Y. Kawamoto, Y. Yokogawa, and S. Kawamura, "The Adhesiveness and Growth of Anchorage-Dependent Animal Cells on Biocompatible

-
- Ceramic Culture Carriers", *Journal of Fermentation and Bioengineering*, Vol.72, No.6, p.450-456, 1991.
57. Y. Yokogawa, M. Toriyama, Y. Kawamoto, T. Suzuki, and S. Kawamura, "Apatite Coating on Yttria Doped Partially Stabilized Zirconia Plate in the Presence of Water Vapor", *J. Ceram. Soc. Jpn. Inter. Ed.*, Vol.100, No. 4, p.602-604, 1992.
 58. C.A. Homsy, T.E. Cain, F.B. Kessler, M.S. Anderson, and J.W. King, "Porous Implant Systems for Prosthesis Stabilization", *Clinical Orthopaedics and Related Research*, No.89, p.220-235, 1972.
 59. M. Jarcho, J.F. Kay, K.I. Gumaer, R.H. Doremus, and H.P. Drobeck, "Tissue, Cellular and Subcellular Events at a Bone-Ceramic Hydroxyapatite Interface", *Journal of Bioengineering*, Vol.1, p.79-92, 1976.
 60. T.S. Golec, "The Use of Hydroxylapatite to Coat Subperiosteal Implants", *The Journal of Oral Implantology*, No. 12, p.20-39, 1985.
 61. J.F. Kay, M. Jarcho, G. Logan, and S.T. Liu, "The Structure and Properties of Hydroxylapatite Coatings on Metal", in "Trans. 12th Ann. Meet. Soc. Biomater.", Minneapolis, St-Paul, Minnesota, USA, p. 13, May 29 to June 1, 1986.
 62. S.D. Cook, J.F. Kay, K.A. Thomas, R.C. Anderson, A.F. Harding, M.C. Reynolds, and M. Jarcho, "Variables Affecting the Interface Strength and Histology of Hydroxylapatite Coated Implant Surfaces", in "Trans. 12th Ann. Meet. Soc. Biomater.", Minneapolis, St-Paul, Minnesota, p. 14, USA, May 29 to June 1, 1986.
 63. K.A. Thomas, S.D. Cook, R.C. Anderson, R.J. Haddad Jr., J.F. Kay, and M. Jarcho, "Biological Response to Hydroxylapatite Coated Porous Titanium Hips", in "Trans. 12th Ann. Meet. Soc. Biomater.", Minneapolis, St-Paul, Minnesota, USA, p. 15, May 29 to June 1, 1986.
 64. J.N. Kent, M.S. Block, J. Kay, M. Jarcho, and I.M. Finger, "Hydroxylapatite Coated and Non-Coated Dental Implants in Dogs", in "Trans. 12th Ann. Meet. Soc. Biomater.", Minneapolis, St-Paul, Minnesota, USA, p. 16, May 29 to June 1, 1986.
 65. J.F. Kay, "Designing Endosseous Dental Implants for Hydroxyapatite Coating", in "Proceedings of the 6th European Conference on Biomaterials", Bologna, Italy, 2 pages, 1986.
 66. J.F. Kay, T.S. Golec, and R.L. Riley, "Hydroxyapatite-Coated Subperiosteal Dental Implants: Design Rationale and Clinical Experience", *The Journal of Prosthetic Dentistry*, Vol. 58, No. 3, p. 339-343, 1987.
 67. M.T. Manley, J.F. Kay, S. Yoshiya, L.S. Stern, and B.N. Stulberg, "Accelerated Fixation of Weight Bearing Implants by Hydroxylapatite Coatings", in "Proceedings of the 33rd Annual Meeting, Orthopaedic Research Society, San Francisco, California, USA, January 19-22, 1987.

-
68. K.I. Gumaer, A.D. Sherer, R.G. Slighter, S.S. Rothstein, and H.P. Drobeck, "Tissue Response in Dogs to Dense Hydroxyapatite Implantation in the Femur", *Journal of Oral and Maxillofacial Surgery*, Vol.44, p.618-627, 1986.
 69. S.J. Yankee, B.J. Pletka, H.A. Luckey, and W.A. Johnson, "Processes for Fabricating Hydroxylapatite Coatings for Biomedical Applications". In "Proceedings of the Third National Thermal Spray Conference", Long Beach, CA, USA, p. 433-438, 20-25 May 1990.
 70. D.P. Rivero, J. Fox, A.K. Skipor, R.M. Urban, and J.O. Galante, "Calcium Phosphate-Coated Porous Titanium Implants for Enhanced Skeletal Fixation", *Journal of Biomedical Materials Research*, Vol. 12, p. 191-201, 1988.
 71. N. Blumenthal, J.L. Ricci, and H. Alexander, "The Effects of Implant Surfaces on Bone Mineral Formation and Attachment in Vitro", *Trans. Soc. Biomater.*, Vol.12, No.5, p.2, 1989.
 72. J.A. Szivek, R.G. Gealer, F.P. Magee, and J. Emmanuel, "Preliminary Development of a Hydroxyapatite-Backed Strain Gauge", *Journal of Applied Biomaterials*, Vol. 1, p. 241-248, 1990.
 73. D.H. Harris, "Overview of Problems Surrounding the Plasma Spraying of Hydroxylapatite Coatings", in "Thermal Spray Research and Applications", Invited Paper, Proceedings of the Third National Thermal Spray Conference, Long Beach, CA, USA, p. 419-423, 20-25 May 1990.
 74. S.J. Yankee and B.J. Pletka, "An Investigation of Plasma Sprayed Hydroxylapatite Splats", in "Proceedings of the Fourth National Thermal Spray Conference", Pittsburgh, PA, USA, p.465-469, 4-10 May, 1991.
 75. R.L. Salsbury, "Quality Control of Hydroxylapatite Coatings: Purity and Crystallinity Determinations", in "Proceedings of the Fourth National Thermal Spray Conference", Pittsburgh, PA, USA, p.471-473, 4-10 May, 1991.
 76. ASTM F 86 - 84. "Standard Practice for Surface Preparation and Marking of Metallic Surgical Implants". *Annual Book of ASTM Standards*, Vol.13.01, 1992.
 77. B.V. Rejda, J.G.J. Peelen, and K. de Groot, "Tri-Calcium Phosphate as a Bone Substitute", *Journal of Bioengineering*, Vol. 1, No. 2, P.93-97, 1977.
 78. G. de With, H.J.A. Van Dijk, N. Hattu, and K. Prijs, "Preparation, Microstructure and Mechanical Properties of Dense Polycrystalline Hydroxyapatite", *Journal of Materials Sciences*, Vol. 16, p.1592-1598, 1981.
 79. A.A. Driessen, P.A. Vingerling, C. De Putter, and K. de Groot, "Fatigue Properties of Pre-Stressed Calcium Phosphate Ceramics", *Science of Ceramics*, Vol. 12, p. 543-549, 1984.
 80. K. de Groot, R. Geesink, C.P.A.T. Klein, and P. Serekian, "Plasma Sprayed Coatings of Hydroxyapatite", *Journal of Biomedical Materials Research*, Vol.21, P. 1375-1381, 1987.

81. P. Ducheyne, W. Van Raemdonck, J.C. Heughebaert and M. Heughebaert, "Structural Analysis of Hydroxyapatite Coatings on Titanium", *Biomaterials*, No. 7, p.97-103, 1986.
82. R.G.T. Geesink, "Experimental and Clinical Experience With Hydroxyapatite-Coated Hip Implants", *Orthopedics*, Vol. 12, p.1239-1243, 1989.
83. J.G.C. Wolke, C.P.A.T. Klein, and V. de Groot, "Plasma-Sprayed Hydroxylapatite Coatings for Biomedical Applications", Invited Paper, in "Thermal Spray Research and Applications". Proceedings of the Third National Thermal Spray Conference, p. 413-417, Long Beach, CA, USA, 20-25 May 1990.
84. C.A. Van Blitterswijk, S.C. Hesselink, J.J. Grote, H.K. Koerten, and K. de Groot, "The Biocompatibility of Hydroxyapatite Ceramic: A Study of Retrieved Human Middle Ear Implants". *J. of Biom. Mar. Res.*, Vol. 24, p. 433-453, 1990.
85. B. Koch, J.G.C. Wolke and K. De Groot, "X-Ray Diffraction Studies on Plasma-Sprayed Calcium Phosphate-Coated Implants", *Journal of Biomedical Materials Research*, Vol. 24, p. 655-667, 1990.
86. C.P.A.T. Klein, J.M.A. de Blicke-Hogervorst, J.G.C. Wolke, and K. de Groot, "Studies of the Solubility of Different Calcium Phosphate Ceramic Particles *in Vitro*", *Biomaterials*, No. 11, p.509-512, 1990.
87. J.G.C. Wolke, K. de Groot, T.G. Kraak, W. Herlaar, and J.M.A. de Blicke-Hogervorst, "The Characterization of Hydroxylapatite Coatings Sprayed with VPS, APS, and DJ Systems", in "Proceedings of the Fourth National Thermal Spray Conference", Pittsburgh, PA, USA, p. 481-490, 4-10 May 1991.
88. J.G.C. Wolke, J.M.A. de Blicke-Hogervorst, W.J.A. Dhert, C.P.A.T. Klein, and K. de Groot, "Studies on the Thermal Spraying of Apatite Bioceramics", *Journal of Thermal Spray Technology*, Vol. 1, No. 1, p.75-82, 1992.
89. ASTM C 633 - 79, "Standard Test Method for Adhesion or Cohesive Strength of Flame-Sprayed Coatings", *Annual Book of ASTM Standards*, Vol. 3.01, 1992.
90. L.M. Sheppard, "Cure it With Ceramics". *Advanced Materials and Process*, No 5, p. 26-31, 1986.
91. H. Oonishi, "Development and Application of Bioceramics in Orthopaedic Surgery". *International Symposium on Fine Ceramics Arita*, p 21-40, 1989.
92. S.J. Mraz , "The Human Body Shop", *Machine Design*, p. 90-94, Nov. 7, 1991.
93. S.A. Barenberg, "Report of the Committee to Survey Needs and Opportunities for the Biomaterials Industry". *MRS Bulletin*, No. 9, p.26-32, 1991.
94. J. Koeneman, J. Lemons, P. Ducheyne, W. Lacefield, F. Magee, T. Calahan, and J. Kay, "Workshop on Characterization of Calcium Phosphate Materials", *Journal of Applied Biomaterials*, p. 79-90, Vol. 1, 1990.

95. J.E. Davies, N. Nagai, and N. Takeshita, "Osteogenesis and Osteoclasts at the Interface With a Bioactive Bone-Substitute", in "Proceedings of the Society for Biomaterials", 15th Annual Meeting, Lake Buena Vista, Florida, USA, p. 5, April 28-May 2, 1989.
96. B.M. Tracy and R.H. Doremus, "Direct Electron Microscopy Studies of the Bone-Hydroxyapatite Interface", *Journal of Biomedical Materials Research*, Vol.18, p.719-726, 1984.
97. P. Ducheyne, L.L. Hench, A. Kagan II, M. Martens, A. Bursens, and J.C. Mulier, "Effect of Hydroxyapatite Impregnation on Skeletal Bonding of Porous Coated Implants", *Journal of Biomedical Materials Research*, Vol. 14, p. 225-237, 1980.
98. W. Van Raemdonck, P. Ducheyne, and P. De Meester, "Auger Electron Spectroscopic Analysis of Hydroxylapatite Coatings on Titanium", *Journal of the American Ceramic Society*, Vol. 67, No.6, p. 381-384, 1984.
99. J.-C. Heughebaert, "Biocéramiques Constituées de Phosphates de Calcium", *Silicates Industriels*, Vol. 53, No. 3-4, p. 37-41, 1988.
100. G. Montel, "Constitutions et Structure des Apatites Biologiques: Influence de Ces Facteurs Sur Leurs Propriétés", *Biologie Cellulaire*, Vol. 28, No. 3, p.179-186, 1977.
101. I. Orly, M. Gregoire, J. Menanteau, M. Heughebaert, and B. Kerebel, "Chemical Changes in Hydroxyapatite Biomaterial under *in Vivo* and *in Vitro* Biological Conditions", *Calcified Tissue International*, Vol.45, p.20-26, 1989.
102. W.R. Lacefield and L. L. Hench, "The Bonding of Bioglass® to a Cobalt-Chromium Surgical Implant Alloy", Revised 19 September 1985, 5 pages, *Biomaterials*, 1986.
103. E. Barth and H. Herø, "Bioactive Glass Ceramic on Titanium Substrate: The Effect of Molybdenum as an Intermediate Bond Coating", Accepted 20 November 1985, 4 pages, *Biomaterials*, 1986.
104. H. Lüthy, J.R. Strub and P. Shärer, "Analysis of Plasma Flame-Sprayed Coatings on Endosseous Oral Titanium Implants Exfoliated in Man: Preliminary Results", *The International Journal of Oral & Maxillofacial Implants*, Vol.2, No.4, p.197-202, 1987.
105. R.E. Baier and A.E. Meyer, "Implant Surface Preparation", *The International Journal of Oral & Maxillofacial Implants*, Vol.3, No.1, p.9-20, 1988.
106. M.J. Edge, "In Vivo Fracture of the Tricalcium Phosphate Coating From the Titanium Body of an Osseointegrating-Type Dental Implant: A Case Report", *The International Journal of Oral & Maxillofacial Implants*, Vol.3, No.1, p.57-58, 1988.
107. H. Lüthy, and J.R. Strub, "Thickness of Plasma Flame-Sprayed Coatings on Titanium Implants Exfoliated in Dogs", *The International Journal of Oral & Maxillofacial Implants*, Vol.3, No.4, p.269-273, 1988.

-
108. G. Daculsi, R.Z. LeGeros, E. Nery, K. Lynch, and B. Kerebel, "Transformation of Biphasic Calcium Phosphate Ceramics *In Vivo*: Ultrastructural and Physicochemical Characterization", *Journal of Biomedical Materials Research*, Vol.23, p. 883-894, 1989.
 109. A. Slósarczyk, and J. Prazuch, "Porous Hydroxyapatite Material for Implantology", *Sprechsaal Int. Ceram. Glass Mag.*, Vol.122, No.8, p.745-746, 1989.
 110. A. Slósarczyk, "Highly Porous Hydroxyapatite Material", *Powder Metall. Int.*, Vol.21, No.4, p.24-25, 1989.
 111. E. Hjørting-Hansen, N. Worsaae, and J.E. Lemons, "Histologic Response After Implantation of Porous Hydroxyapatite Ceramic in Humans", *The International Journal of Oral & Maxillofacial Implants*, Vol.5, No.3, p.255-263, 1990.
 112. F.B. Bagambisa, U. Joos, and W. Schilli, "The Interaction of Osteogenic Cells With Hydroxylapatite Implant Materials *In Vitro* and *In Vivo*", *The International Journal of Oral & Maxillofacial Implants*, Vol. 5, No. 3, p.217-226, 1990.
 113. E. Lugscheider, T.F. Weber, and M. Knepper, "Production of Biocompatible Coatings of Hydroxyapatite and Fluorapatite", in "Thermal Spray Technology. New Ideas and Processes", *Proceedings of The National Thermal Spray Conference*, p. 337-343, Cincinnati, Ohio, USA, 24-27 October 1988.
 114. R.M. Pilliar, "Porous-Surfaced Metallic Implants for Orthopedic Applications", *Journal of Biomedical Materials Research: Applied Biomaterials*, Vol. 21, No. A1, p. 1-33, 1987.
 115. R.M. Pilliar and M.J. Filiaggi, "Mechanical Characterization of Plasma-Sprayed Hydroxyapatite-Titanium Alloy Interfaces", in "Bioceramics", Vol.4, Ed. by W. Bonfield, G.W. Hastings and K.E. Tanner, *Proceedings of the 4th Int. Symposium on Ceramics in Medicine*, London, U.K., Sept. 1991, p. 343-350, 1991.
 116. M.J. Filiaggi, N.A. Coombs, and R.M. Pilliar, "Characterization of the Interface in the Plasma-Sprayed Hydroxylapatite Coating / Ti-6AL-4V Implant System", (draft from the authors), to be published in *Journal of Biomedical Materials Research*.
 117. A. Krajewski, A. Ravaglioli, R. Mongiorgi, and A. Moroni, "Mineralization and Calcium Fixation Within a Porous Apatitic Ceramic Material After Implantation in the Femur of Rabbits", *Journal of Biomedical Materials Research*, Vol. 22, p.445-457, 1988.
 118. A. Ravaglioli, A. Krajewski, and R.Z. Le Geros, "Manufacture of Calcium Phosphate Bioactive Ceramics and Glasses: Modalities and Problems", *Interceram* No. 2, p.22-23, 1989.
 119. J. Li, and L. Hermansson, "Mechanical Evaluation of Hot Isostatically Pressed Hydroxylapatite", *Interceram*, Vol. 39, No. 2, p. 13-15, 1990.
 120. P. Royer and C. Rey, "Calcium Phosphate Coatings for Orthopaedic Prosthesis", *Surface and Coatings Technology*, Vol. 45, p.171-177, 1991.

-
121. G. Tackett and J. Huber, "Storage of Grit Blasted Biomedical Components: Effects on Ti-6AL-4V Porous Coating Bond Strength", in "Thermal Spray Research and Applications", p.431-432, Proceedings of the Third National Thermal Spray Conference, Long Beach, CA, USA, 20-25 May 1990.
 122. H. McDowell, T.M. Gregory, and W.E. Brown, "Solubility of $\text{Ca}_5(\text{PO}_4)_3\text{OH}$ in the System $\text{Ca}(\text{OH})_2\text{-H}_3\text{PO}_4\text{-H}_2\text{O}$ at 5, 15, 25, and 37 °C", *Journal of Research of the National Bureau of Standards-A. Physics and Chemistry*, Vol. 81A, No. 2-3, p. 273-291, 1977.
 123. S. Chander and W. Fuerstenau, "Interfacial Properties and Equilibria in the Apatite-Aqueous Solution System", *Journal of Colloid and Interface Science*, Vol. 70, No. 3, p. 506-516, 1979.
 124. H. Newesely and J.F. Osborn, "Structural and Textural Implications of Calcium Phosphates in Ceramics", in "Mechanical Properties of Biomaterials", edited by G.W. Hastings and D.F. Williams, John Wiley & Sons Ltd, Chap. 37, p.457-464, 1980.
 125. J.L. Miquel, L. Facchini, A.P. Legrand, X. Marchandise, P. Lecouffe, M. Chanavaz, M. Donazzan, C. Rey, and J. Lemaître, "Characterisation and Conversion Study into Natural Living Bone of Calcium Phosphate Bioceramics by Solid State NMR Spectroscopy", *Clinical Materials*, Vol. 5, No. 2-4, p. 115-125, 1990.
 126. M.A. Bredig, "Phase Relations in the System Calcium Orthosilicate-Orthophosphate", *Am. Mine.*, Vol. 28, p. 594-601, 1943.
 127. R.W. Nurse, J.H. Welch, and W. Gutt, "High-Temperature Phase Equilibria in the System Dicalcium Silicate-Tricalcium Phosphate", *J. Chem. Soc., Part I*, p. 1077-1083, 1959.
 128. B. Dickens and W.E. Brown, "The Crystal Structure of $\text{Ca}_5(\text{PO}_4)_2\text{SiO}_4$ (Silico-Carnotite)", *TMPM Tschermaks Min. Petr. Mitt*, Vol. 16, p. 1-27, 1971.
 129. M.B. Tomson and G.H. Nancollas, "Mineralization Kinetics: A Constant Composition Approach", *Science*, Vol. 200, p. 1059-1060, 1978.
 130. P.G. Koutsoukos, Z. Amjad, M.B. Tomson, and G.H. Nancollas, "Crystallization of Calcium Phosphates. A Constant Composition Study", *Journal of the American Chemical Society*, Vol. 102, p. 1553-1557, 1980.
 131. P.G. Koutsoukos and G.H. Nancollas, "Crystal Growth of Calcium Phosphates - Epitaxial Considerations", *Journal of Crystal Growth*, Vol. 53, p.10-19, 1981.
 132. M. Fulmer and P.W. Brown, "The Effects of Particle Size and Solution Chemistry on the Formation of Hydroxyapatite", *Mat. Res. Soc. Symp. Proc. of the Materials Research Society*, Vol. 174, p.39-44, 1990.
 133. P.W. Brown, N. Hocker, and S. Hoyle, "Variations in Solution Chemistry During the Low-Temperature Formation of Hydroxyapatite", *J. Am. Ceram. Soc.*, Vol. 74, No. 8, p. 1848-1854, 1991.

-
134. M.W. Barnes, M. Klimkiewicz, and P.W. Brown, "Hydration in the System $\text{Ca}_2\text{SiO}_4\text{-Ca}_3(\text{PO}_4)_2$ at 90 °C", J. Am. Ceram. Soc., Vol. 75, No. 6, p.1423-1429, 1992.
 135. J.M. Toth, W.M. Hirthe, W.G. Hubbard, W.A. Brantley, and K.L. Lynch, "Determination of the Ratio of HA/TCP Mixtures by X-Ray Diffraction", Journal of Applied Biomaterials, Vol. 2, p. 37-40, 1991.
 136. A.J. Ruys and E.R. McCartney, "Progress in Developing High-Strength Resorbable Bone Implants". Materials Science Forum, Vol. 34-36, p. 399-401, 1988.
 137. S.J. Yankee, B.J. Pletka, and R.L. Salsbury, "Quality Control of Hydroxylapatite Coatings: The Surface Preparation Stage", in "Proceedings of the Fourth National Thermal Spray Conference", Pittsburgh, PA, USA, 4-10 May, 1991, p.475-479.
 138. R.B. Heimann, D.Lamy, and T.N. Sopkow, "Parameter Optimization of Alumina-Titania Coatings by a Statistical Experimental Design", in "Thermal Spray Research and Applications", p.491-496, Proceedings of the Third National Thermal Spray Conference, Long Beach, CA, USA, 20-25 May 1990.
 139. R.B. Heimann, D.Lamy, and T.N. Sopkow, "Optimization of Vacuum Plasma Arc Spray Parameters of 88WC12Co Alloy Coatings Using a Statistical Multifactorial Design Matrix", Journal of the Canadian Ceramic Society, p. 49-54, Vol. 59, No. 3, Aug. 1990.
 140. C.C. Berndt, "Instrumented Tensile Adhesion Tests on Plasma Sprayed Thermal Barrier Coatings", J. Materials Engineering, Vol. 11, No. 4, p. 275-282, 1989.
 141. C.C. Berndt and K.A. Gross, "Characteristics of Hydroxylapatite Bio-Coatings", in Proceedings of the Internatioanl Thermal Spray Conference & Exposition, Orlando, Florida, USA, p. 465-470, 28 May-5 June 1992.

APPENDIX

Plasma Spraying Equipment

A commercial plasma spray coating system, from Miller Thermal Technologies, Inc., Plasmadyne Division, was used to produce the coatings. The system included as well a containment chamber that allows for spraying in low pressure (or so-called "vacuum" spraying) or in controlled atmospheres. However, all spraying activities for this work were performed in air, although the spray gun was installed in the containment chamber. Most components of the spraying system are shown in Figure A.1.

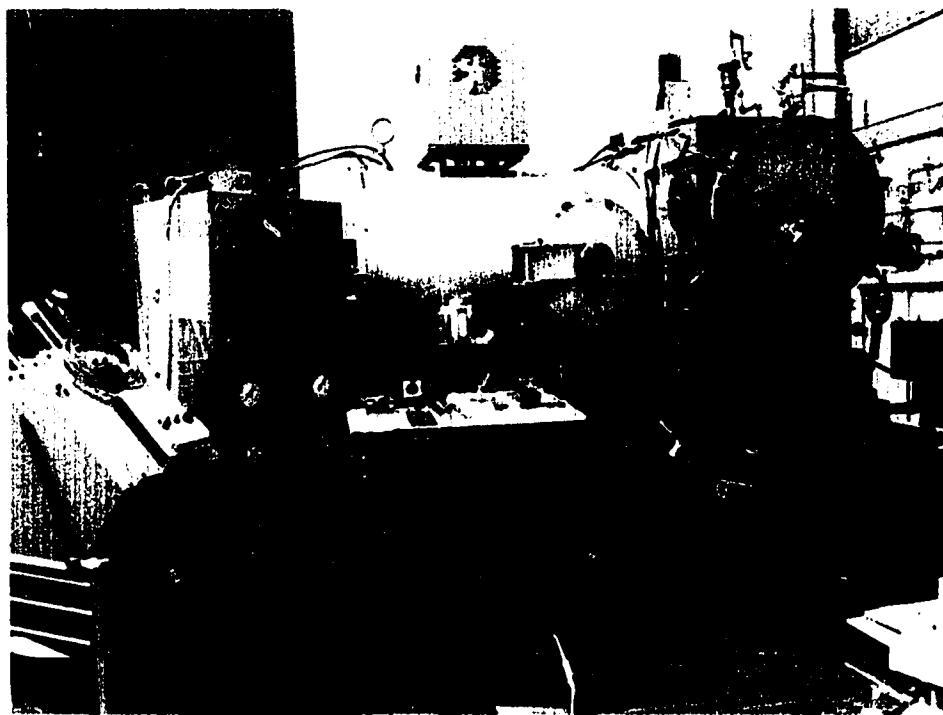


Figure A.1 Plasma spray coating system.

The Model 3610-D automatic production plasma spray system includes the following main elements:

- PS-100 Power Supply which permits selection of the operating current level.

-
- Model 1228 High Frequency Unit, which permits the start-up of the arc. This is the small orange square box located on top of the gray cylinder (containment chamber), center top of Figure A.1.
 - Model 3610 Control Console, which contains all the necessary controls for operation of the spray system as well as a micro-processor (automatic) control module, which shuts off the system when faulty conditions are detected, such as low water pressure, high gas pressure, etc. This is the vertical orange cabinet with various dial indicators, Figure A.1.
 - Model 1275 Dual Roto-Feed Hopper. The two powder sources are controlled by a common electronic system. Selection of either powder is controlled remotely from the control console. The hopper is located at the extreme left, Figure A.1.
 - SG-100 Plasma Spray Gun, operated from subsonic conditions up to Mach I and Mach II levels (referring to the exit conditions of the plasma stream). These conditions are obtained through the combination of proper powder settings and gun configuration (cathode, anode, and gas injector).

In addition to these elements, a water cooling system is required to circulate water through the containment chamber and through the gun itself. A venting system is also required to evacuate the gases and particles away from the spray chamber.

In addition to the spraying system, a control console was used to control the gun movement (up and down) and the specimen holder (back and forth, laterally). Gases are required to produce the plasma (argon and helium) and for powder particles transportation (argon).

The SG-100 plasma spray gun components are shown in Figure A.2. The gun is routinely disassembled for maintenance and to install proper components required for each configuration. Components which are varied are the cathode, the anode, and the gas injector. These components are shown in Figure A.3 with a scale indicating their respective size. In this work, a 40 kW subsonic configuration was used, with a 2083-175 anode (90 ° injection, general purpose, for spraying both metals and ceramics), a 1083A-129 cathode, and a 2083-130 (four hole) gas injector.

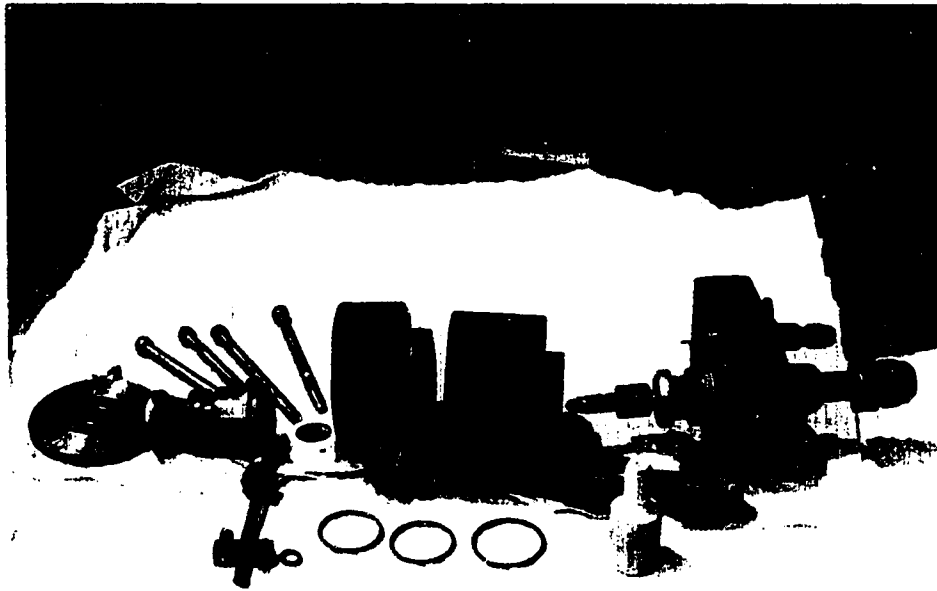


Figure A.2 SG-100 plasma spray gun components.

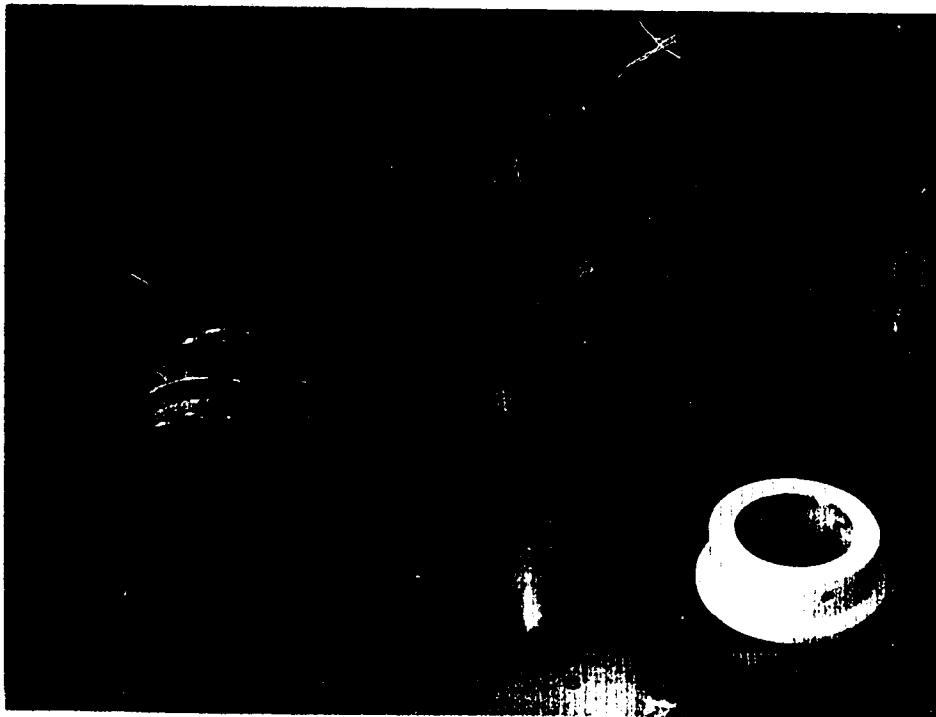


Figure A.3 Anode (#175), left, cathode (#129), center, and gas injector (#130), right.